2009-12-18

Correlation between High Resolution Sequence Stratigraphy and Mechanical Stratigraphy for Enhanced Fracture Characteristic Prediction

Laiyyan M. Al Kharusi
University of Miami, lkharusi@rsmas.miami.edu

UNIVERSITY OF MIAMI

CORRELATION BETWEEN HIGH RESOLUTION SEQUENCE STRATIGRAPHY AND MECHANICAL STRATIGRAPHY FOR ENHANCED FRACTURE CHARACTERISTIC PREDICTION

By

Laiyyan M. Al Kharusi

A DISSERTATION

Submitted to the Faculty
of the University of Miami
in partial fulfillment of the requirements for
the degree of Doctor of Philosophy

Coral Gables, Florida

December 2009

UNIVERSITY OF MIAMI

A dissertation submitted in partial fulfillment of
the requirements for the degree of
Doctor of Philosophy

CORRELATION BETWEEN HIGH RESOLUTION SEQUENCE STRATIGRAPHY AND MECHANICAL STRATIGRAPHY FOR ENHANCED FRACTURE CHARACTERISTIC PREDICTION

Laiyyan M. Al-Kharusi

Approved:

_____
Gregor P. Eberli, Ph.D.
Professor of Marine Geology
and Geophysics

_____
Terri A. Scandura, Ph.D.
Dean of the Graduate School

_____
Christopher G.A. Harrison, Ph.D.
Professor of Marine Geology
and Geophysics

_____
Timothy H. Dixon, Ph.D.
Professor of Marine Geology
and Geophysics

_____
Volker C. Vahrenkamp, Ph.D.
Carbonate Geology Specialist
ND-ADCO
Abu Dhabi, United Arab Emirates

AL KHARUSI, LAIYYAN (Ph.D., Marine Geology and Geophysics)
Correlation Between High Resolution Sequence; Stratigraphy And Mechanical Stratigraphy For Enhanced Fracture Characteristic Prediction. (December 2009)

Abstract of a dissertation at the University of Miami.

Dissertation supervised by Professor Gregor Eberli.
No. of pages in text. (152)

Sequence stratigraphy relates changes in vertical and lateral facies distribution to relative changes in sea level. These relative changes in carbonates effect early diagenesis, types of pores, cementation and dissolution patterns. As a result, in carbonates, relative changes in sea level significantly impact the lithology, porosity, diagenesis, bed and bounding surfaces which are all factors that control fracture patterns. This study explores these relationships by integrating stratigraphy with fracture analysis and petrophysical properties. A special focus is given to the relationship between mechanical boundaries and sequence stratigraphic boundaries in three different settings: 1) Mississippian strata in Sheep Mountain Anticline, Wyoming, 2) Mississippian limestones in St. Louis, Missouri, and 3) Pennsylvanian limestones intermixed with clastics in the Paradox Basin, Utah.

The analysis of these sections demonstrate that a fracture hierarchy exists in relation to the sequence stratigraphic hierarchy. The majority of fractures (80%) terminate at genetic unit boundaries or the internal flooding surface that separates the transgressive from regressive hemicycle. Fractures (20%) that do not terminate at genetic

unit boundaries or their internal flooding surface terminate at lower order sequence stratigraphic boundaries or their internal flooding surfaces. Secondly, the fracture spacing relates well to bed thickness in mechanical units no greater than 0.5m in thickness but with increasing bed thickness a scatter from the linear trend is observed. In the Paradox Basin the influence of strain on fracture density is illustrated by two sections measured in different strain regimes. The folded strata at Raplee Anticline has higher fracture densities than the flat-lying beds at the Honaker Trail. Cemented low porosity rocks in the Paradox Basin do not show a correlation between fracture pattern and porosity. However velocity and rock stiffness moduli's display a slight correlation to fracture spacing. Furthermore, bed thickness is found to be only one factor in determining fracture density but with increasing strain, internal bedforms and rock petrophysical heterogeneities influence fracture density patterns.

This study illustrates how integrating sedimentologic and sequence stratigraphic interpretations with data on structural kinematics can lead to refined predictive understanding of fracture attributes.

To my loving parents

Mohamed Ali Al-Kharusi and Rahima Hafidh Al-Busaidi

For all your love, understanding, support and patience

To my dear grandparents

Ali Said Al-Kharusi and Suda Mohamed Al-Shaqsi

For instilling in all your children and grandchildren the most important values in life,

Honor, Respect, Education and Kindness

To my wonderful husband Nasser Salim Al-Rashdi

For giving me all the treasures in the world;

Happiness, Faith and Love

You're simply the Best!

To my sweet daughter Anais-Inas

May God bless you always in life, and may you grow up to be humble, strong,

honorable and loving

Finally to my grandmother

Azza Salum Al-Riyami

Thank you for making me your princess

You are and forever will be my Angel

Acknowledgements:

There are many people that I need to do justice by for all that they have done to enable me to accomplish what I have:

To Allah my God, thank you for making this possible and for all the blessings that you have enriched my life with.

To our Sultan, His Majesty Sultan Qaboos bin Said Al-Said, for without his development of the country and enforcement of education I may be today building a campfire in the desert!

To my family (and coming from the Middle East that is no small thing). Yet a special mention to the following; my parents Mohamed and Rahima (you sacrificed a lot for me and I hope I get the chance to give you back one day), my grandfather Ali, and my two grandmothers Suda and Azza (I'll never forget). To my brother Faysal (will always remember your magic in my life), and my other brothers; Al-Mu'uthar, Al-Salt and Hafidh (thanks for all the times you all protected me). To my sisters; Ijlaal and Souda (thank you for making me beautiful inside and out). To my aunties Asiah, Soad and Shadia Al-Kharusi (funny how the women in our family are more stronger and influential then the men!). To my special cousin Sattam (you're my brother, you always took care of me and wished the best for me). To Lubna Kharusi (for all your honesty, integrity, wisdom and faith). To Nasra, Shadia and Ghaniya Al-Rashdy (I couldn't have made it this far without your kind words!).

To two very special people in my life; my husband Nasser; thank you for all the love and patience you have given me. Thank you for not letting me take the easy road out and encouraging me to just go do it, but most of all thank you for all the times that I hurt

you and you made it better. I have discovered the mystery of happiness with you. And to my sweet daughter Anais-Inas, for being a sweet baby and letting mommy leave you to go make something of her life, you're my miracle from God. I love you baby girl.

To my supervisor Gregor Eberli, you are an inspiration! I owe you a debt and I was such a lucky girl to get you as my supervisor; you are part of my family now. To Mara Diaz, Chris Harrison, Peter and Greta Swart, Tim and Jackie Dixon, Larry Peterson, Gene Rankey, Karen Neher, Amal Al-Said, Alan Buck and Terri Vilamore; What can I say except RSMAS would have not been what it was if not for all of you!!!

To Volker Vahrenkamp, the man who started it all, it was an honor and a pleasure.

To my friends from Miami, Gregor Baechle, Brigitte Vlaswinkel, Bill and Barbie Anderson, Ben Dow, Miriam Andres, Kelly Bergman, Ralf Weger, Kelley Steffan, Guido Bracco Gartner, Carlos Alvarez and many more, you were my support group, my advisors and my playmates. Thank you for sharing with me the good, the bad and the ugly!

To my wonderful friend from Oman, Sheikh Khalfan Al-Esri, all I can say is thank you. You know the rest.

To "Petroleum Development of Oman", for making this Ph.D. a reality and to "Occidental Oil and Gas" for enabling me to complete it.

TABLE OF CONTENTS

LIST OF FIGURES

LIST OF TABLES

Chapter 1: Introduction

Shallow water carbonates are commonly deposited in depositional cycles that stack to form larger stratigraphic units. The stacking of these cycles or genetic units as they will be called in this document appears to be hierarchical on different orders. Rock mechanical studies reveal that fractures are also hierarchical in the sense that they affect beds, sets of beds and composites of beds. The structural setting combined with a variety of other factors control the fracture density and length. For example, bed thickness is an important factor for fracture attributes (Gross, 1995). Thus although attributes of the strata have been implicitly incorporated into fracture models, the relation between high resolution sequence stratigraphy and fractures is unknown. The working hypothesis of this study is to test if a correlation exists between stratigraphic boundaries and mechanical boundaries (Fig.1). The main criterion for the stated hypothesis is based on the knowledge that the mechanical properties of a rock are generated by the combined effects of facies and diagenesis. Furthermore, Underwood et al. (2003) stressed the impact of stratigraphy on fracture patterns, by demonstrating how organic partitionings and mud horizons at bed bounding surfaces acted as mechanical boundaries to fracture propagation.

If this hypothesis is found to be correct, then the significance of the study would be to link high resolution sequence stratigraphy and mechanical stratigraphy, which will produce a better understanding of the fracture behavior that is important in assessing reservoir behavior and the impact may enhance production levels, due to better modeling of different flow rates within different mechanical units.

The goal is to incorporate the stratigraphic architecture and the vertical facies variation information to lead to a better understanding of the attributes which will affect fracture distribution and help to determine the various reservoir flow units and their connectivity within a stratigraphic sequence. In addition, incorporating the kinematics of the area will increase predictability of the various fracture attributes (length/spacing) within a mechanical unit. This study is a step forward to the evaluation of a reservoir and its flow units, because it will improve the understanding of the distribution of fractures as they can play a critical role in enhancing or reducing the permeability of a reservoir.

Hence, forming a link between high-resolution sequence stratigraphic boundaries and mechanical boundaries would bridge sequence stratigraphy and mechanical stratigraphy. This bridging of the two concepts is possible because high resolution sequence stratigraphy is a tool, which captures the attributes, such as facies and diagenesis, which have an impact on the mechanical behavior of the rock (i.e. its fracture characterization).

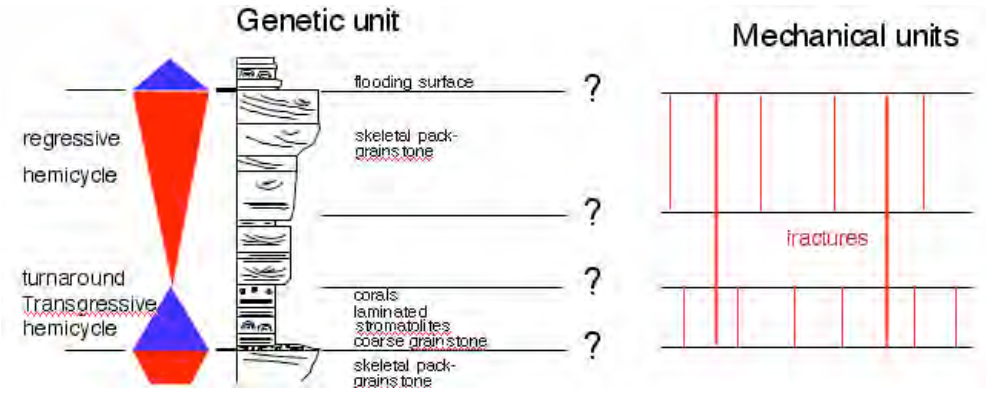

Figure 1.1: Diagram illustrating the working hypothesis of the study that says the genetic unit boundaries and the turnaround from transgressive to regressive hemicycles are also mechanical unit boundaries and, thus, a correlation exists between high-resolution sequence stratigraphy and mechanical stratigraphy.

Specific aims to test hypothesis

In order to test the hypothesis if high resolution sequence stratigraphic boundaries correlate to mechanical boundaries, several specific aims are addressed:

- Do genetic unit boundaries and their subdivisions act as mechanical boundaries to fracture propagation?
- Is there a fracture hierarchy which relates to the sequence stratigraphic hierarchy?
- What are the factors controlling fracture distribution in rocks?
- What are the major stratigraphic parameters controlling fracture length and spacing, besides stress and kinematics?
- Can dynamic modulus and other calculated moduli give a significant statistical correlation to fracture intensity?

These questions are examined by investigating fracture attributes (e.g. spacing, length), facies, stratigraphic subdivisions and physical properties in carbonates and mixed carbonate-siliciclastic successions in three areas.

Approach

The approach is documenting correlations between high-resolution sequence stratigraphic boundaries and their subdivisions and mechanical stratigraphic boundaries in carbonate strata. Study sites were selected where sequence stratigraphic analysis had been established by previous workers, in order to decrease any bias in the correlation and hence assess the influence of the stratigraphic control on the structural style and the fracture distribution. The mechanical units of the carbonate strata are defined by measuring the fracture spacing and lengths in the genetic units. Lithological descriptions, porosity and velocity determinations are the criteria for assessing the intrinsic rock

properties of the mechanical unit, whereas bed thickness and internal bedforms (laminations, cross bedding) are the extrinsic properties evaluated.

Geologic Concepts

Sequence Stratigraphy & Genetic Unit

Interpretation of seismic cross sections led to the concept of sequence stratigraphy by Vail and his co-workers in 1977 that was defined by Haq et al. (1988) as: "Sequence stratigraphy is the branch of stratigraphy which subdivides the rock record using a succession of depositional sequences composed of genetically related strata as regional and interregional correlative units". Important assumptions of sequence stratigraphy are:

1. Chronostratigraphic significance of seismic reflections
2. Facies co-existence with genetically related strata
3. Facies partitioning within one sea level cycle

Sequence stratigraphy tracks the migration of facies by integrating time and relative sea level changes (Loucks and Sarg, 1993). The potential to predict facies within a chronostratigraphic constrained framework of unconformity bound depositional sequences is the greatest strength of sequence stratigraphy (Haq et al., 1987; Posamentier and Vail, 1988; Vail et al., 1977; Van Wagoner et al., 1990; Loucks and Sarg, 1993). The term sequence was originally defined by Mitchum et al. (1977) as: "A stratigraphic unit composed of a relatively conformable succession of genetically related strata bounded at its top and base by unconformities or their correlative conformities".

In this study, the concentration is on the smallest unit recognized in sequence stratigraphy. This unit is termed genetic unit and consists of a transgressive and regressive hemicycle (Homewood et al., 1992). A genetic unit is assumed to be deposited

during a high-frequency (orbital controlled) sea level change. Thus a genetic unit is synonymous to depositional cycles of 4th to 5th order (Goldhammer et al., 1994) or high frequency sequences used by the ExxonMobil group. A "genetic unit" starts with the initial flooding, where the stratigraphic deposits demonstrates a deepening, where the rate of relative sea level rise is greater than the rate of sedimentation. The turnaround point of the cycle occurs at the maximum flooding (i.e. the most transgressive – onshore deposits) and from there the deposits regress away from the shoreline, and the rate of sedimentation is greater than the rate of accommodation space created by relative changes in sea level. Each genetic unit is usually composed of several beds of different lithologies that reflect its position within one high frequency cycle of creation and filling of accommodation space.

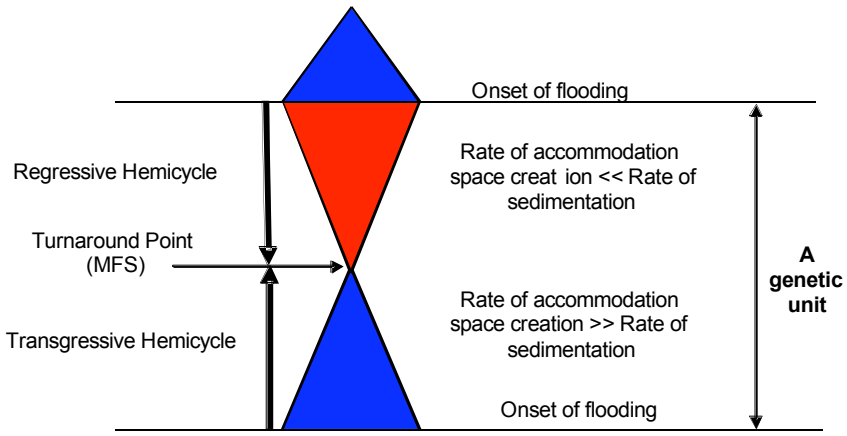

Figure 1.2: Diagram representing a genetic unit. It starts with the onset of flooding, where the stratigraphic deposits demonstrate a deepening, and the rate of relative sea level rise is greater than the rate of sedimentation. The turnaround point of the cycle occurs at the maximum flooding (i.e. the most transgressive – onshore deposits) and from there the deposits regress away from the shoreline, where the rate of sedimentation is greater than the rate of accommodation space created by relative changes in sea level.

The importance of considering these stratigraphic boundaries for this study is because these stratigraphic boundaries are considered to also behave as mechanical boundaries (i.e. boundaries which prevent fracture propagation), due to cementation during periods of non deposition or periods of exposure, dissolution and diagenetic changes that occur to the rock.

Mechanical Stratigraphy

The term "Mechanical Stratigraphy" is used to differentiate different types and intensities of deformation in different layers according to subtle changes in the rocks petrophysical and petrological properties (Nelson, 1985). Corbett et al. (1987) defined mechanical stratigraphy as layers with different fracture density of the same type of mode of fracturing (Fig. 1.3). Hence, a mechanical unit can consist of a single sedimentary bed or several sedimentary beds. Gross (1995) introduced that the concept of fracture partitioning, which refers to the difference in brittle failure mode from one layer to the next within a given rock column subjected to an applied remote stress." Fracture partitioning is the result of differences in failure mechanisms between layers of different lithologies, and is independent of the structural position or regional variation in the differential stress (Gross, 1995). As a result, the mechanical stratigraphy of a rock sequence may consist of un-fractured layers, layers characterized by faults, or layers which predominantly contain opening mode 1 joints (Gross, 1995).

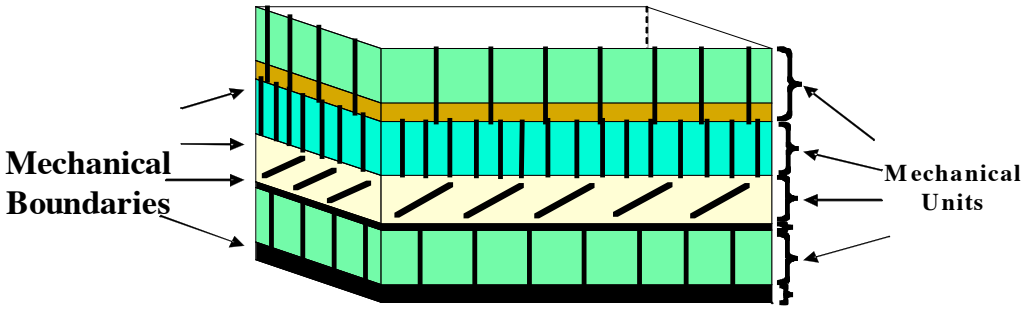

Figure 1.3: Diagram representing the concept of mechanical stratigraphy, and mechanical layers caused by variations in fracture density to different mode types of fracturing.

Relative fracture intensity is one of the basis for partitioning layers into mechanical stratigraphy, and the mechanical layer boundaries are related to the vertical persistence of the fractures: for each boundary, they quantify how many joints terminate versus how many traverse the boundary. This definition is used in this study. If a minimum of 75% of fractures terminate at the boundary it is considered to be a significant mechanical boundary. For comparison Underwood et al. (2003) labeled their minimum cut off at 50%.

Fractures

Fractures are defined as mechanical discontinuities or breaks in rocks with or without displacement (Lacazette, 2000). They are formed by strains that occur from stress concentrations around flaws, heterogeneities, and physical discontinuities within the rock fabric (Rock Fractures & Fluid Flow, 1996).

Fracture formations are controlled by several factors, such as the overall tectonic setting, the geodynamic evolution, and the stress strain conditions. In addition in a similar

tectonic regime, rocks fracture differently due to differences in lithology, mineralogy, bed thickness and porosity. For instance, in siliciclastic strata, shale layers act as mechanical boundaries to fracture propagation, because shales deform ductilely and not brittlely (Gross, 1995). Fractures will utilize microscopic flaws and grow from there (Cooke and Underwood, 2001). These flaws can be discontinuities such as cements present within the rock, or moldic pore spaces. All these factors affect the brittleness of the rock and will determine when and where the rock will fail. The bed thickness plays a dominant role in determining fracture spacing (Price, 1996, Huang and Angelier, 1989, Wu and Pollard, 1995, Gross et al., 1995, and Narr and Suppe, 1991). The bed bounding surfaces can affect to where a fracture will propagate or terminate (Cooke and Underwood 2001).

The various controls mentioned above affect different fracture types to varying degrees. Fracture types can be subdivided according to their size, and the integration between the fracture scales and the major controls on them is displayed in a simple diagram below:

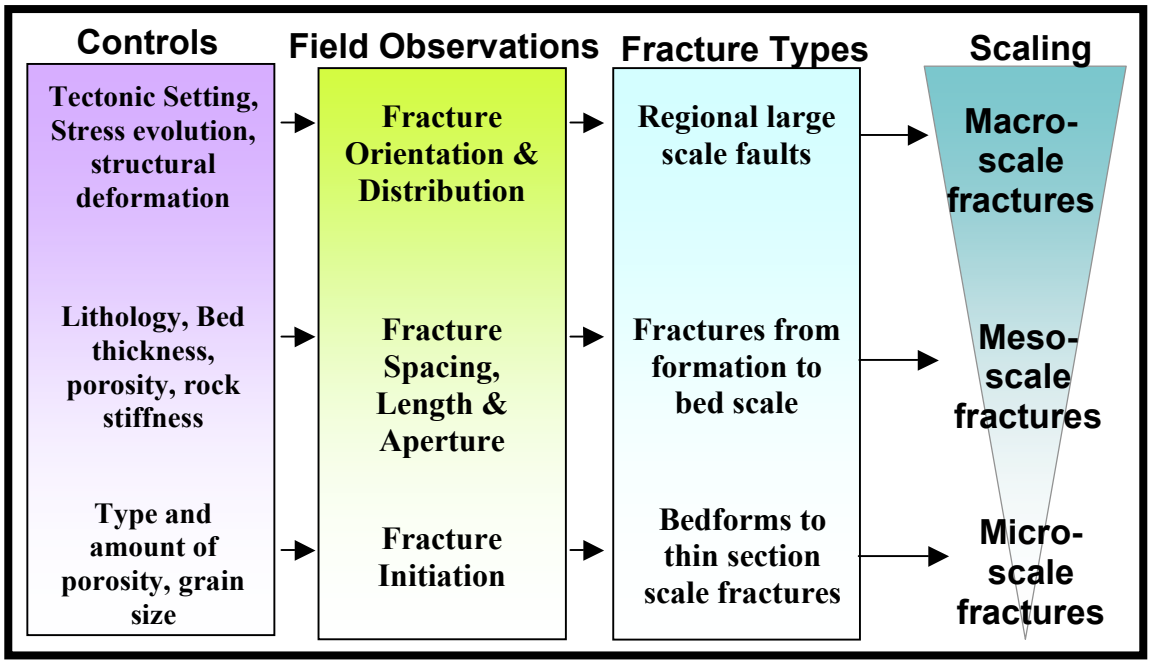

This study concentrates on describing meso-scaled fractures (i.e. fractures which their scale ranges from centimeter to several meters in length) and their controls empirically versus a first principle mechanistic approach. Many efforts at observing and documenting extrinsic (stresses, mechanical layer thickness) and intrinsic (lithology, porosity) in order to predict fracture patterns have focused only on one parameter at a time (Hanks et al., 1997, Gross et al., 1995, Hugman and Friedman, 1979 and Hatzor and Palchik, 1997). A brief summary of these various controls and their significance in the role they play in controlling fracture properties (length, spacing) is presented here.

1. Kinematics of Area:

A major parameter that controls fracture intensity and mode of fracturing at a particular area is the kinematics of that area. Lorenz et al. (1997) defines regional fractures as fractures, which are generally attributed to combination of factors such as basin maturation, basin subsidence or uplift. These factors are commonly influenced by far field stresses or distant tectonic events. These regional fractures are extensive, generally orientated normal to bedding and form parallel or sub-parallel to the regional maximum horizontal compressive stresses (Lorenz et al., 1997).

2. Lithology & Diagenesis:

Although structure and tectonics create the stresses which initiate fracturing within rocks, lithology still remains the primary control on the fracture susceptibility (Lorenz et al., 1997). At higher stress conditions, however, the stresses will override the lithologic control and become the dominant factor.

Lithology and diagenesis include a broad spectrum of variables that can affect fracture behavior. Mineralogy affects the stiffness of the rock. For example, anhydrite is much stiffer than dolomite and dolomite is stiffer than calcite (Yale and Jamieson, 1994). Grain size and grain size distribution are known to influence rock strength and fracture initiation (Hugman and Friedman, 1979 and Hatzor and Palchik, 1997).

Hanks et al. (1997) also found that in the Mississippian Lisburne Formation carbonates, lithology was the primary control on fracture density. Where grainstones were less densely fractured than dolomitic mudstones, and that the density of fractures in fracture sets increases with increasing carbonate mud content. However, they suggested that the local structural setting plays an even greater role in the overall character of the fractures as well as their density. Fabbri et al. (2001), documented similar lithological controls within interbedded sandstones and mudstones, where the jointing was confined to the sandstone units and the mudstones did not fracture at all.

3. Porosity:

The strength of the rock is in a large part due to porosity, where more porous rocks were much weaker than non-porous rocks (Corbett et al., 1987). Fracture initiation is not only due to maximum tension, because fractures also initiate at local concentrations of tensile stress around flaws (heterogeneities), (Cooke and Underwood, 2001). In beds where the flaws are evenly distributed, fracture initiation is then based solely on where tensile stresses are the greatest (Gross, 1993; Gross et al., 1995; Cooke and Underwood, 2001). Therefore, larger flaws will produce larger stress concentrations, and hence the location of fracture initiation will depend on the distribution of the largest flaws. The stress for crack initiation is dependent on the initial length of the flaw (Hatzor and Palchik, 1997).

In low porosity rocks, the critical flaw length (length at which fracturing occurs) was related to the mean grain size, but in high porosity rocks, the fracture initiation was more dependent on the porosity, and the grain size effect was insignificant. In contrast other studies such as (Hugman and Friedman, 1979), demonstrated that the influence of grain size on the rock strength was inversely proportional in carbonate rocks such as limestones and dolomites, but Hatzor and Palchik (1997) demonstrated that in carbonate rocks grain size and arrangement can vary dramatically.

4. Mechanical Layer Thickness:

In mechanical stratigraphy, Gross 1993, defines a "mechanical layer" as "a unit of rock that behaves homogeneously in response to an applied stress". A mechanical layer may consist of one or more sedimentary beds. A mechanical layer thickness is the thickness of a mechanical unit, which has deformed in a manner different to the unit below or above it (Gross et al., 1995). Therefore a mechanical layer thickness may range anywhere from 2 mm to 5 m. Another factor to take into account when measuring the thickness of a mechanical layer is that it is always not laterally continuous. This lateral variability will affect the fracture lengths and, to some degree, the fracture spacing. When observing fracture spacing in relation to bed thickness. Gross et al. (1995) suggested that mechanical layer stiffness influences the joint spacing, because stiffer layers have wider stress shadows since the width of a stress shadow is dependent on the elastic modulus of a layer. Consequently, stiffer beds (i.e. beds with higher elastic moduli) are more closely fractured, because when layers of different moduli are subjected to a uniform stress, the stiffer beds fracture at lower strains than the softer beds (Gross et. al., 1995). Yet, with

continued stress, infilling fractures occur within the stiffer beds and that causes them to have more closely spaced joints.

Hanks et al (1997) found that, although fracture spacing can be approximated by using bed thickness, this approximation does not hold up when stresses that form the fractures are the controlling factor.

5. Bed Bounding Surfaces:

Previous field investigations have concentrated on fracture termination in strata consisting of interbedded brittle and ductile rocks (Cooke and Underwood, 2001, Dyer, 1988; Baer, 1991; Helgeson and Aydin, 1991; Narr and Suppe, 1991; Gross, 1993; Underwood, 1999). These studies demonstrate that fractures initiate within stiffer units (e.g. limestone or dolomite) and terminate at the contact of more ductile units (e.g. shales and marls) (Cooke and Underwood, 2001). The importance of weak bedding contacts on fracture termination is documented in a series of studies (Dyer, 1988; Baer, 1991; Helgeson and Aydin, 1991; Narr and Suppe, 1991; Gross, 1993; Underwood, 1999; Cooke and Underwood, 2001).

Baer (1991) documented that some dike segments terminated at bedding planes within dolomite, rather than propagating to shale contacts and terminating at the brittle-ductile transition between the dolomites and shale. He attributed these terminations to bedding-plane slip along the bed contacts. Another study of interbedded dolostone-chert and mudstone/shale, observed fracture terminations at boundaries with mudstone layers (Narr and Suppe; 1991). Some fractures terminated at mechanical layer boundaries with slickensides, which were indicative of interlayer slip. Underwood (1999) documented

that, within dolostone rocks, fractures tended to terminate at both thin mud layers and at weak interfaces (e.g. thin organic partings and shallowing-upward cycle boundaries).

Cooke and Underwood (2001) demonstrated that an interface with a low tensile strength would fail by de-bonding and subsequently open in the presence of the fracture tip stress field. It is then postulated that, when the fracture intersects the open interface, the stress singularity at the fracture tip is lost and the fracture will not propagate across that open interface (Cooke and Underwood, 2001). Moreover, a fracture will also terminate against a sliding interface since the shear stress at the interface had exceeded its own shear strength and the fracture tip becomes dull (Cooke and Underwood, 2001). These observations are consistent with the results of Teufel and Clark (1984), who discovered that higher interface-normal compressive stresses are required for fractures to propagate across interfaces with little to no friction. Renshaw and Pollard (1995) concluded that once slip occurs along the interface then the tensile stresses are no longer being transmitted across that interface and fracture growth is hence barred. In many cases the fracture which crosses over an interface does develop not just ahead of the initial fracture, but it can step to either side, forming a step-over fracture (Renshaw and Pollard, 1995).

Cooke and Underwood (2001) state that "fractures would generally propagate thorough bedding contacts that are strongly welded or well cemented" and that these surfaces may be approximated by bonded interfaces. Fractures approaching moderate-strength contacts will terminate at the contact if the stresses are insufficient to initiate new fractures or step-over to either side of the initial fracture, or produce a step over fracture (Cooke and Underwood, 2001).

In this study we determine if the mechanical boundaries to fracture propagation are high resolution sequence stratigraphic surfaces. If so, then it would lead to an understanding to the reasons why sequence stratigraphy is correlateable to mechanical stratigraphy.

Study Areas

Three areas with different sequence stratigraphic, diagenetic and tectonic settings were selected to test the hypothesis. All areas had easy access to the outcrop, the sequence stratigraphic units had been previously defined and it was possible to perform mechanical stratigraphy analysis.

Sheep Mountain Anticline, Wyoming

The first study area is at Sheep Mountain Anticline near Greybull, Wyoming. It is an asymmetric, doubly plunging anticline, from a blind thrust fault (Hennier and Spang, 1983). In the core of the anticline the Madison Formation is exposed and composed of six 3rd order sequences and one second order super-sequence. The genetic units defined at Sheep Mountain Anticline are 5th order cycles, which consist of regressive interbedded calcitic grainstones and transgressive dolomitic mudstone beds.

The Sheep Mountain Anticline, located in the northern Bighorn Basin of Wyoming (Fig. 1.4), and is a simple doubly plunging asymmetric anticlinal structure on the east limb of the Bighorn Basin (Hennier & Spang, 1983; Sonnenfeld, 1996).

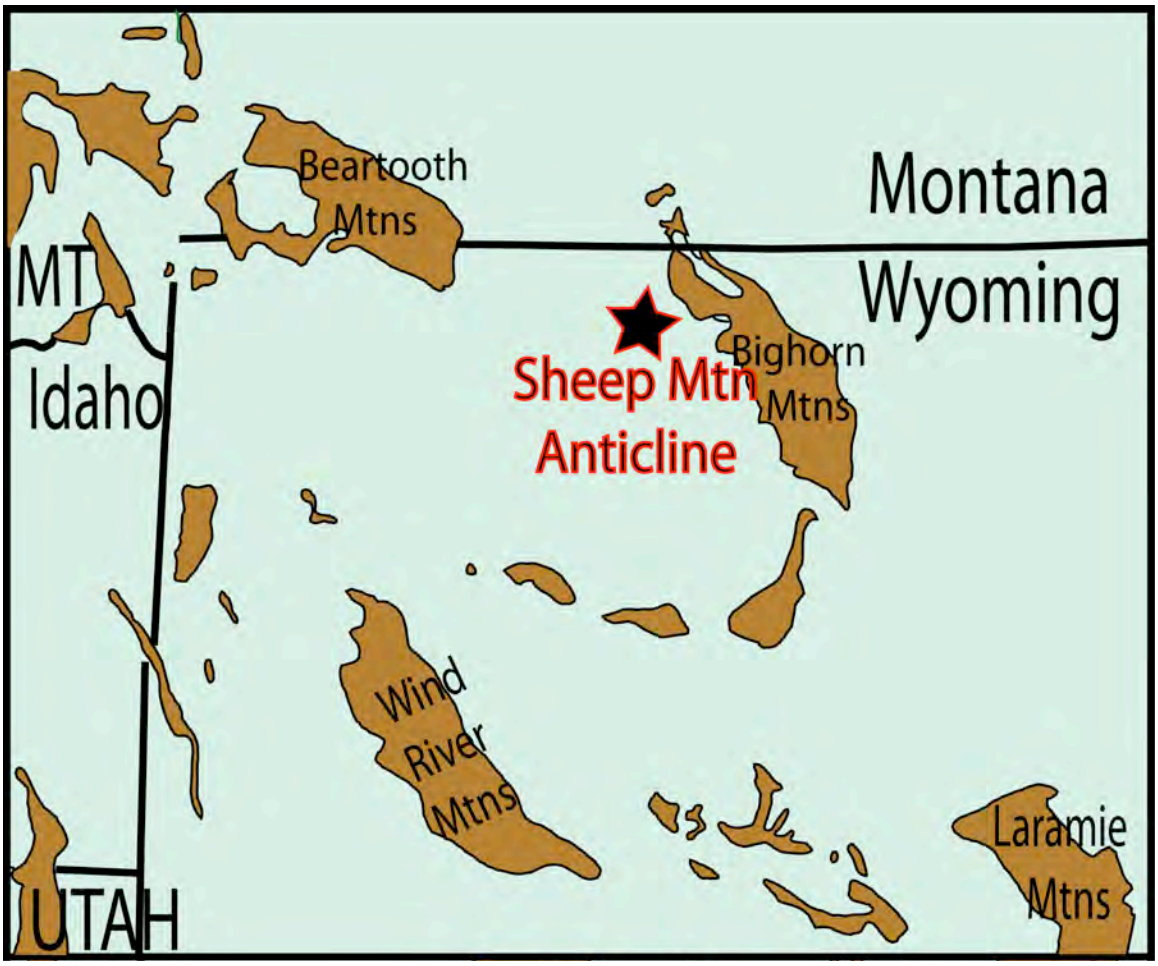

Figure 1.4: Location map of Sheep Mountain Anticline, in Wyoming. Area of study off of Greybull. Modified from Sonnenfeld, 1996.

The Sheep Mountain anticline and other associated folds in the Bighorn Basin are Laramide compressional structures and the anticline trends northwest-southeast, which is subparrallel to the orientation of the Bighorn Mountain Uplift (Fig. 1.5); (Hennier & Spang, 1983). Sheep Mountain formed as a basement-cored, doubly plunging asymmetric fold, whereby the steep northeastern limb dips between 40 and 90 degrees northeast (Bellahsen et al., 2006). The shape of the anticline is inconsistent along the fold axis, whereby it plunges 20 degrees to the northwest and about 10 degrees to the southwest (Bellahsen et al., 2006).

The strata within the anticline are the Madison Formation that is Mississippian in age. It consists of 6 sequences of shallow-water carbonates (Sonnenfeld, 1996; Smith et al, 2004).

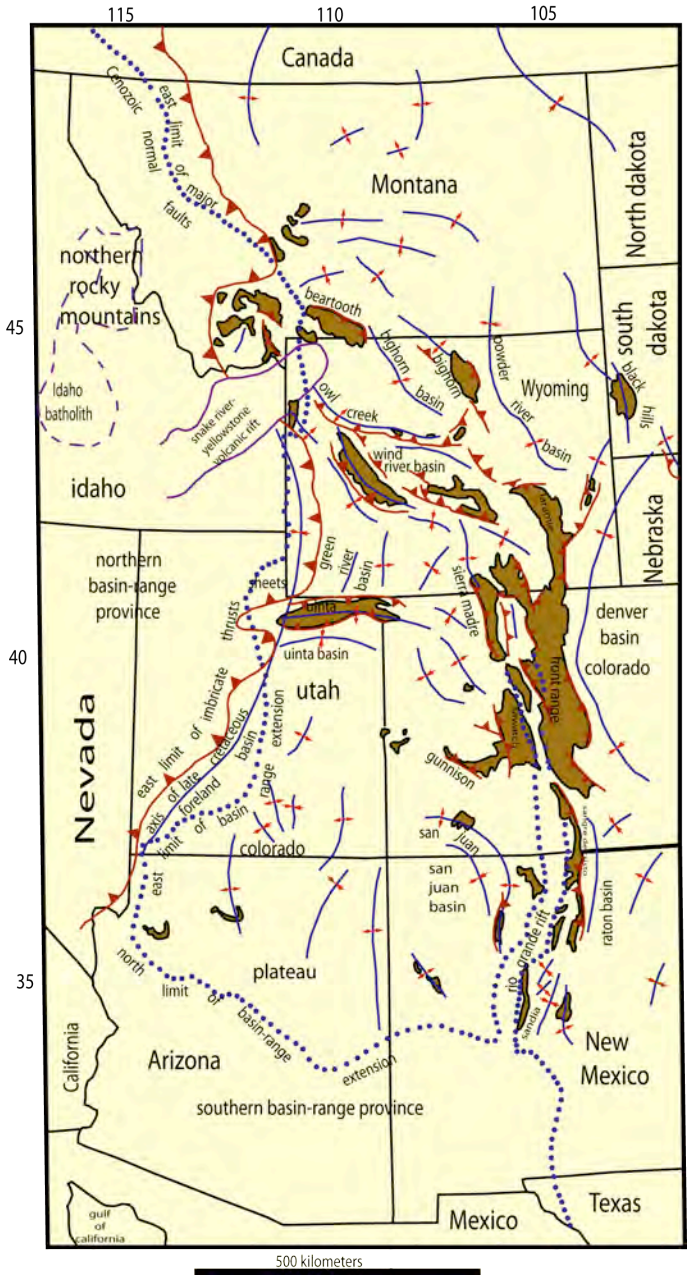

Figure 1.5: Major structures associated with Laramide tectonics, and basement cored uplifts. Sheep Mountain Anticline is one of many anticlines trending NE-SW. (Taken from Smith & Eberli, 2000).

Sequence Stratigraphy:

The Lower Mississippian Madison Formation at Sheep Mountain Anticline is composed of a hierarchy of six sequences (Fig. 1.6; Sonnenfeld, 1996 and Smith & Eberli, 2000). The higher order sequences and the genetic units stack into 6 major 3rd order sequences, which themselves stack up into two major long term composite sequences of 2nd order.

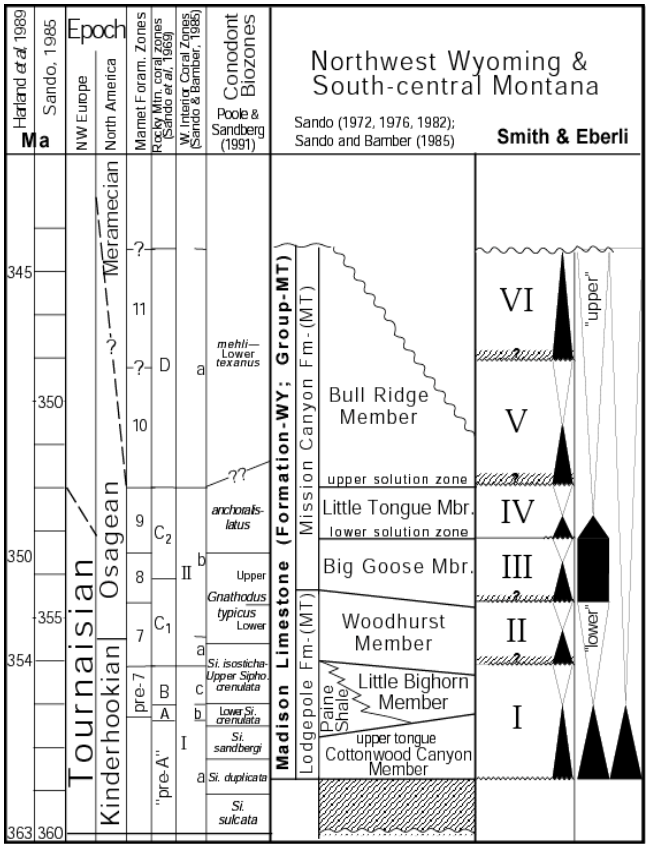

Figure 1.6: Sequence stratigraphy, biostratigraphy and formation names of the Madison Formation (Taken from Smith & Eberli, 2000 and Sonnenfeld, 1996).

Sonnenfeld (1996) and Cooke (2000) were the first to correlate mechanical units to stratigraphic units in Sheep Mountain Anticline. Sonnenfeld found that generally the

sequence stratigraphy may highlight fracture styles and that not all stratigraphic bedding or cycle boundaries are mechanical breaks (Fig. 1.7).

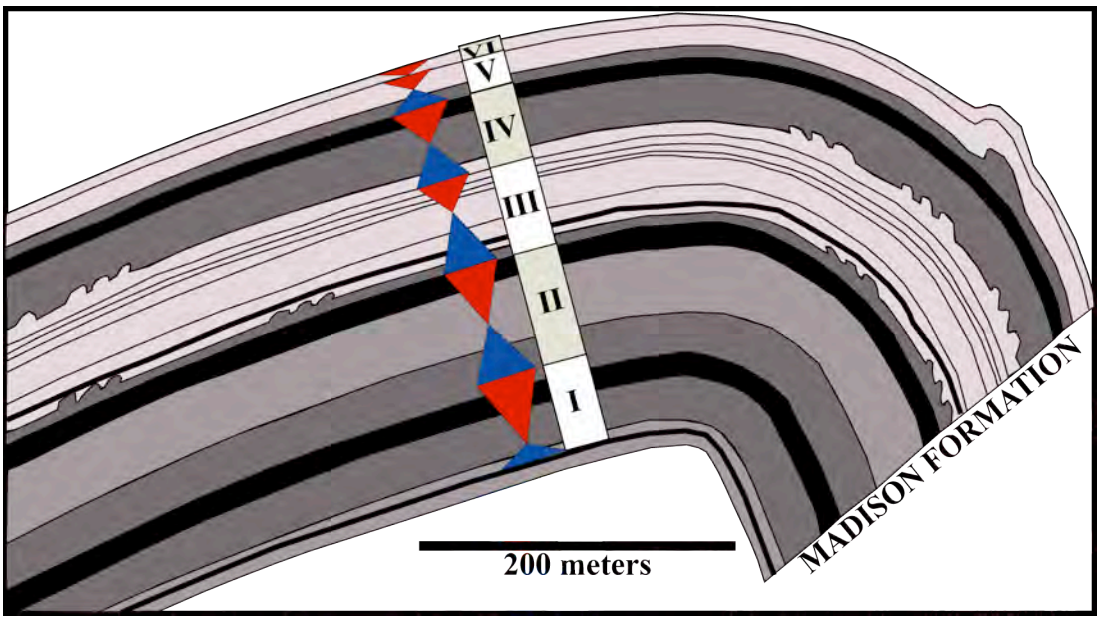

Figure 1.7: Sonnenfeld (1996) depiction of the mechanical stratigraphy of the Madison formation at Sheep Mountain Anticline.

In contrast to Sonnenfeld, this study concentrated on the relationship of the fractures to the depositional genetic units.

Illinois Basin at Missouri

The second area of study is the Middle Mississippian (Visean) carbonates of the St. Louis Basin, Missouri. The main formations considered in this area are the Warsaw and Salem formations which are predominantly limestones with shale's, for which Rankey (2003) described several type sections. In contrast to the Sheep Mountain Anticline, all the sections selected in this site in the mid-continent are flat lying beds with little regional

tectonism. This provides a good tectonic counterpart and will allow for the comparison of different stress and strain effects on fractures.

The measured sections are located along highway I-270, in the St. Louis and Jefferson counties, Missouri (Fig. 1.8). The stratigraphic interval is constrained to the Lower Carboniferous, Visean carbonates. Five sections are measured, from the Upper Warsaw and Salem Formations. The sequence stratigraphy and depositional analysis follows the work of Rankey (2003).

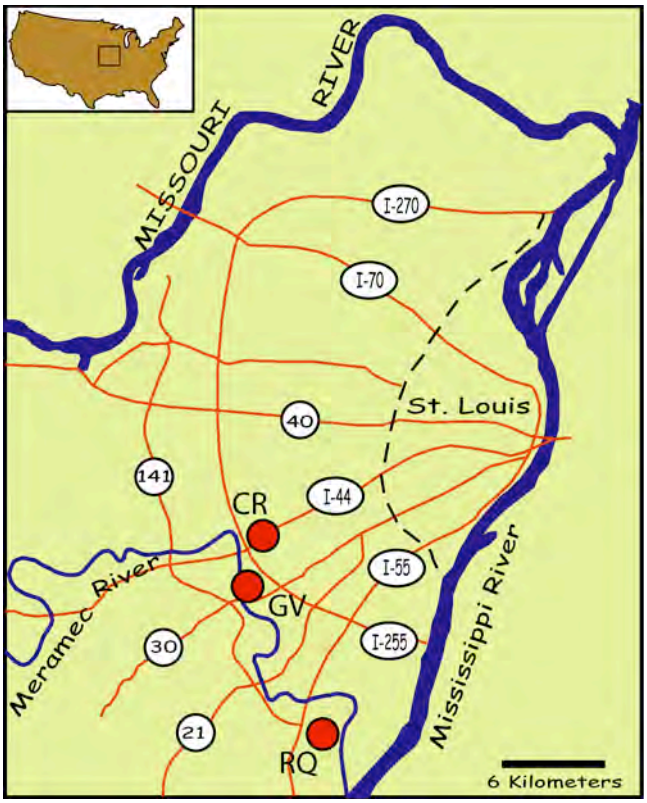

Figure 1.8: Location map showing of measured section. From Rankey 2003. The red lines indicate interstates, and the dotted line indicates St. Louis city outskirts. Sections are Cragwald Road (CR), Gravois Road (GV) and Cardinal Quarry (RQ).

The area of study is bounded to the east by the Illinois Basin. To the south-southeast the area is underlain by a complex rift system known as the "New Madrid Rift Complex". Late Proterozoic to early Cambrian extension created the "Reelfoot Rift", occurred as a 'failed' rift which extends northeastward from Arkansas and Tennessee into southern Illinois, with an eastern extension known as the "Rough Creek Graben" into western Kentucky and an inferred "St. Louis Arm" into Missouri, which crosses the Sparta Shelf and the northeastern flank of the Ozark Dome (Fig. 1.9); (Kolata & Nelson 1991).

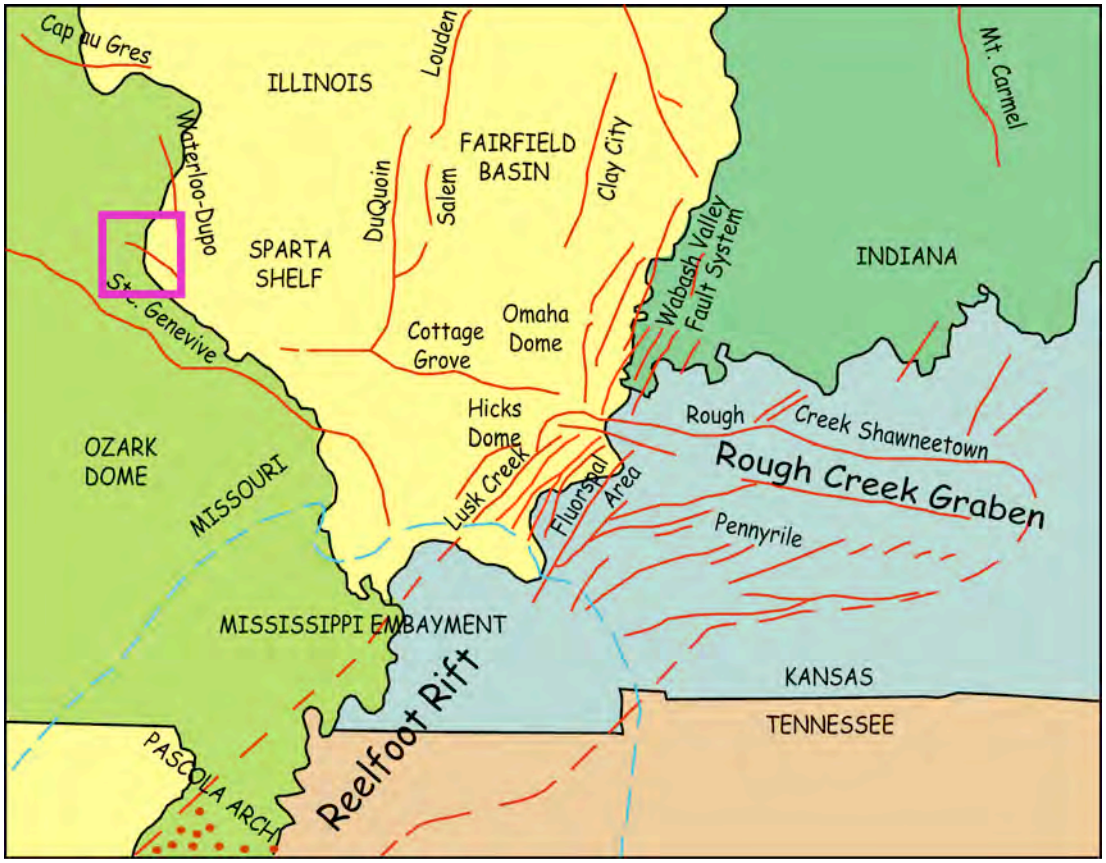

Figure 1.9: Tectonic overview setting showing the Reelfoot Rift, Rough Creek Graben, as well as normal faults present in the area of study, from Kolata & Nelson (1991). Red lines denote fault lines, and blue denotes extent of the Mississippi embayment. Area of study lies within purple box.

From Late Cambrian to Early Ordovician, thermal subsidence dominated within the New Madrid Rift Complex, and then the rates of subsidence decreased dramatically and remained relatively slow during the rest of the Paleozoic era. (Kolata & Nelson, 1991). Deformation occurred in the mid-continent with the Late Paleozoic Ouachita and Alleghenian orogenies, where most of the major anticlines and fault systems were formed or reactivated during this time. The St. Louis area is bounded to the east by the Waterloo Dupo Anticline and the Illinois basins, to the north by the Cap au Gres faulted flexure (a fractured monocline) and to the south by the St. Genevieve fault zone and the Ozark Dome (Kolata & Nelson, 1991).

Sequence Stratigraphy:

Depositionally, the Warsaw and Salem strata include heterogeneous grainstones both laterally and vertically, which contain both calcite cementation and dolomitization (Rankey, 2003). Facies range in environments from subwavebase, deeper marine to tidally influenced oolitic and crinoidal shoals to tidal flat. Rankey (2003) states that "facies group to form parasequences, generally manifest as cleaning-upward packstone-grainstone cycles, although considerable variation is present as a function of the sequence stratigraphic and paleogeographic setting." The Salem and Warsaw formations form the highstand sequence set of a composite sequence and include highly progradational facies belts (Fig. 1.10); (Rankey, 2003).

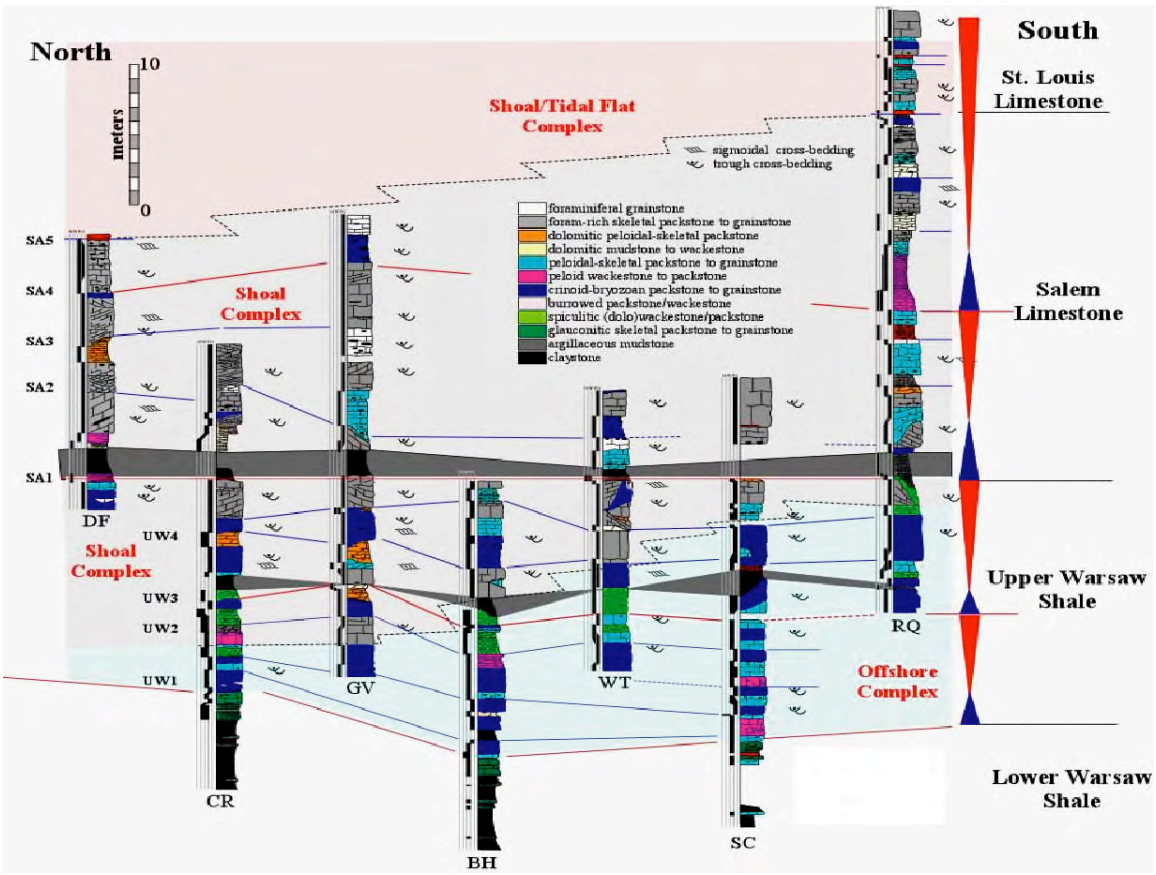

Figure 1.10: Stratigraphic framework of the Warsaw and Salem formations in St. Louis County, from Rankey (2003). Sections studied include Gravois Road Section (GV), Cragwald Road Section (CR) and Cardinal Quarry Section (RQ).

In this study measurements were done along road sections, which have been excavated by blasting. The measured fractures were not caused by blasting (no radial fracturing). Based on the fact that some contained cement infilling and were perpendicular to bedding, which is characteristic of mode 1 fractures, and hence assumed to be tectonically induced. Fracture length, spacing, and terminations were measured to define the mechanical stratigraphy. The continuous exposure allows description and collection of a statistically significant data set of attributes of mechanical properties.

Paradox Basin, Utah

The third area of study is in the Paradox Basin, which is a mixed carbonate siliciclastic system of Pennsylvanian age, and in particular, the Ismay and Desert Creek intervals of the Paradox Formation were extensively documented by previous workers in regards to facies, tectonics and sequence stratigraphic analysis (Goldhammer et al., 1991; Grammer et al., 2000; Baars and Stevenson, 1982 and Weber et al., 1995).

The Paradox Basin is an elongate, intracratonic basin that extends from northwestern New Mexico to east-central Utah and covers an area of approximately 27,000 km^2 (Fig.1.11). The mechanical analysis was preformed in two different tectonic settings, the folded strata at Raplee Anticline, and the flat lying beds along Honaker Trail.

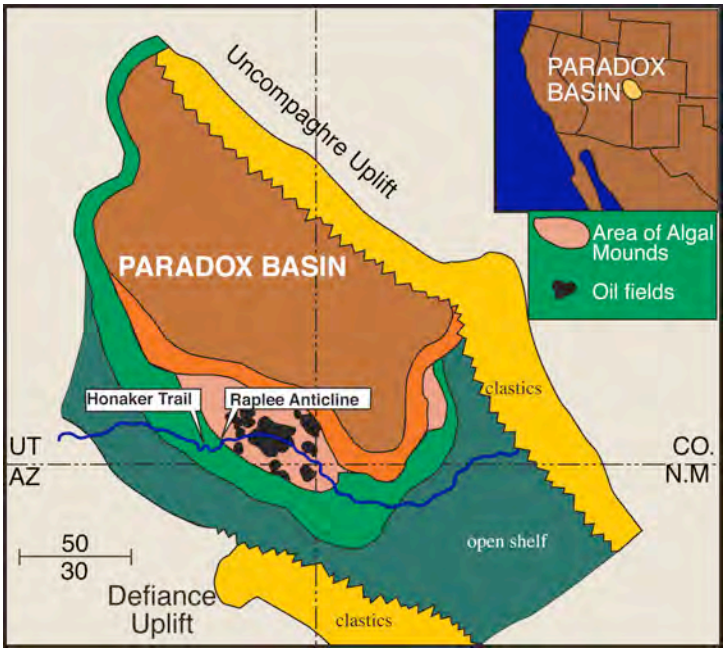

Figure 1.11: Regional map showing extent of Paradox Salt Basin taken from Eberli (2000). Area of study lies to the west of the Aneth oil field.

The Paradox Basin resides in the Colorado Plateau province. The tectonic fabric of the province was well established in Precambrian times and reactivated in Late Paleozoic. The Paradox Basin lies at the crossing area of two major lineaments; the Olympia Wichita lineament and the Colorado lineament (Stokes, 1988; Baars and Stevenson, 1982); (Fig. 1.12). Baars & Stevenson (1982) state these Precambrian lineaments were reactivated due to the compression of the Pennsylvanian Ancestral Rocky Mountains Orogeny creating uplift areas with topographic lows (i.e. Paradox Basin). Most of the structures observed today in the Paradox Basin are due to the west-east compressional forces of the Laramide Orogeny which caused the monoclines across reactivated high angle basement thrust faults, as well as uplift and erosion (White, 1995). Tectonic origin of the Paradox Basin is a controversial subject; Barbeau (2003) finds evidence for a foreland type basin, while Baars and Stevenson (1982) demonstrated it to be an extensional basin with strike slip motion.

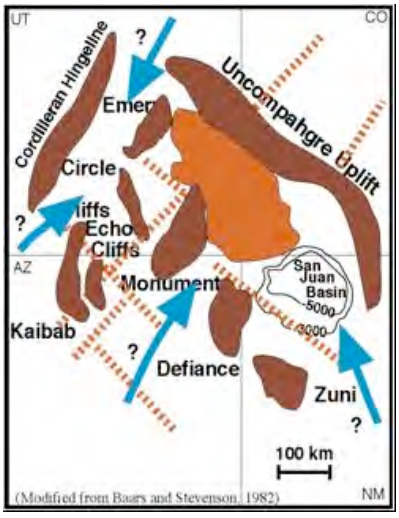

Figure 1.12: Regional tectonic map displaying areas of uplift and major basement lineaments. Arrows indicate water flow and projected clastic input. From Grammer et. al. (1996).

Sequence Stratigraphy:

The studied strata were deposited during the Pennsylvanian as a cyclic mixed carbonate-siliciclastic system (Weber et al., 1995; Sarg et al., 1999). The strata are from the Desert Creek and Ismay intervals which form the top of the shelfal equivalence of the paradox Formation.

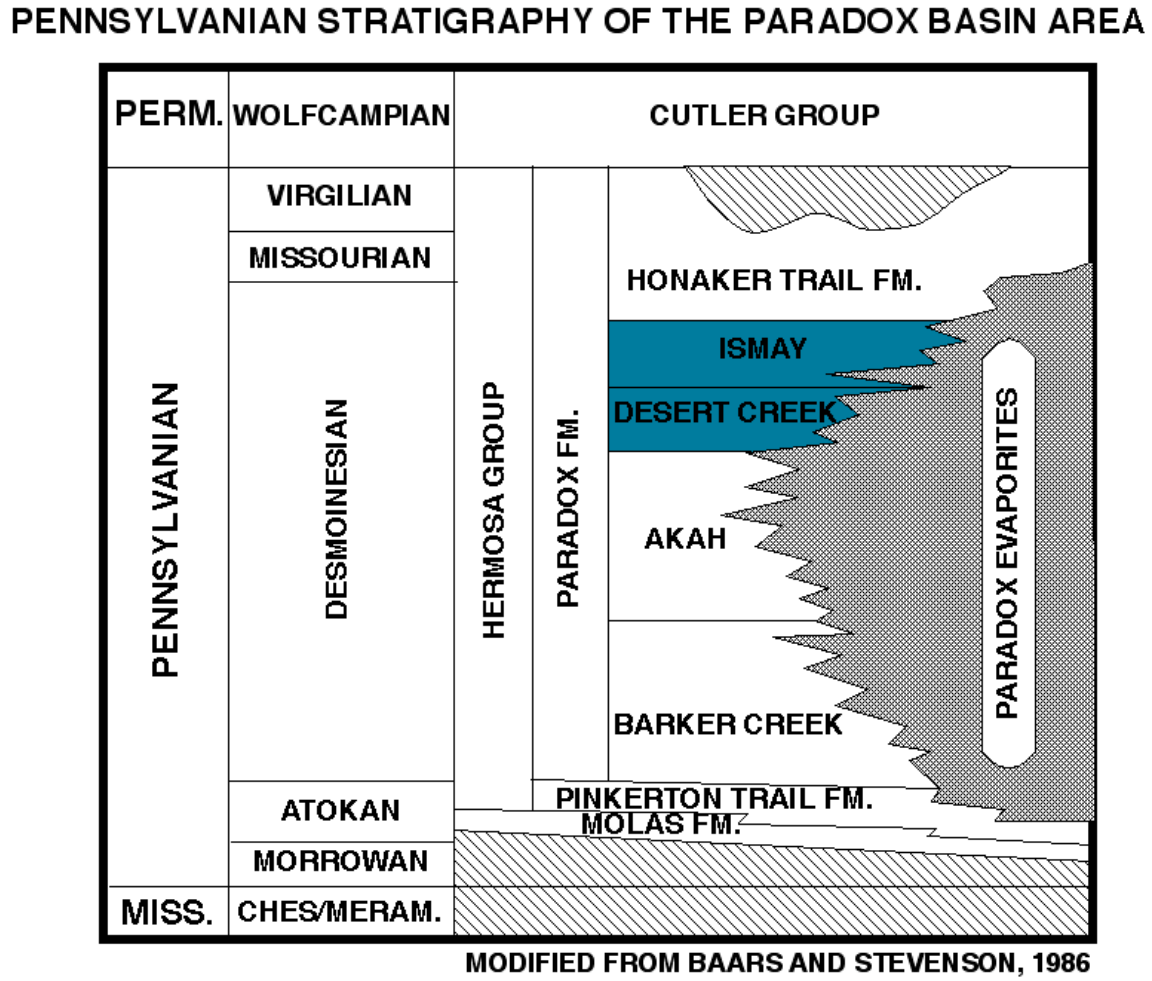

Figure 1.13: Pennsylvanian stratigraphy of the Paradox Basin. The Desmoinesian age of the studied Desert Creek and Ismay intervals are shown. Taken and modified from Goldhammer et al. (1991) and Baars and Stevenson (1982).

Both the Desert Creek and Ismay intervals are characterized by algal buildups and the strata shows three superimposed orders of cyclicity (Goldhammer et al., 1991). The

general exposure-bounded 4th order sequences of the Desert Creek and Lower Ismay are composed of higher frequency 5th order depositional cycles (Goldhammer et al., 1991).

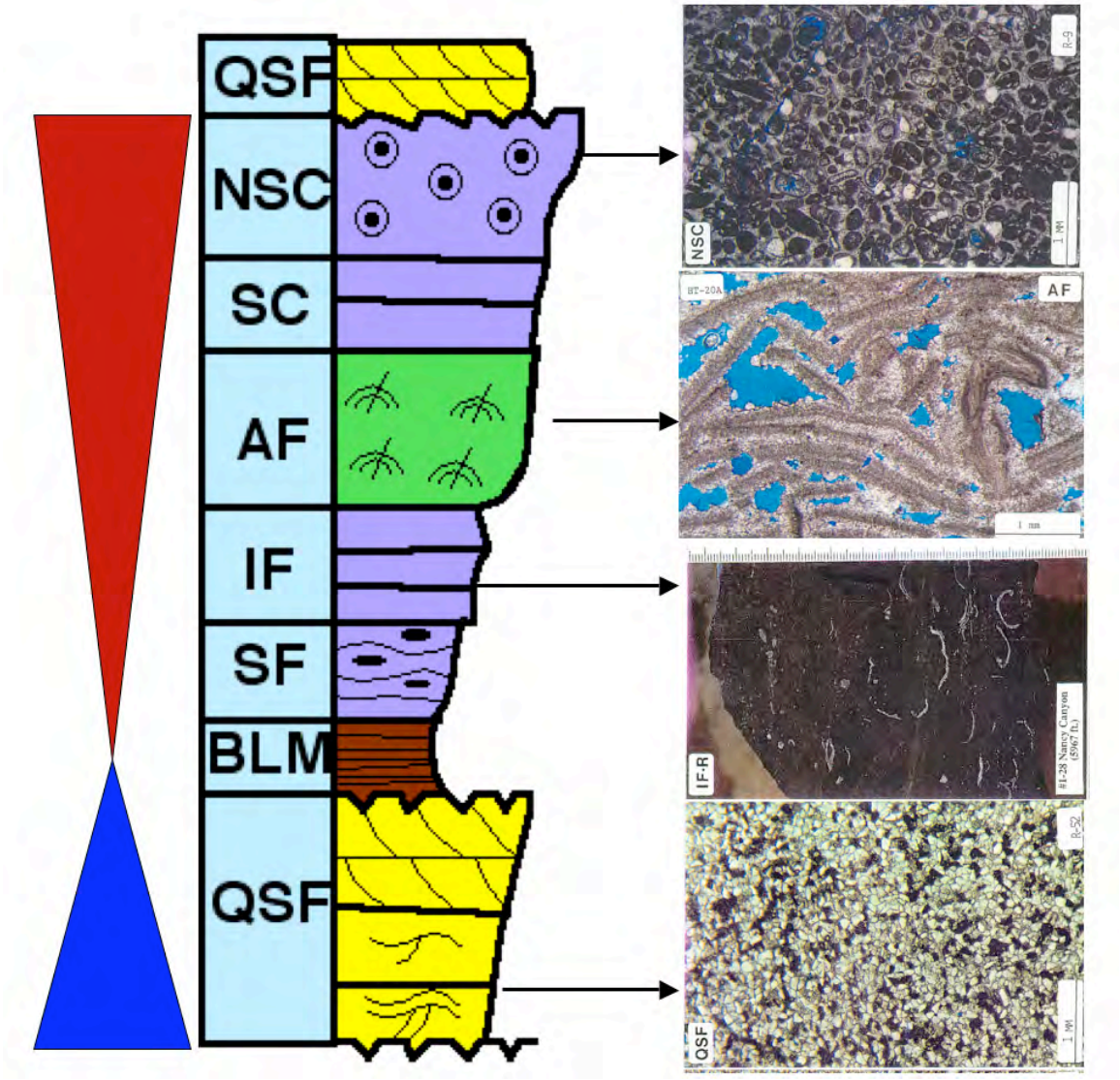

Figure 1.14: Schematic drawing of a typical high frequency depositional cycle of the Desert Creek and Lower Ismay intervals at the Paradox Basin. The average cycle is 6m thick and capped by a transgressive quartzitic sandstone as defined by Goldhammer et al. (1991).

An ideal cycle consists of 7 facies deposited during one high-frequency sea level change. During transgression eolian deposits are reworked and overlain by black laminated mudstone. The regressive hemicycle shelf carbonates were deposited and during times of

maximum water depth algal mounds developed on several locations that are capped by skeletal/nonskeletal grainstone (Fig.1.14); (Goldhammer et al., 1991; Grammer et al., 1996).

Chapter 2: Methodology

Areas of Study

The areas of study were selected for the following reasons: (1) To determine if in three different sequence stratigraphic, diagenetic and tectonic settings, the hypothesis works where the sequence stratigraphy relates to the mechanical stratigraphy (2) the areas were highly fractured; (3) it was possible to perform a mechanical stratigraphy analysis; (4) Sequence stratigraphic analysis in the areas have been previously defined; (5) different lithologic contents of genetic unit's limestone, limestone-dolomite interbeds, mixed carbonate siliciclastic settings.

Fieldwork

Stratigraphic Analysis

In each area, the sequence stratigraphy and the genetic units were known. The previously studied subdivisions were used largely in this study, with minor changes due to my own independent analysis. At each location, the genetic units were confirmed and understood based on lithological descriptions and identification of key sedimentary structures. The lithologies and sedimentary features interpretation was used to subdivide the facies into transgressive and regressive hemicycles, through understanding of depositional environments and relative sea level rise and fall. In the Paradox Basin area, samples were cored with a power drill in the field, and generally two samples (vertical and horizontal) were taken per stratigraphic bed whenever possible.

Mechanical Analysis

Fractures were measured using the scan density line method (Narr and Lerche, 1984, Wu and Pollard, 1995 and Enegelder et al, 1997). The scan density line method uses a traverse line parallel to bedding plane. The line is perpendicular to the average strike of the fracture set, generally along cross sections of the layer or along the layer's surface (Wu and Pollard, 1995). All fractures, which intercept that line are measured for length and spacing. The first fracture is the zero point, and from that fracture the spacing along the strike line is measured to the next fracture. At each fracture the length of that fracture is measured, and the termination levels are also recorded.

Wu and Pollard (1995) demonstrated potential errors that may be introduced when using the scan density line method for outcrop fracture characterization. They compared the area method, which measures fractures on the surface of the bed, to the scan density line method. The data revealed similar results in well-developed fracture patterns, but in poorly developed fracture patterns the scan-line method produced scattered results that differed from the area method by more than 50%. They attributed the differences to the selection of the positioning of the two end points of the line. The area method is superior to the scan-line method, and thus is the recommended method for measurement of fracture spacing. The area method, however, can only be applied when the top surface of the bed is present. Unfortunately, in the study areas, the top surface of the bed is rarely well exposed; leaving the scan-line method as the only one applicable method.

Keeping the limitations in mind, several measures are taken in our study to reduce the errors introduced by using the scan-line method. These are: (1) a longer scan-line than that mentioned by Wu and Pollard (1995) in their study, (2) a larger number of fracture

measurements per scan-line to decrease the data bias and (3) the endpoints of the scan-line are located at fractures. In this study we are mainly concerned with mode 1 opening fractures.

Table 2.1 below details the measured and observed mechanical properties, and gives a brief description of the various parameters that affect them.

Fracture Measurements	Definition, Description and Methodology
Fracture Types	Joints – Opening mode, no shear displacement (Mode 1) fractures, which also include veins and displacement perpendicular to the plane. Faults – Displacements with measurable shear offset.
Fracture Spacing	The perpendicular distance between fractures that is generally parallel or sub parallel to the bedding plane for joints (vertical open mode 1 fractures).
Fracture Length	Measured in the field using either a ruler or tape measure and placing it along the length of the fracture. The distance of fracture propagation is mostly influenced by the bed to bed contact which may inhibit or enhance the fracture from propagating. It may also cause fracture "step over" propagation as described by Cooke and Underwood (2001).
Abutting/ Crosscutting Relationships	This method is applicable to areas where it is possible to attain the top surface view of a bed. The top surface enables the determination of one or more than one generation of fractures. Orientations of the different fracture sets are measured. If one fracture set commonly terminates, or steps-over another set, then this indicates that it is a later, secondary generation of fractures.
Sketches & Photos	Field sketches and photographs were taken of each section, to visually demonstrate the different mechanical units and to gain a broader prospective of fracture hierarchy within the sequences.

Table 2.1: Brief description of different types of fracture properties and methods of measurements.

Laboratory Analyses

Grain Density and Porosity:

Grain density and porosity were determined using the Comparative Sedimentology Laboratory's "Helium Picnometer". The Helium Picnometer reads out the grain volume and grain density of the core plug. The total volume is calculated using a digital caliper by measuring the diameter and height of the plug. Several measurements are done and the average is taken to reduce inaccuracies. From subtracting the total volume by the grain volume, we determine the pore volume, and from that the porosity and bulk density are calculated.

Velocity:

Velocity measurements are performed to observe if different mechanical units differ strongly in their various dynamic moduli. Previous works by Yale and Jamieson (1994), demonstrated a correlation between static and dynamic moduli. Measurements were carried out at the Comparative Sedimentology Laboratory.

Statistical Analysis & Calculations

A number of statistical analyses were carried out to observe relationships mainly between fracture spacing and other factors. These are listed below.

Fracture Density/Intensity:

The fracture density is defined as "the average number of fractures intersected per linear meter" Corbett et al. (1987).

Fracture Spacing Ratio:

Fracture spacing ratio (FSR) is defined by Gross (1993) by the ratio of the mean bed thickness and the median joint spacing. Hence to determine the fracture spacing the data was sorted from lowest to highest, and take the median value and divide it by the average thickness of the mechanical bed.

Dynamic Moduli:

Dynamic moduli are derived from measurements of Vp, Vs and grain density. Through the following equations, the various rock moduli are determined:

- Bulk Modulus (K) = $\lambda + [(1/3) * 2\mu]$
- Young's Modulus (E) = $(9\ K\lambda)/ (3K + \mu)$
- Poisson's Ratio (σ) = $\lambda / [2*(\lambda + \mu)]$

Where (ρ) is the bulk density and λ and μ are Lame's constants and are calculated from:

$Vp = \sqrt{(\lambda + 2\mu)/\rho}$ where; $\lambda = (Vp^2 * \rho) - 2\mu$

$Vs = \sqrt{(\mu/ \rho)}$ where; $\mu = Vs^2 * \rho$

Rigidity Ratio:

The Rigidity Ratio is the ratio of the "softer" shear modulus divided by the "stiffer" shear modulus (Shackelton et al., 2005). It is used to determine fracture propagation across different rock unit boundaries.

Dataset

Field Dataset

Sheep Mountain Anticline Data Acquisition:

Six sections were measured at Sheep Mountain Anticline (SMLA, SMLB, SMLC, SMSA, and SMLR (Table 2.2). At each section one or more genetic units were identified, each of which contained between two to five mechanical units.

In sequence one of the Madison Formation at Sheep Mountain, fracture parameters across a single bed was measured along the strike from one limb to the other of the anticline to test the influence of change in dip of the bed across the anticline on fracture attributes (Table 2.2.1).

Field Data from; Wyoming, Sheep Mountain Anticline		
Section	***Mechanical Units***	***Total Number of Fractures***
SMLA	1	100
	2	57
SMLB	1	102
	2	70
SMLR	1	100
	2	85
SMLC	1	101
	2	60
	3	50
	4	53
	5	100
SMSA	1	54
	2	91
	3	35

Table 2.2: Number of sections measured at Sheep Mountain Anticline, and the number of mechanical units identified as well as the total number of fractures measured.

Table 2.2.1: Dip and dip direction of fracture distribution along Sheep Mountain Anticline				
Fracture	Spacing (cm)	Height (cm)	Fracture Dip/Direction	Bed Dip/ Direction
1	0	190	72/176	20/210
2	75	140	68/176	20/210
3	225	163	82/038	20/210
4	120	250	56/068	20/210
5	50	250	80/042	20/210
6	73	71	86/220	20/210
7	124	180	70/210	20/210
8	90	320	84/170	20/210
9	25	220	86/198	20/210
10	60	290	84/020	20/210
11	28	295	86/194	20/210
12	48	300	90/000	20/210
13	360	350	86/216	20/210
14	240	380	90/000	20/210
15	220	405	82/060	20/210
16	155	447	86/102	10/227
17	230	485	90/000	10/227
18	250	515	70/022	10/227
19	170	532	74/174	10/227
20	260	540	72/224	10/227
21	360	540	76/168	10/227
22	690	500	72/170	10/227
23	660	500	70/162	10/227
24	410	450	78/162	10/227
25	700	400	86/206	16/170
26	140	400	82/186	16/170
27	250	400	72/200	16/170
28	900	425	72/210	16/170
29	560	350	82/208	16/170
30	410	350	80/100	16/170
31	180	375	82/144	16/170
32	600	375	86/200	16/170
33	480	400	90/000	16/170
34	370	400	72/174	16/170
35	385	400	88/230	16/170
36	840	350	78/226	16/170
37	440	400	N.A.	16/170
38	310	400	86/190	46/354
39	470	450	62/212	46/354
40	230	450	76/136	46/354
41	240	500	78/174	46/354
42	110	475	82/236	46/354
43	580	425	64/190	46/354
44	430	400	62/218	42/040
45	350	360	86/150	42/040
46	290	450	88/250	42/040
47	1330	540	90/000	42/040
48	330	630	82/110	42/040
49	250	630	70/156	42/040
50	700	630	90/000	42/040

St. Louis - Data Acquisition

The St. Louis area has several well exposed outcrops which were several 100s of meters long that provided an excellent opportunity to observe facies heterogeneity and fracture pattern variations within large heterogeneous sedimentary bodies.

The sections measured include the Cragwald, Gravois Road and Cardinal Quarry sections. Another well exposed section on the Meramec highway was also measured. This section has not been previously measured by Rankey (2003) and this will be one of the test sections, to observe if our final predictive tools can be applied to other sections. Lithologicaly, the strata were not highly diageneticaly altered and facies description was much easier to follow.

Table 2.3: Field Data from Missouri, St. Louis-Flank of Illinois Basin

Section	Mechanical Units	Total No. Fractures
Gravois	1	96
	2	102
	3	100
	4	110
	5	98
Cragwald	1	124
	2	115
	3	109
	4	102
	5	97
	6	104
Cardinal	1	102
	2	102
	3	100
	4	110
	5	112
	6	110
	7	108

Paradox - Data Acquisition:

Fracture analysis on the upper Desmoinsian strata in two structurally different areas. Flat-lying strata (6 sections) of the Honaker Trail area and the tectonically deformed strata at Raplee Anticline (3 sections) were again used to test the concept that elements of the genetic unit correspond to the mechanical units in areas with different strain conditions. The Paradox Basin was also an ideal case to test both methodologies; the scan density line method and the surface area mapping of fracture networks.

Table 2.4: Field Data from Utah - Paradox Basin (Honaker Trail)

Section	Mechanical Units	Total No. Fractures
1	1	85
	2	99
	3	100
	4	80
	5	90
	6	100
2	1	100
	2	88
	3	100
3	1	100
	2	85
Hornpoint	1	100
	2	100
4	1	86
	2	92
	3	100
	4	98
5	1	92
	2	100
	3	99

Table 2.5: Field Data from Utah - Paradox Basin (Raplee Anticline)		
Section	Mechanical Units	Total No. Fractures
1	1	100
	2	100
	3	90
	4	90
	5	100
	6	100
	7	100
	8	100
	9	100
	10	100
2	1	100
	2	100
	3	100
	4	100
	5	100
	6	100
	7	100
3	1	100
	2	100
	3	100
	4	100

The total number of fractures represents the number of fractures measured in each mechanical unit. A total of 100 fractures are measured to reduce any statistical bias in the dataset. But, in some cases outcrop conditions did not allow for completion of 100 fracture measurements.

Laboratory Dataset

Paradox Basin, Utah - Petrophysics:

Measurements of petrophysical properties (density, porosity and ultrasonic velocity) in laboratory from 80 outcrop samples were taken. This data was used to determine the dynamic moduli of the different mechanical units. These measurements were constrained

only to the Paradox Basin where very little diagenetic alteration has occurred from the original depositional rock fabric, which would enable us to accurately assess fracture formation and constraints without the added complication of heavily altered rock fabrics.

Chapter 3: Relationship between high-resolution sequence stratigraphy and mechanical units

We know that the architecture of carbonates is characterized by a hierarchical stacking of stratigraphic units that can act as flow units. Similarly, fractures are often hierarchical, in that they affect beds, bed-sets or larger units. What is not known is, if there is any correlateable relationship between the stacking of sedimentary beds into stratigraphic units of different time magnitudes, with the stacking of sedimentary beds into mechanical units. The working hypothesis in this chapter here is that the rock properties generated by the combined effect of facies and diagenesis in each stratigraphic unit controls the mechanical properties of the strata. Consequently, a relationship between the stratigraphic units and the mechanical units can be expected. This relationship is evaluated in this study.

The main goal of this study is to test the hypothesis that there is a relationship between mechanical stratigraphy and high resolution sequence stratigraphy. If valid, this result would permit prediction of fracture partitioning and mechanical boundaries to flow, from stratigraphic information. The impact of this study can be applied to reservoirs, and enhance production levels, due to better modeling of different flow rates within different mechanical units. To reach this goal the following questions are addressed: Are fractures limited to sedimentary beds or stratigraphic units and if so, then to what scale? Do mechanical unit boundaries coincide with genetic unit boundaries?

Sheep Mountain Anticline – Greybull, Wyoming

The Sheep Mountain Anticline is located in the northern Bighorn Basin of Wyoming and Montana. The structure of Sheep Mountain Anticline is a simple doubly plunging asymmetric anticline on the east limb of the Bighorn Basin (Hennier & Spang, 1983; Sonnenfeld, 1996; Smith et al., 2004). Sheep Mountain anticline trends northwest-southeast, and is sub-parallel to the Bighorn Mountain Uplift (Hennier & Spang, 1983). Sheep Mountain Anticline and other associated folds in the Bighorn Basin are Laramide compressional structures. In Early and Middle Mississippian, the Madison Formation was deposited on an extensive carbonate shelf, bounded to the west by the Antler Highlands (due to the Antler Orogeny during Late Devonian) and to the east by the Transcontinental Arch and to the north by the Central Montana Trough. The strata was faulted and folded during the Late Cretaceous to Eocene times (Smith et. al., 2003); (Fig. 3.1).

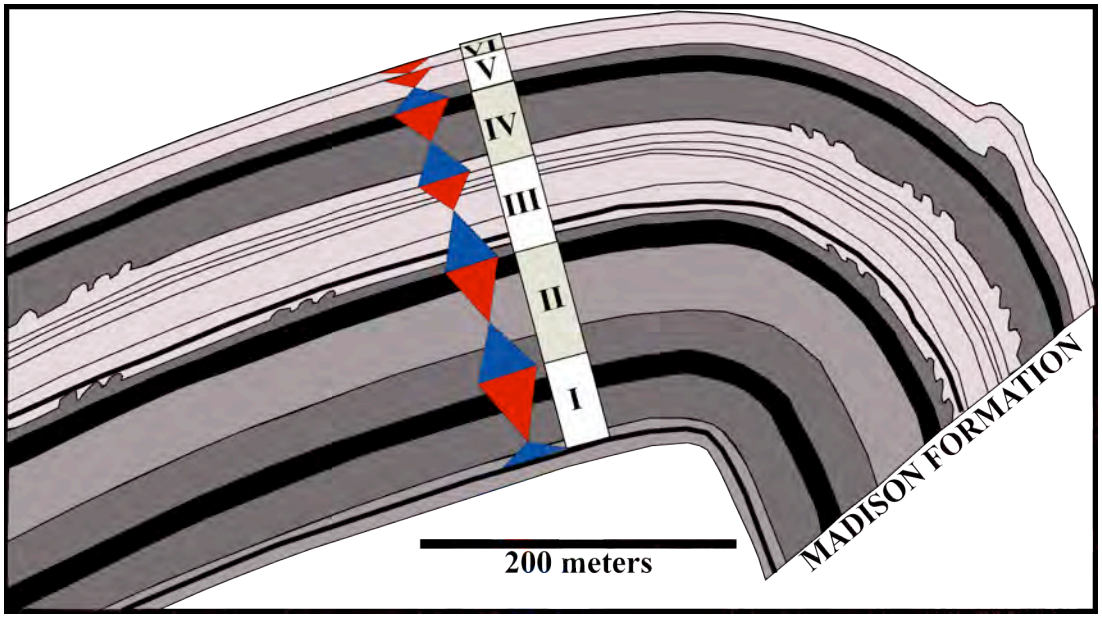

Figure 3.1: Schematic cross section view of Sheep Mountain Anticline, displaying the asymmetry of the anticline and the 6 major third order sequences. Modified from Sonnenfeld, 1996.

The Lower Mississippian Madison Formation at Sheep Mountain Anticline, Greybull, Wyoming is composed of a hierarchy of sequences (Fig. 3.2), (Sonnenfeld, 1996; Smith et. al, 2004). These previous works document that higher order sequences and the genetic units stack into 6 major 3rd order sequences, which stack up into two important long term composite sequences of 2nd order.

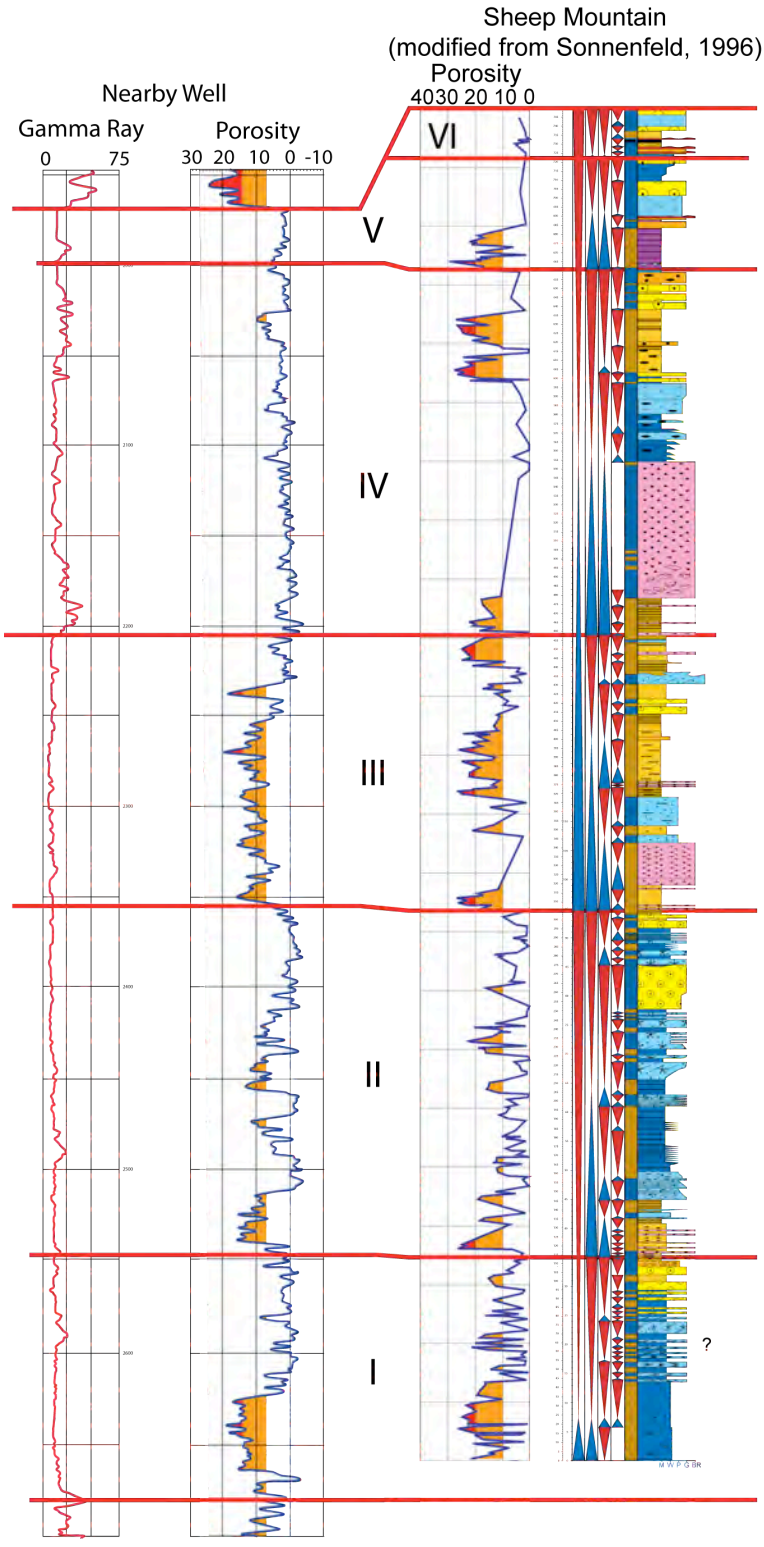

Figure 3.2: Facies, porosity and sequence stratigraphy of the Madison Formation at Sheep Mountain Anticline as described by Smith et al. 2004.

Lithofacies Description:

The lithofacies described below are a general composite based on more detailed lithofacies described by Sonnenfeld (1996), who subdivided the Madison Formation into 16 major lithofacies. In this paper, and from a more structural point of view, only 9 lithofacies are considered, some of which are a composite of two lithofacies identified by Sonnenfeld (1996).

Type of Lithofacies	Description
Laminated to bioturbated limestone	This facies is observed as thin bedded black to dark limestone, alternating with a more orangish dolostone, and contains crinoids and bryozoan fragments, peloids and brachiopods. Typical sedimentary structures include fining upwards from packstones to mudstones, some parallel laminated tops and sometimes burrowed. The laminated to bioturbated limestone facies is interpreted to be deposited in a dysaerobic sub storm-wave base outer ramp.
Bioturbated microskeletal dolowackestone/mudstone	This facies varies from thin to massive bedded, medium gray bioturbated dolomite with rare fauna. (Some crinoid fragments and brachiopods). Some stylolites present. The depositional environment for this facies is interpreted to be sub storm-wave base, open marine, middle ramp.
Skeletal lime packstone to dolomudstone	This thin to medium bedded, cherty dolomitic limestone and dolomite, is gray in color and contains crinoids, brachiopods, rugose corals and bryozoans. Sedimentary features are abundant from hummocky to swaley cross stratification, wave rippled tops and non-amalgamated storm beds. The depositional environment of this facies is interpreted to be open marine, lower shoreface.
Cross-stratified skeletal packstone to grainstone	A massive to medium bedded, medium gray limestone to dolomitic limestone, poorly sorted Packstone to grainstone, this facies is rich in its biodiversity containing crinoids, brachiopods, rugose corals, bryozoans, peloids, red algae and ooids. Sedimentary features include amalgamated storm beds, with hummocky and trough cross bedding, with firmground caps and intraclasts. This facies depositional environment is interpreted to be open marine, middle upper shoreface, within fair weather wave-base.

Cross-stratified skeletal oolitic grainstone	The Oolitic grainstone is gray to buff in color, massive to medium bedded, dolomitic limestone to limestone. This facies contains ooids, peloids, crinoids, brachiopods and rugose corals. Amalgamated trough and planar tabular cross bedding, as well as some ripple cross stratification and bi-directional cross beds are typical sedimentary features. This facies is interpreted to be deposited in a restricted, tidally influenced, upper shoreface within fair weather wave-base conditions.
Ostracod-peloidal grainstone to dolomudstone	Light gray to buff limestone and dolostone. Contains peloids, ostracods and green algae, and is generally massive to medium bedded, pervasively bioturbated and sometimes cherty. Depositional environment is interpreted as a restricted inner to outer lagoon.
Wave-rippled dolomudstone/wackestone	This mudstone wackestone facies is thin to medium bedded, with bioturbated bases, grading into parallel laminated to wave rippled zones. It is buff colored, with peloids, intraclasts and rare ostracods. Contains minor subvertical burrows, and is interpreted to be deposited in a restricted, low energy, inner shoal environment.
Stromatolitic laminated mudstone to laminated dolomudstone	Gray mudstone to stromatolitic bindstone, occurs as both limestone or dolomite, with sparse presence of intraclasts, and bluish chalcedonic nodules due to evaporates. Very thin to medium bedding, laminated and may contain mud cracks, thin wave ripples and rare fenestrae. Depositional environment is upper intertidal to supratidal.
Evaporite solution collapse breccia	The evaporite solution collapse breccia is generally a medium to thin bedded, argillaceous, greenish white to tan, dolomitic collapse breccia mudstones. Depositional environment is interpreted to be supratidal, sabkha deposition.

Table 3.1: Brief description of the various lithofacies present in the Madison Formation (from Sonnenfeld 1996).

Idealized Genetic Cycle

Sonnenfeld (1996), defined 4 major small scale "fundamental" 5th order cycles. These are:

1. **Deep subtidal cycles:**

   This cycle contains the deepest facies present in the Madison study area. This cycle consists mainly of bioturbated, microskeletal dolowackestone to mudstone, which contains some crinoid fragments, brachiopods and solution seams. The depositional environment is interpreted as oxygenated below storm wave-base deposits. The regressive hemicycle is represented by grainier microskeletal peloidal packstones, and the transgressive hemicycles as thin argillaceous mudstones rich in solution seams.

2. **Subtidal storm proximality cycles:**

   This cycle is generally a shallowing upward cycle, where the transgressive hemicycle is represented by any distinguishable lithofacies, and the regressive hemicycle consists of a coarsening upward cycle from dolomitized mudstones, to skeletal lime packstones, which coarsen into cross stratified skeletal Packstones grainstones with the top of the hemicycle being represented by cross-stratified Oolitic grainstones.

3. **Lagoonal cycles:**

   The lagoonal cycles demonstrate an overall fining upward grain size profile. This fining upwards demonstrates the dissipation of current energy, and generally overlies the skeletal Oolitic grainstone. Their base is generally composed of the ostracod micropeloidal grainstone, which then fines upwards into the ostracod-peloidal dolowackestone to mudstone. The top of this cycle is generally capped by wave rippled to mudcracked dolomudstones.

4. **Peritidal cycles:**

The peritidal cycle is generally the shoaling upwards from inner lagoonal facies to intertidal and supratidal facies. These facies include the mudcracked conglomeratic dolomudstone, as well as the stromatolitic laminated mudstone, and the supratidal dolomudstone rich evaporite collapse breccia, as well as the laminated argillaceous dolomudstones.

Sheep Mountain Anticline - Results

The observations and correlations of the genetic boundaries and mechanical boundaries of each section are described. The sections are increasing in their stratigraphic order from youngest to oldest (Fig. 3.3). A total of six sections were measured from Sheep Mountain Anticline. These sections are:

1. SMLB: Sheep Mountain Low Angle Limb – B
2. SMLA: Sheep Mountain Low Angle Limb – A
3. SMSA: Sheep Mountain Steep Angle Limb – A
4. SMLC: Sheep Mountain Low Angle Limb – C
5. SMLR: Sheep Mountain Low Angle Limb – R

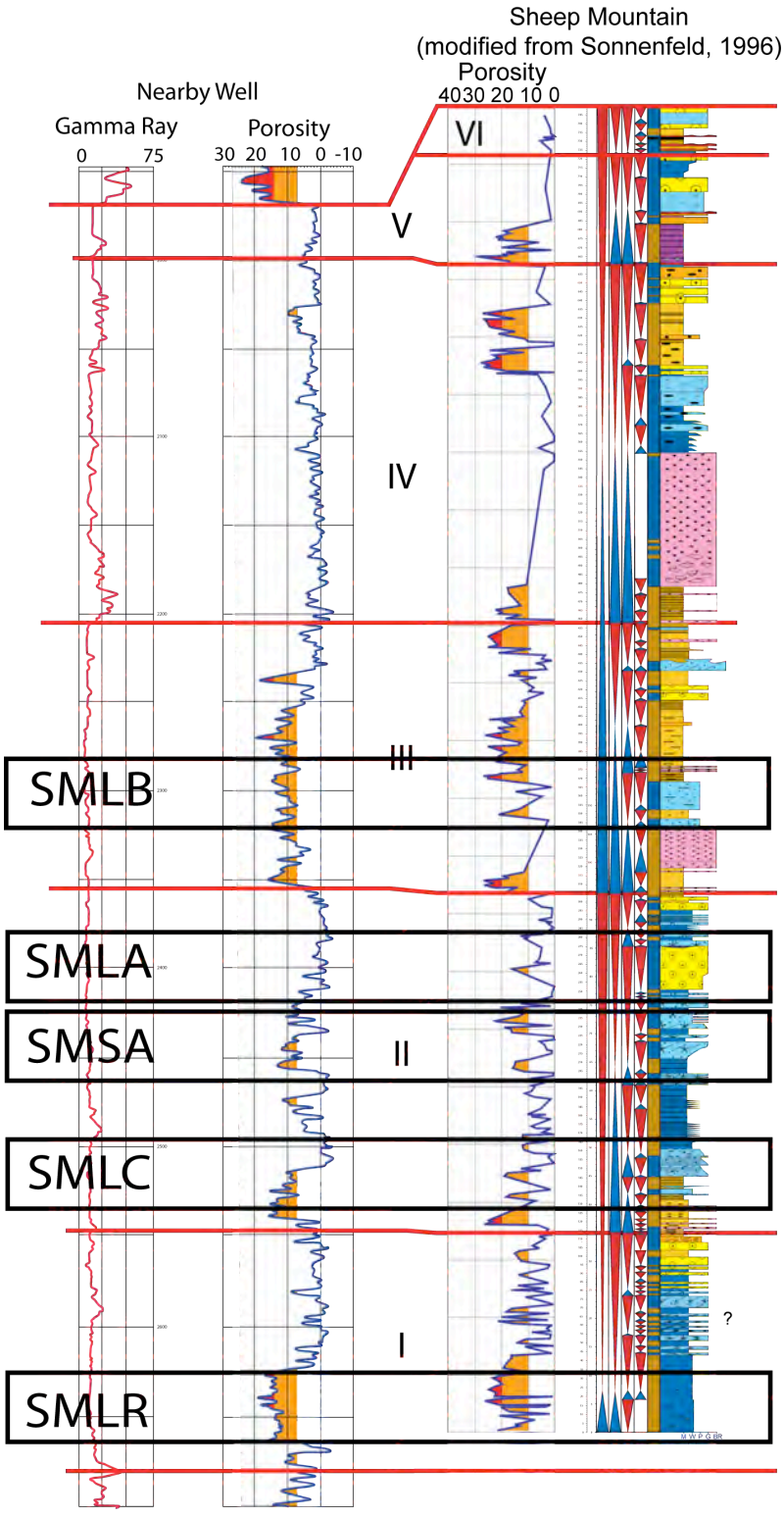

Figure 3.3: Stratigraphic locations of measured sections in Sheep Mountain Anticline. Stratigraphic Interpretation taken from Smith et. al., 2004.

Section SMLB:

Measured section SMLB is just above the major evaporite solution collapse breccia in sequence III (Fig. 3.4). This section consists of two genetic cycles and is about 9.70m thick. The transgressive hemicycle of the first genetic cycle is a ~2.00m thick dolomitic mudstone to wackestone and the regressive hemicycle is composed of a 5.00 meter thick peloidal crinoid packstone. The transgressive hemicycle of the next genetic cycle above the genetic unit boundary is composed of finely laminated dolomitized peloidal mudstone/wackestone (~1.5m thick) and its overlaying regressive hemicycle is composed of a ~10cm thick evaporite solution collapse breccia deposit (Fig. 3.4).

The fractures measured are in the regressive hemicycle portion of the basal genetic cycle and the transgressive hemicycle portion from the upper genetic cycle. Three mechanical units were identified based on the mechanical boundaries. The fractures in the regressive portion (peloidal/crinoidal packstone) of the lower genetic unit do not extend down into the underlying mudstone layer (the transgressive hemicycle). All 100 fractures measured originated from the base of the packstone or from within it (Fig. 3.4). The turnaround point from the transgressive to the regressive hemicycle is therefore a mechanical boundary. Another mechanical boundary is identified at the top of the regressive peloidal/crinoidal packstone where 98% of the fractures terminate at the genetic unit boundary. The third mechanical boundary is at the top of the thinly laminated dolomitic unit where 85% of the fractures do not propagate across a bedding plane below the breccia unit. This bedding plane is again interpreted as the turnaround point from the transgressive to the regressive hemicycle. Hence, three mechanical units are identified in

section SMLB and the four mechanical boundaries identified coincide with the genetic unit boundaries or turnaround points between hemicycles (Fig. 3.4).

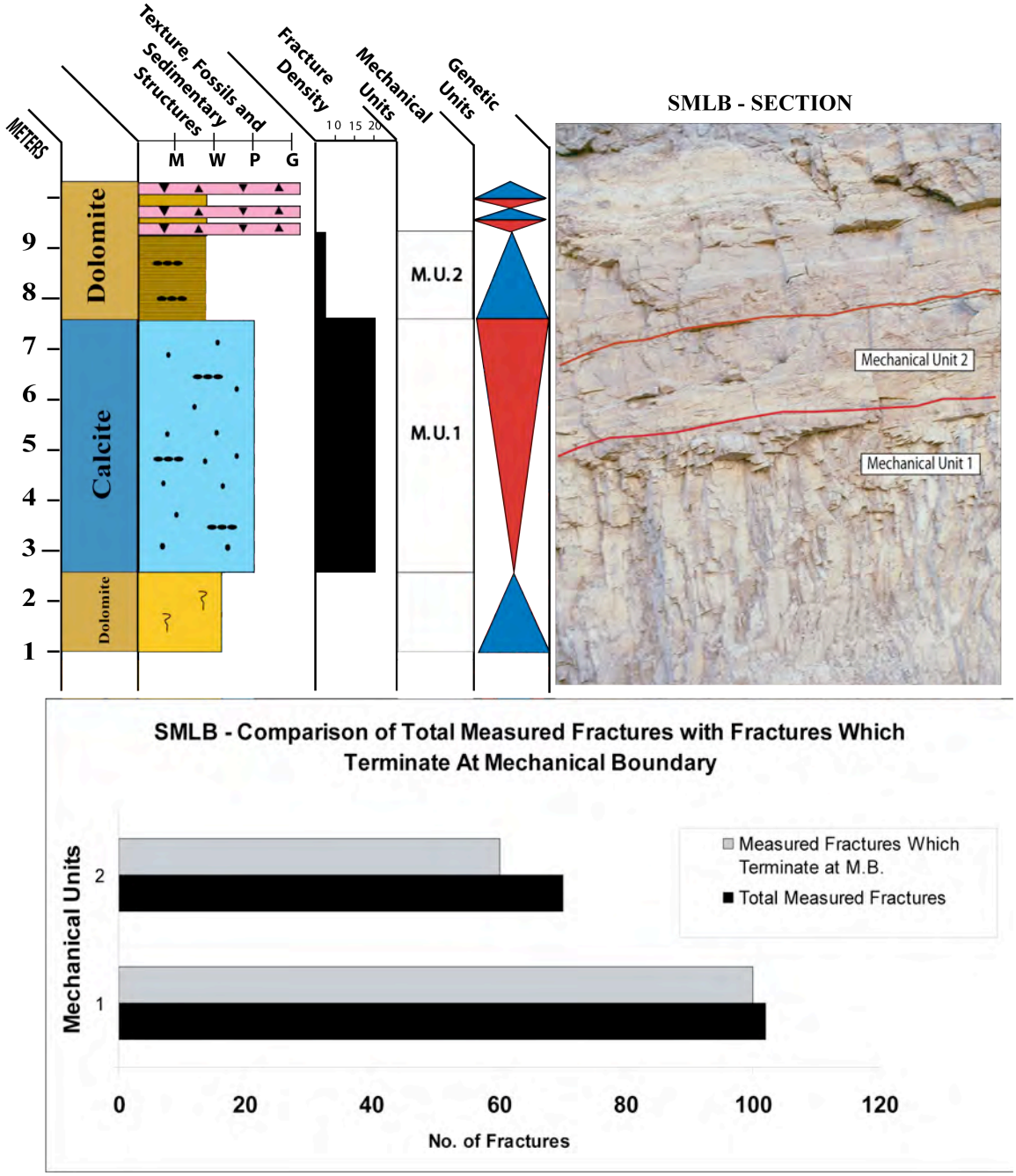

Figure 3.4: Section SMLB within sequence III of the Madison Formation. Fracture density variations reflect the different mechanical units. The mechanical units correlate with the genetic unit boundaries or the turnaround points between transgressive (blue triangles) and regressive (red triangles) hemicycles.

Section SMLA:

Section SMLA straddles the boundary between sequence II and sequence III. (Fig. 3.3) This measured section consists of three genetic cycles and is about ~5.35m thick. The transgressive hemicycle of the first genetic cycle is a ~2.00m thick dolomitic mudstone to wackestone and the regressive hemicycle is composed of a 6.00 meter thick oolitic grainstone, which displays an erosional surface at the top, forming a genetic unit boundary. In the next genetic cycle, the transgressive hemicycle is condensed onto the cycle boundary; as a result the regressive hemicycle, composed of a crinoidal grainstone deposit (~1m thick), stacks directly onto the underlying regressive unit. The next genetic cycle consists of a transgressive hemicycle expressed by ~0.4m thick mudstone and its overlaying regressive hemicycle is composed of a ~0.8m crinoidal grainstone bed (Fig. 3.5).

The fractures measured were in the regressive hemicycle portion of the basal genetic cycle and the next two genetic cycles. Three mechanical units were identified based on the mechanical boundaries. The first mechanical boundary is at the base of oolitic grainstone, the regressive portion of the genetic unit; because the fractures measured do not propagate below the grainstone bed (Fig. 3.5). This turnaround point from transgressive to regressive hemicycle is therefore a mechanical boundary. At the top of the regressive oolitic grainstone where 89% of the fractures terminate at the genetic unit boundary, forming a mechanical boundary. The third mechanical boundary is at the genetic unit boundary of the third genetic cycle where 85% of the fractures terminate. Hence, the three mechanical units identified in section SMLA coincide with the genetic unit boundaries or their turnaround points. However, not every genetic unit boundary or

turnaround point is a mechanical boundary in this section, as is demonstrated with the second genetic cycle and the turnaround point of the third genetic cycle (Fig. 3.5).

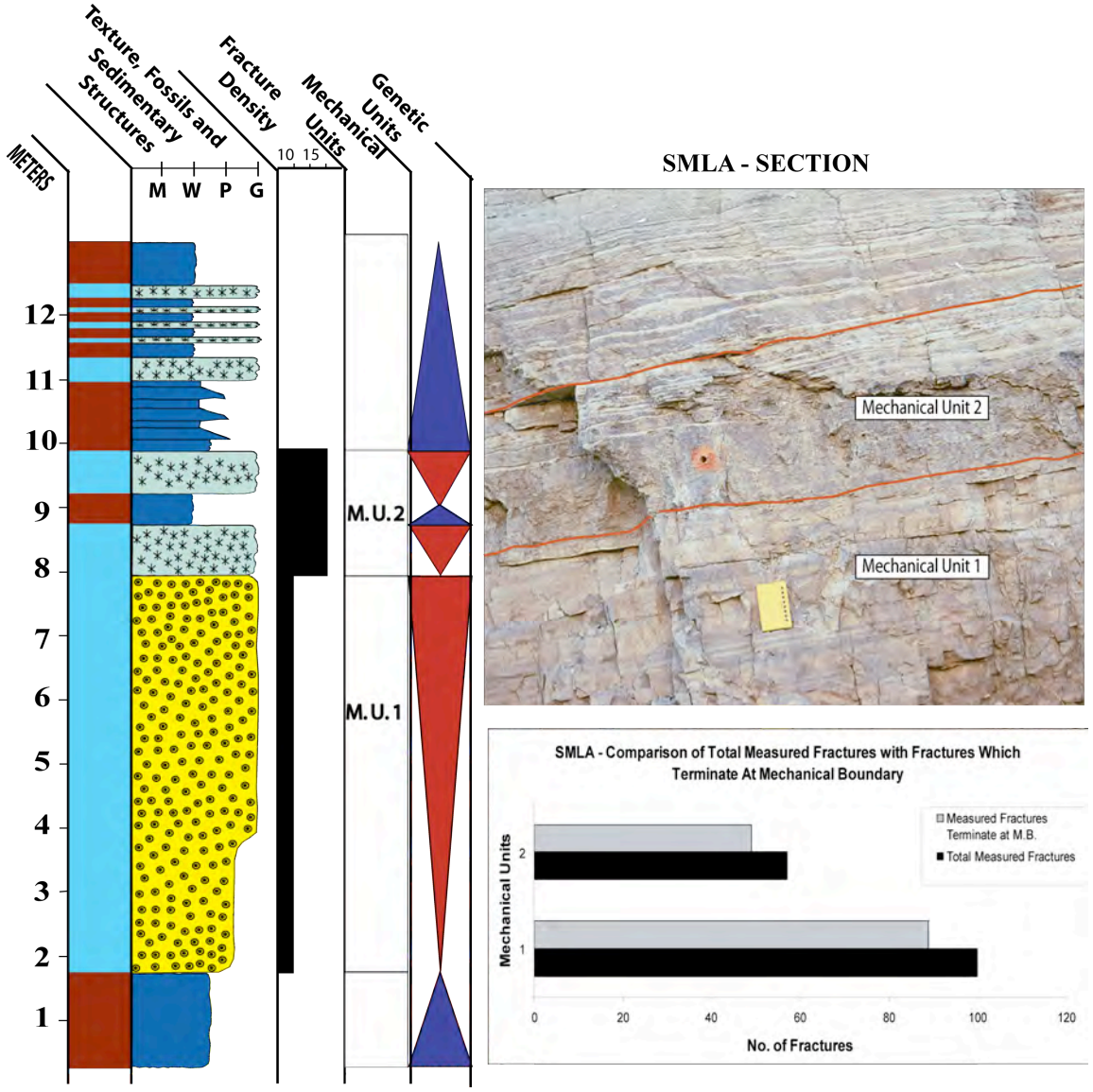

Figure 3.5: Boundary between upper sequence II and basal sequence III of the Madison Formation section SMLA. A sequence boundary is present between mechanical units 1 and 2. Fracture density variations reflect the different mechanical units. The mechanical units correlate with the genetic unit boundaries and internal flooding surfaces.

Section SMSA:

The total thickness of this section is ~5.50 meters thick and is located just below the base of the oolitic grainstone from section SMLA in sequence II (Fig. 3.3). Section SMSA is measured on the steep angle limb of Sheep Mountain anticline. This measured section consists of two genetic cycles, where the transgressive hemicycle of the first genetic cycle is a ~1.00m thick dolomitic mudstone and the regressive hemicycle is composed of a 1.80 m thick crinoidal packstone grading upwards into a grainstone. Above the genetic unit boundary, the transgressive hemicycle of the next genetic cycle is composed of finely laminated dolomitized mudstones capped by a 10 cm thick crinoidal grainstone bed; its overlaying regressive hemicycle is composed of a ~1.2 m thick crinoidal grainstone deposit (Fig. 3.6).

Within this succession four mechanical units were identified. In the regressive portion (crinoidal packstone to grainstone) of the lower genetic unit all fractures measured originated from either the base or within the crinoidal packstone/grainstone (Fig. 3.6). The base of the bed, which is the turnaround point from transgressive hemicycle to regressive hemicycles, is hence a mechanical boundary. Likewise, the top of the regressive crinoidal grainstone is a mechanical boundary because 88% of the fractures terminate at the genetic unit boundary. is the overlaying bedsets of thinly laminated dolomitic mudstones are a mechanical unit as 97% of the fractures do not propagate into the second crinoidal grainstone unit. This lithoigical boundary is the turnaround point from the transgressive to the regressive hemicycle and constitutes also a mechanical unit boundary. The fourth mechanical boundary is derived from the fractures measured in the second regressive hemicycle where 91% of the fractures terminate at the genetic unit

boundary. Hence, four mechanical units are identified in section SMSA and the mechanical boundaries identified coincide well in this section with the genetic unit boundaries and their turnaround points (Fig. 3.6).

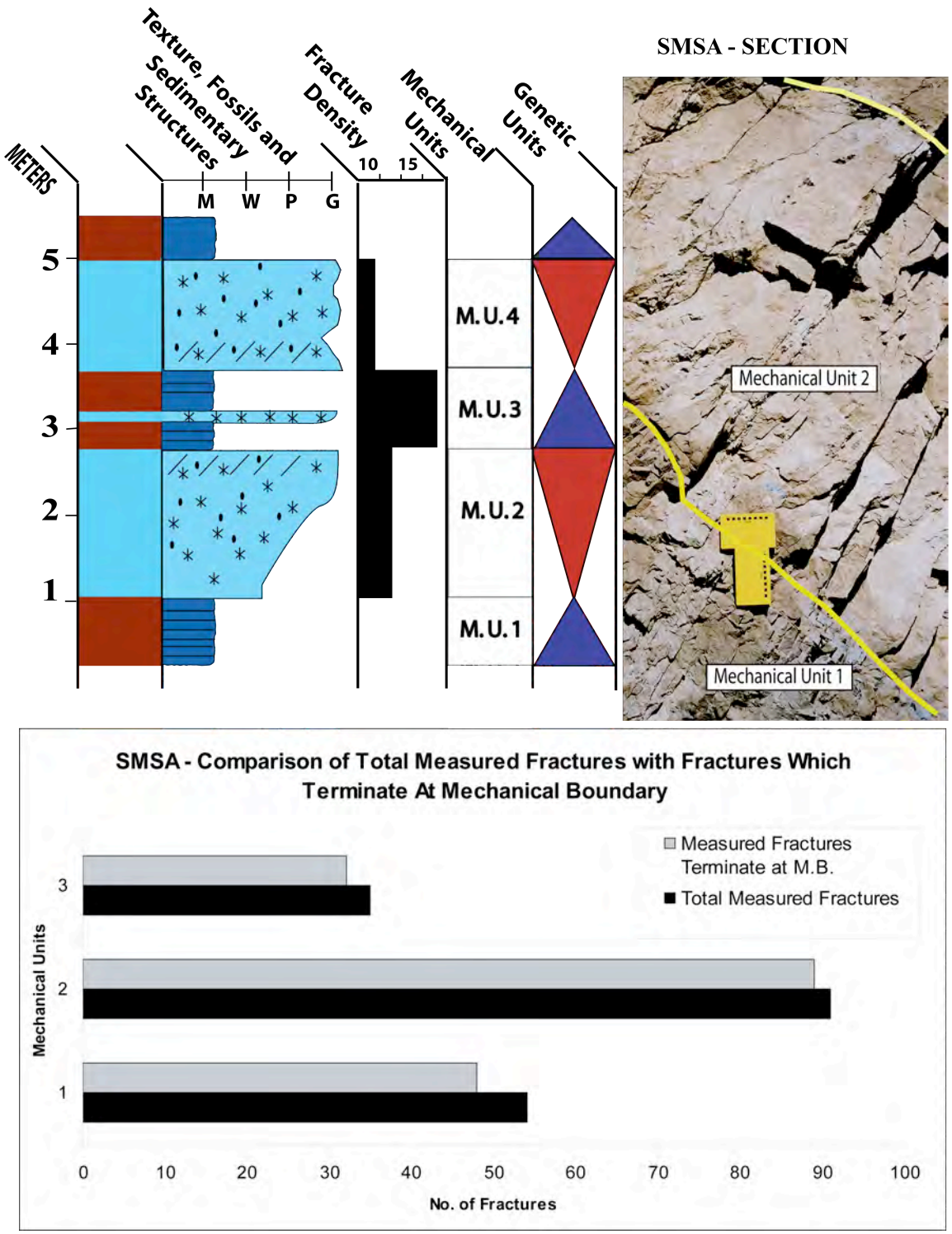

Figure 3.6: Section SMSA in the upper part sequence II of the Madison Formation. Fracture density variations reflect the different mechanical units. This again confirms that the mechanical units correlate with the genetic unit boundaries and internal flooding surfaces.

Section SMLC:

Section SMLC, in the middle of sequence II, is 5.50 meters thick and consists of three genetic cycles (Fig. 3.3). The first genetic cycle is about a meter thick. A calcitic crinoidal packstone makes up the transgressive hemicycle while the regressive hemicycle is composed of a thin unit of dolomitic mud at the base and capped by another calcitic crinoidal grainstone. The next genetic cycle's transgressive hemicycle is composed of layers of dolomitic mud- to wackestone interbedded with crinoidal grainstone. The overlaying 1.5m thick laminated crinoidal grainstone forms the regressive hemicycle. Above genetic unit boundary, the next transgressive hemicycle is expressed by 2 m thick interval of finely laminated dolomitized peloidal mudstone to wackestone, and the overlaying regressive hemicycle is composed of a thick crinoidal grainstone with cross-bedding and pressure dissolution features (Fig. 3.7).

In this succession, six mechanical units were identified and the fractures were measured in five of them. 94% of the fractures in the transgressive hemicycle of the first genetic cycle in the succession did not propagate into the overlying regressive hemicycle, thus identifying the turnaround point from transgression to regression as a mechanical boundary. All 100 fractures measured within the regressive hemicycle do not extend into the next genetic cycle above, making the genetic unit boundary also a mechanical boundary (Fig. 3.7). The third mechanical boundary is identified at the turnaround point of the second genetic unit where 80% of the measured fractures do not propagate into the thick regressive crinoidal grainstone. All the measured fractures within the regressive hemicycle terminate at the genetic unit boundary. The last mechanical boundary of the succession is identified where 89% of the fractures terminate at the turnaround point of

the third genetic unit. In summary, six mechanical units are identified in section SMLC and the mechanical boundaries identified coincide with the genetic unit boundaries or their turnaround points (Fig. 3.7).

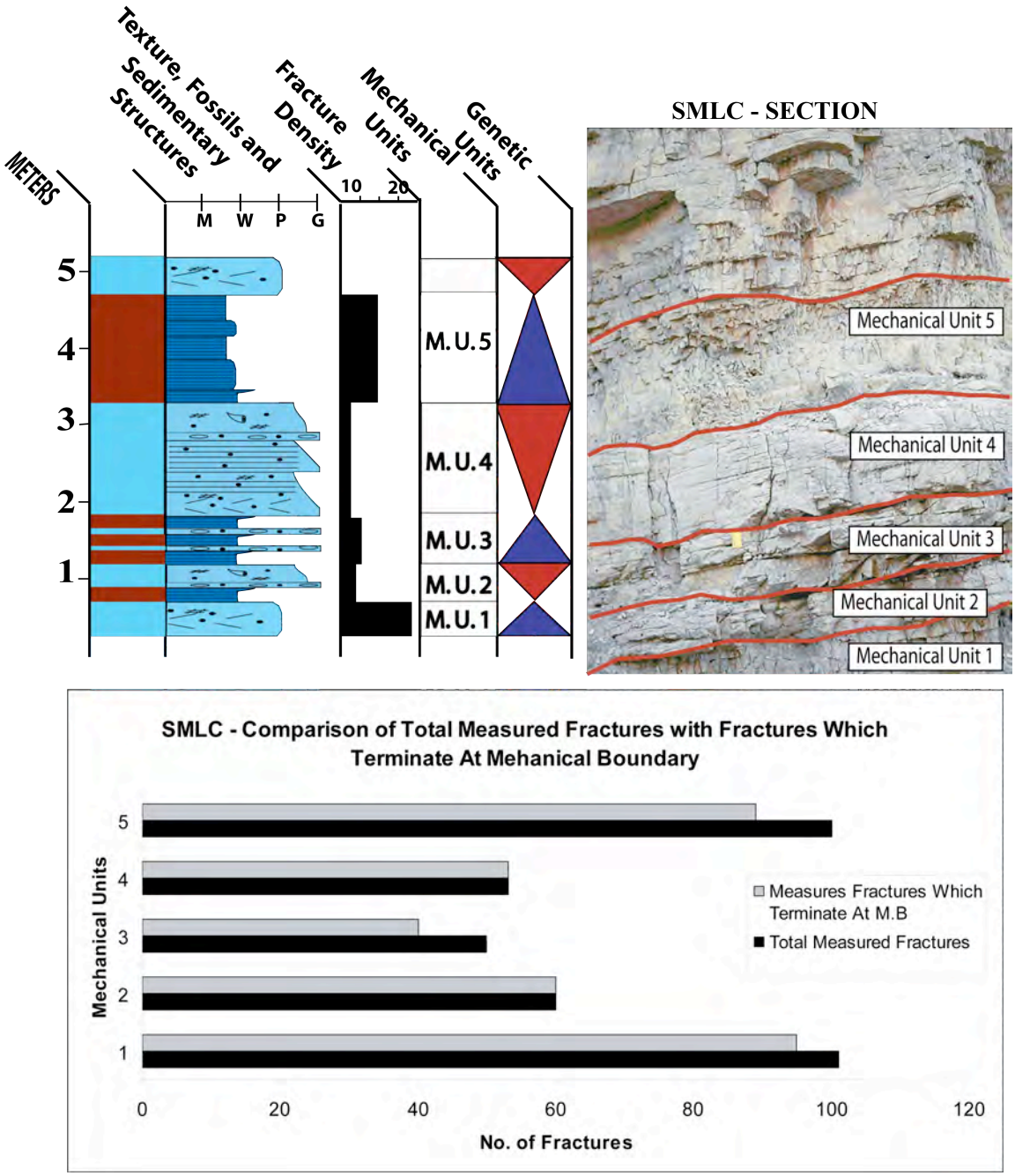

Figure 3.7: Mid-sequence II of the Madison Formation section SMLC. Fracture density variations reflect the different mechanical units. The mechanical units correlate with the genetic unit boundaries and internal flooding surfaces.

The interpretation of the second sequence boundary between mechanical unit 4 and 5 has been altered from Smith et al. (2004) where they place it in the middle of mechanical unit 4 and I place it at the top. The reason for me changing the original interpretation is because there was no indication of a sequence boundary found in the middle of mechanical unit 4.

Section SMLR:

Section SMLR encompasses the first two genetic units in sequence I of the Madison Formation identified by Smith and Eberli, (2000), (Fig. 3.3). This section was measured on the other side of the river where accessibility to the outcrop was limited and consists of one complete genetic cycle and is over 5 meters thick. The entire section is composed of highly dolomitized wackestones to mudstone-wackestones. The first measured unit is the regressive hemicycle exposed at the base and is a ~1.50m thick dolomitic wackestone which, in thin section consists of fabric destructive dolomite containing some crinoidal and brachiopod fragments. The genetic cycle above begins with a transgressive hemicycle and is composed of a 0.60 meter thick fabric destructive dolomitized wackestone to mudstone. The overlaying regressive hemicycle is composed of a more massive thick dolomitic wackestone with sporadic echinoid and brachiopod fragments and is ~4m thick (Fig. 3.8).

The fractures measured were from all the hemicycles present in the section. Three mechanical units were identified based on the mechanical boundaries. 99% of the fractures present in the regressive portion of the lower genetic unit terminated at the high resolution sequence boundary, thus forming a mechanical boundary. At the next mechanical unit, which coincides with the transgressive hemicycle 98% of the measured

fractures terminated at the turnaround point from the transgressive hemicycle to the regressive hemicycle is therefore also a mechanical boundary. Another mechanical boundary is identified at the top of the massive regressive hemicycle where the fractures can be seen to terminate sharply at the genetic unit boundary and not propagate across (Fig. 3.8). Hence, three mechanical units are identified in section SMLR and the four mechanical boundaries identified coincide with the genetic unit boundaries and their turnaround points (Fig. 3.8). In this section, identification of the mechanical units was enhanced due to variations in fracture density, where the middle transgressive hemicycle is highly fractured in comparison to the units below and above it, which both represent the regressive hemicycles (Fig. 3.8).

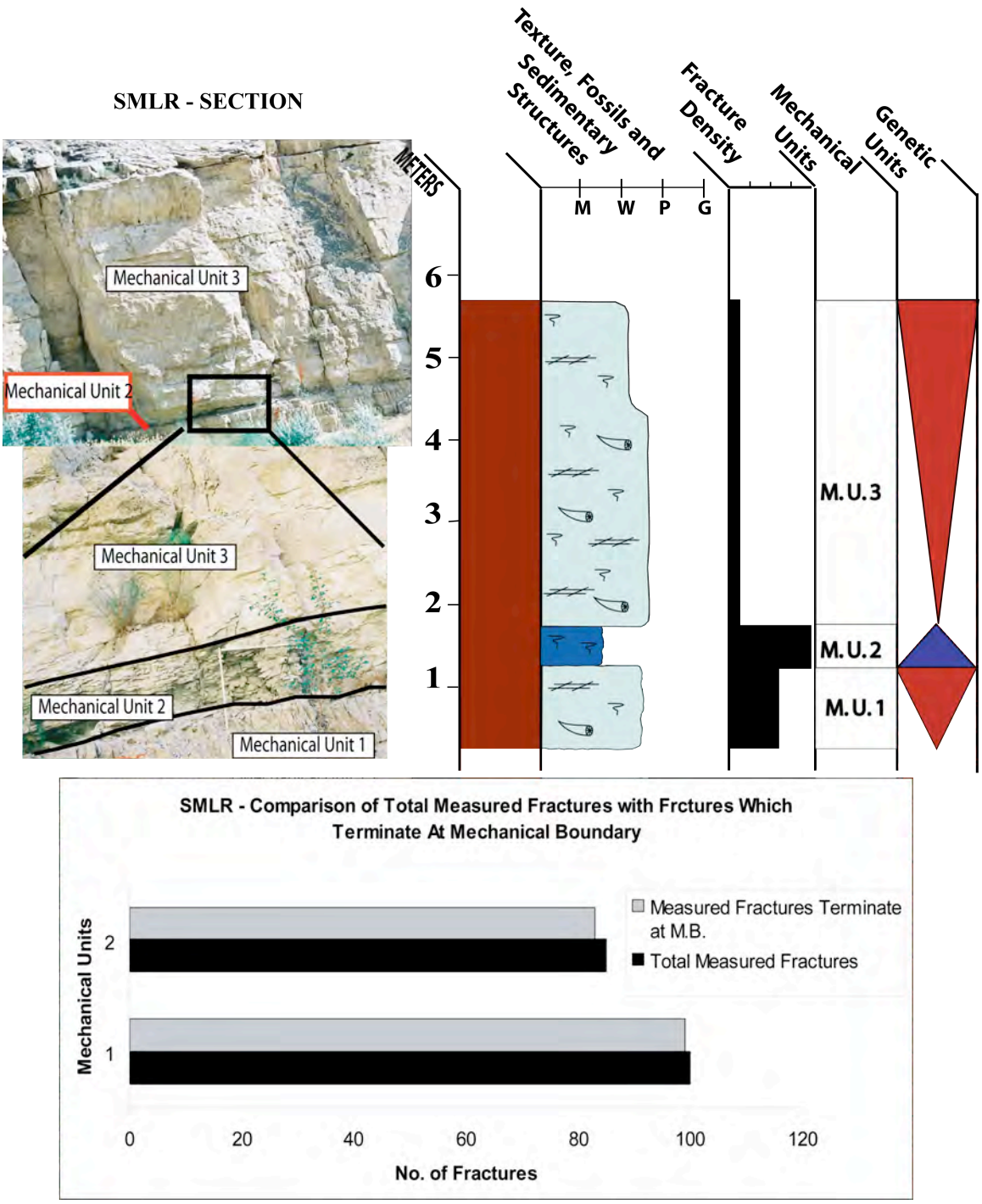

Figure 3.8: Basal sequence I of the Madison Formation section SMLR. Fracture density variations reflect the different mechanical units. The mechanical units correlate with the genetic unit boundaries and internal flooding surfaces

Sheep Mountain Anticline - Conclusion

Genetic unit boundaries in general correlate with mechanical unit boundaries and hence it can be concluded that high frequency genetic unit boundaries generally act as boundaries to fracture propagation.

However, a genetic unit is usually composed of two mechanical units. In most cases, fracture partitioning exists between the transgressive and the regressive hemicycle. This fracture partitioning is directly related to the facies partitioning in the muddier transgressive hemicycles and the grainier regressive hemicycles. In addition, diagenetic partitioning into dolomitized transgressive and calcareous regressive hemicycles is believed to have enhanced this effect. Hence, the transgressive hemicycles are generally more dolomitized, contain higher percentages of intercrystalline porosity and are also generally more fractured than the regressive hemicycles.

This implies the need for subdividing the genetic unit (or one sedimentary cycle) in reservoir modeling to describe accurately the fracture and porosity distribution of the strata.

Flank of Illinois Basin - St. Louis, Missouri

Overview

During early Carboniferous time, a relatively deep-water carbonate ramp setting also developed in the Illinois Basin (Lineback, 1972; Lasemi et al., 1998).

The Meramecian (Middle Mississippian) sequence of eastern Missouri consists of four formations (Howe and Koenig, 1961). From bottom to top these are: the Warsaw, Salem, St. Louis, and Ste. Genevieve formations. This study investigates the carbonate sequences of the Warsaw and Salem formations (Middle Mississippian) of eastern Missouri along the western margin of the Illinois basin.

Before and during Early Carboniferous time, the proto-Illinois Basin area was a broad, slowly subsiding, cratonic embayment that opened southward toward the deep ocean. The embayment was initially established during the latest Precambrian to Early Cambrian time when the Reelfoot Rift-Rough Creek Graben, a 'failed' rift, formed (Kolata & Nelson, 1991). After initial thermal subsidence during Late Cambrian and Early Ordovician time, the rate of subsidence decreased dramatically and remained relatively slow during most of the remainder of the Paleozoic era (Kolata & Nelson, 1991 and references therein).

The proto-Illinois Basin embayment was relatively deep (at least 300m according to Lineback, 1966) in the southern part of the basin and shallowed onto "shelves" at the western, northern, and eastern fringes during Early Carboniferous time (Cluff et al., 1981). Organic-rich black shale, the new Albany Shale, was deposited within this embayment during Late Devonian and Early Carboniferous time (Cluff et al., 1981). Following deposition of the New Albany Shale, the influx of siliciclastic sediment

ceased, and the environment became conducive to carbonate production. Subsequently in western Illinois a crinoidal carbonate 'shelf', the eastern extent of the Burlington Shelf (Lane, 1978; Lineback, 1972), developed, and about 60m of carbonate rocks, including the Fern Glen, Burlington and Keokuk Formations were deposited. Perhaps because of continued lowering of relative sea level and/or renewed tectonic activity in the northern Appalachians, siliciclastic sediments again slowly entered the basin from the east and northeast, initially as a 'pro-delta shale' (Springville Shale) and then as a tongue-shaped wedge of siltstone, the Borden Siltstone. The Borden wedge was confined on the north and west by the Burlington Shelf and was absent in the deepest south-central part of the basin. Borden siliciclastic sediments were also being deposited at about the same time in southwestern Indiana and farther east in central and eastern Kentucky. Toward the end of Borden deposition, siliciclastic sediments (Lower Warsaw Shale) prograded to the west and northwest over the Burlington Shelf, and a carbonate ramp developed on the wedge in the basin (Lineback 1972; Lasemi et al., 1998).

Depositional History

The lithologic characters and associated sedimentary structures of the Warsaw-Salem lithofacies suggest that the facies sequence represents the deposits of a single regressive outbuilding or shoaling of a carbonate ramp (Ahr, 1973).

The critical stage in this ramp outbuilding, however, was the development of a chain of biohermal mud mounds that divided the shelf into two distinct depositional regimes:

- An eastern open, shallow marine shelf of normal marine sedimentation (Fig. 3.9)

- A western restricted part of the ramp where shoals, lagoons, tidal flats, and strandplains developed under fluctuating marginal marine conditions (Bhattacharyya and Seely, 1994).

Incidentally, these two depositional regimes nearly conform to the two stratigraphic formations, the Warsaw and the Salem, respectively, designated in the area (Fig. 3.10). The uppermost member of the Warsaw Formation (the biohermal mound), thus, formed a transition zone between the normal marine and restricted marine depositional environments, and was influenced, in part, by the depositional and diagenetic processes of both regimes (Bhattacharyya and Seely, 1994). But, by virtue of being a physical barrier of dense mudstone lithology, it also served as a barrier to the fluids of early diagenetic origin within the two regimes (Bhattacharyya and Seely, 1994).

Along the outer margin of this ramp, the argillaceous lime mudstones were deposited under shallow, open marine conditions below the influence of wave or current energies prevalent during fair weather (Bhattacharyya and Seely, 1994). During periodic high-energy (storm) events, storm generated surges brought in the coarser inner shelf bioclastic material across the biohermal mound barrier on to the open shelf as density currents from which the graded grainstones were deposited as thin sheets on the muddy, open marine shelf (Bhattacharyya and Seely, 1994). The transition from biohermal mudstone to cross-bedded, very coarse grained grainstone and packstone illustrates the transition from open marine shelf to a restricted shelf under the influence of tidal currents and waves. The trough cross-bedded grainstones represent the deposits of tidal channels, shoals and washover fans. The mudstones were deposited in restricted lagoons and tidal flats behind the complex of biohermal barrier and tidal channels. The final phase of the

first shoaling event is represented by the strandplain grainstones with its characteristic texture and very shallow wave and current-dominated structures (Bhattacharyya and Seely, 1994).

Figure 3.9: General paleogeographic of the Warsaw and Salem Formations during Early Visean time (modified from Lane, 1978)

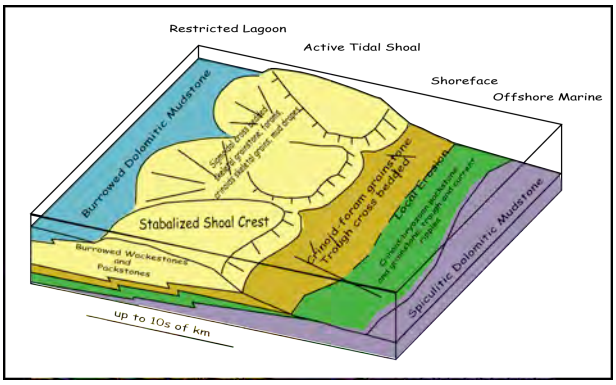

Figure 3.10: General interpretive facies model of the Upper Warsaw and Salem intervals.

Lithofacies Description

Lithofacies described from the Warsaw and Salem Formations at the studied outcrops are based on previous work done by Rankey (2003). Rankey identified 11 major facies subdivisions in his study. All 11 facies are included in this study.

Type of Lithofacies	Description
Foram rich skeletal grainstone-packstone facies	Thin to thick bedded facies, present in the upper Warsaw and Salem, containing a diverse assemblage of forams, crinoids, fenestrate bryozoans, peloids as well as brachiopods, bivalves, gastropods, with ubiquitous troughs and current ripples with some wavy laminations. This deposit represents a high energy, shoal complex.
Peloidal-skeletal packstone-grainstone facies	This unit occurs in outcrop throughout the Warsaw and Salem units, but occurs more commonly in the Salem. Present as a thin to thick bedded unit, and also documented as channel infills, it contains a diverse assemblage of fauna from peloids, forams, crinoids, fenestrate bryozoans as well as brachiopods, bivalves and gastropods. Sedimentary features include wavy laminations, trough cross bedding, current ripples as well as some sigmoid and mud drapes. The mud drapes represent a tidally-influenced environment, with high energy, shoal complex.
Crinoid-bryozoan packstone-grainstone facies	This unit is present in abundance in the Warsaw section. In outcrop it occurs from thin to thick bedded and is identifiable by it dominant abundance of crinoids and both ramose and fenestrate bryozoans. Glauconitic rich, it also has an abundance of brachiopods, peloids, and both rugose and syringoporid corals. Sedimentary structures associated with this unit include wavy laminations, occasional trough cross bedding, coarse to fine layering and the occasional Glossifungites. The presence of diverse grains and internal bedforms indicate an open marine environment with moderate energy.
Glauconitic skeletal packstone-grainstone facies	This facies is present only in the lower part of the Upper Warsaw unit. It occurs in outcrop as a thin to thick bedded deposit, dominated by crinoids, bryozoans (ramose and fenestrate), brachiopods, peloids, rugose and syringoporid corals. It is also rich in glauconite and has a faint green tinge color to it and occasional Glossifungites may be present. Sedimentary features associated with this unit are some wavy laminations and phosphatized grains or surface burrows with coarse to fine layering. This deposit is interpreted to be a sediment starved sub-wave base marine deposit.
Dolomitic peloidal-skeletal packstone facies	This facies occurs throughout the section in both the Warsaw and Salem. Varies from thin to thick bedded, this unit is rich in peloids, crinoids and forams, and is generally associated with wavy laminations and calcite filled vugs. This facies is interpreted to be deposited under restricted low energy conditions in the subtidal to intertidal zone. The calcitic vugs are thought to be due to argillaceous rare evaporitic molds.

Burrowed packstone-wackestone facies	This facies occurs throughout the Warsaw and Salem section. In outcrop it occurs as both thick and thin bedded, with brachiopods, crinoids and bryozoans present within it. Any previous sedimentary structures have been destroyed by the intense burrowing. This facies is thought to be deposited in an open marine, low energy deposit.
Peloidal wackestone-packstone facies	Thin to thick bedded grainstones, occurs throughout the section and are typically composed of forams, crinoids and peloids. No distinguishable sedimentary structures are present. This facies is interpreted to be a low energy, open marine deposit.
Dolomitic spiculitic wackestone-packstone facies	Present throughout the section, this facies occurs either as thin or thick bedded in outcrop, and is commonly associated with burrows and some wavy laminations. Typical grains present include crinoids, peloids, sponge spicules and fenestrate bryozoans. Depositional environment is interpreted to be an open marine low energy.
Dolomitic mudstone-wackestone facies	This facies occurs in both the Warsaw and Salem in outcrop. It's rich in peloids, crinoids and forams, and is generally associated with wavy laminations and calcite filled vugs. This facies is interpreted to be deposited under restricted low energy conditions in the intertidal zone. The calcitic vugs are thought to be argillaceous rare evaporitic molds.
Argillaceous mudstone facies	The argillaceous mudstone is only found in the Warsaw Unit in outcrop, as a thick bedded mudstone deposits, with some wavy laminations and rare presence of brachiopods and crinoids. This deposit is interpreted to represent sub-wavebase marine conditions and is generally associated in the transgressive part of the sequences.
Claystone/Shale facies	The Claystone shale facies occurs in outcrop only in the Warsaw unit, as a thin, platy, laminated bedded unit, with very rare brachiopods and crinoids present. It is interpreted to represent sub-wavebase marine deposits and is generally associated as the onset of the transgressive sequence.

Table 3.2: Lithofacies of the Warsaw and Salem Formations taken from Rankey 2003.

High Resolution Sequence Stratigraphic Cycles

The genetic cycles defined here is modified from Rankey (2003), where three major cycles are separated out. There is an overall 4th order shallowing upwards trend from the lower Warsaw to the Salem. The fifth order cycles are broken into the Salem Formation idealized cycle, the upper part of the Upper Warsaw formation, and the lower part of the Upper Warsaw formation (Fig. 3.11).

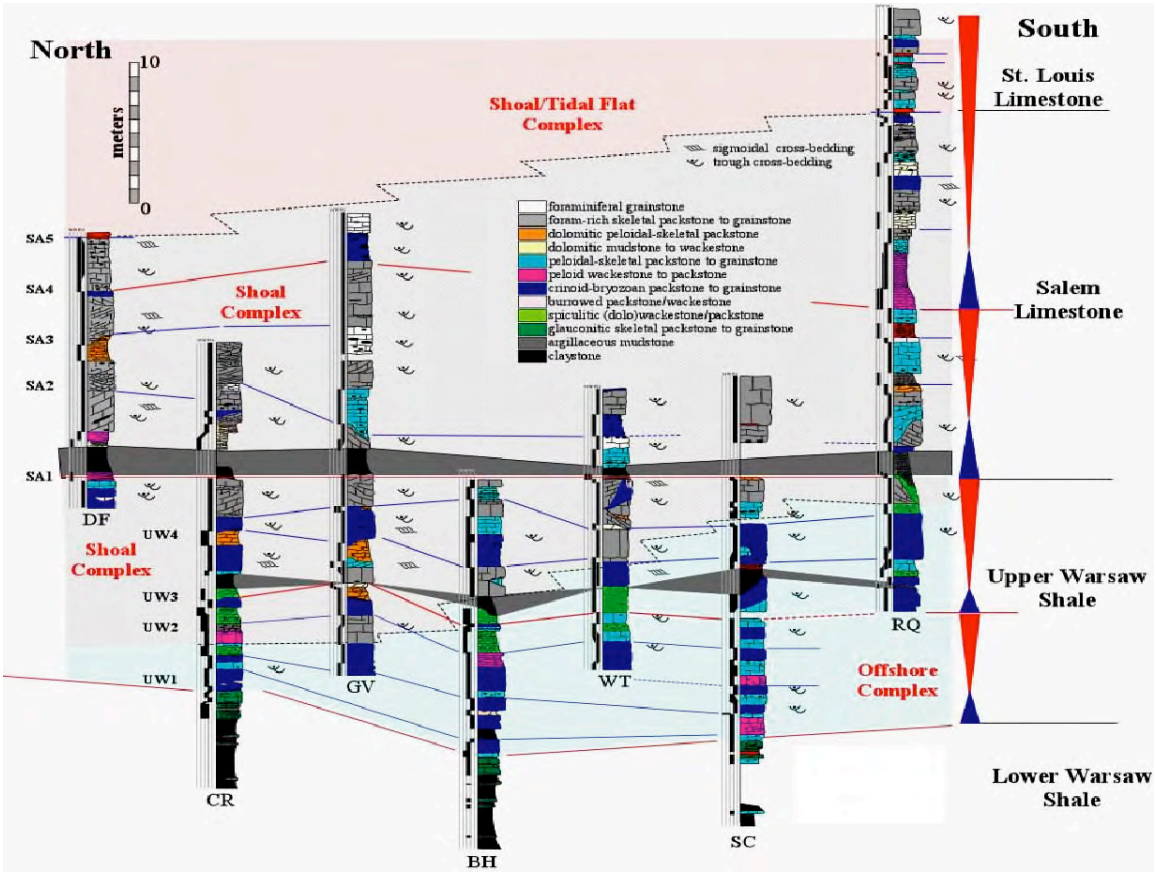

Figure 3.11: Stratigraphic cross-section of the Middle Mississippian Lower Warsaw Shale-basal St. Louis, south of St. Louis County, Missouri.

The lower part of the Upper Warsaw Genetic Cycle:

The lower part of the Upper Warsaw cycle is generally typified at the base by a spiculitic, argillaceous, laminated peloidal, skeletal wackestone to packstone which shoals into a grainstone and is capped at the top by a cross bedded, crinoidal bryozoan grainstone.

The upper part of the Upper Warsaw Genetic Cycle:

Two genetic cycles are identified in the upper part of the Upper Warsaw. As the Upper Warsaw varies laterally, an up dip genetic cycle is identified and a down dip cycle.

The updip genetic cycle consists at its base of a cross bedded to sigmoidally cross bedded grainstone which transgresses into a dolomitic wackestone, and is capped by a skeletal grainstone.

The down dip cycle's base is generally represented by a grey shale and an argillaceous peloidal-skeletal which shoals into a sometimes burrowed crinoidal, skeletal packstone, which shoals further into a skeletal grainstone.

Salem Formation Genetic Cycle:

The ideal Salem Formation genetic cycle varies between 3 to 6 meters thick, and its base generally consists of either a peloidal packstone to a dolowackestone packstone, or a claystone which forms the initial transgression from the Upper Warsaw into the Salem Formation. A foram skeletal grainstone, with trough or sigmoid cross bedding, and muddy drapes overlies the lower packstone unit. This grainstone is the initial regressive hemicycle of the Salem formation. This is overlain by a dolomitic packstone, which again is the next transgressive hemicycle, and is capped by the regressive foram skeletal grainstone.

Flank of Illinois Basin - St. Louis, Missouri – Results

Three main sections from previous work done by Rankey (2003) were measured for mechanical stratigraphy and comparison with the genetic hierarchy (Fig. 3.12). The measured sections are:

1. Gravois Road Section (GV)
2. Cragwald Quarry Section (CR)
3. Cardinal Quarry Section (RQ)

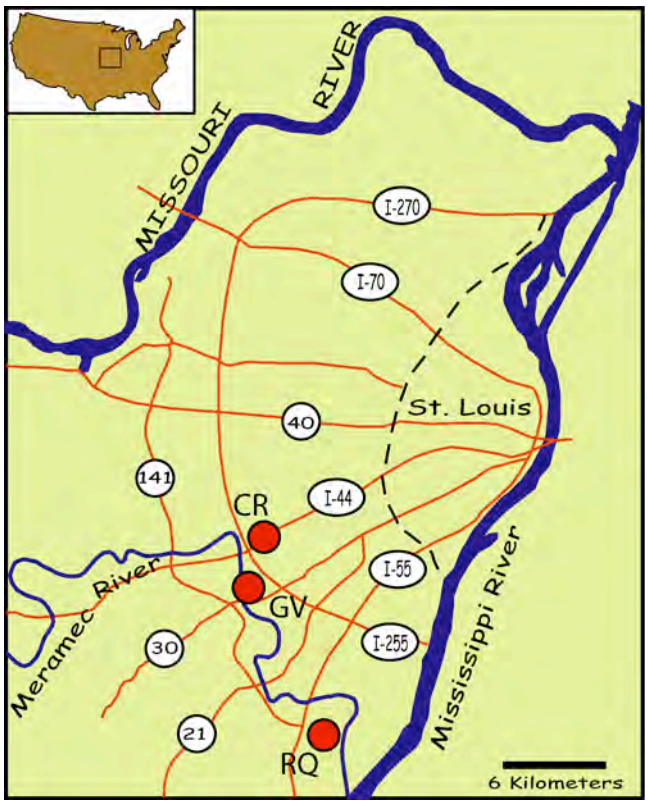

Figure 3.12: Map displaying locations of measured sections of the Lower Visean carbonates in St. Louis, Missouri. The red lines indicate interstates, and the dotted line indicates St. Louis city outskirts. Sections are Cragwald Road (CR), Gravois Road (GV) and Cardinal Quarry (RQ).

Gravois Road Section:

The Upper Warsaw-Salem Formations consist of genetic units in which interbedded grainstones to packstones of variable grain composition (crinoids, bryozoan, foraminifera) are interpreted to represent the regressive hemicycle while dolomitic wackestones, mudstones and claystones are interpreted to represent the transgressive hemicycle of the genetic unit. This interpretation is consistent with the facies interpretation in the lower order sequences as described by Rankey (2003). At the Gravois Road section four genetic units in the uppermost part of the Upper Warsaw Formation was measured (Figure 3.13). The base of the section is a coarsening upward crinoidal-bryozoan packstone to grainstone, which is overlain by bed of similar facies but that contains small evaporite rosettes. The evaporitic bed is interpreted as the regressive hemicycle, and the underlying packstone is considered the transgressive hemicycle. A sharp boundary forms the top genetic unit boundary. The overlying peloidal packstone bed is dolomitized that is capped by a dolomitic mudstone represents the next transgressive hemicycle. The top of the mudstone is interpreted as the mfs within this cycle that has a foram-skeletal packstone regressive hemicycle. A partially dolomitized peloidal packstone which then grades into a dolomitic peloidal packstone represents the onset of a new transgression, and the deposition of the third genetic unit.

In this unit, the regressive hemicycle consists of a thick large cross-bedded crinoidal, bryozoan packstone, which is capped by a dolomitic packstone that forms a discontinuous lens. This dolomite lens is interpreted as the onset of a small transgression, before it is overlain by a foram-skeletal packstone, which represents the final regressive

hemicycle within the Gravois section of the Upper Warsaw Formation. The facies in the overlaying Salem Formation is a thick grey claystone unit (Fig. 3.1.3; Rankey 2003).

Five mechanical units were measured in this Gravois Road section (Fig. 3.13). Within the units the majority of the fractures (>85%) terminate at bedding surfaces, which are therefore defined as mechanical unit boundaries (Figure 3.13). The data also show that these mechanical boundaries correspond to either a genetic unit boundary or the turnaround point within the genetic cycle (Figure 3.13). Furthermore, the regressive hemicycles are usually less fractured with fracture densities ranging from 1 to 2 fractures per meter than the transgressive hemicycles which have fracture density ranging from 3 to 4 fractures per meter (Figure 3.13).

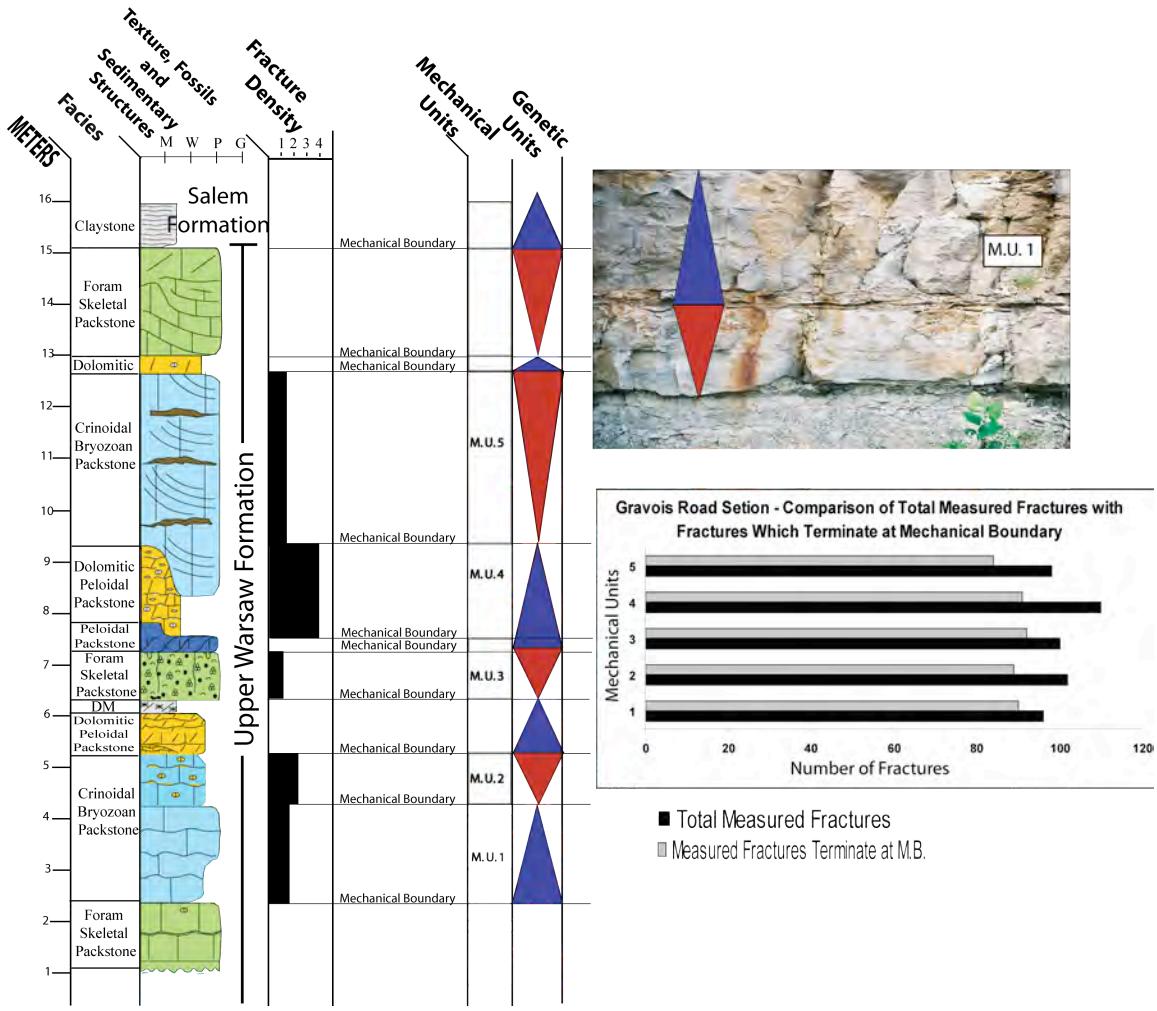

Figure 3.13: Gravois Road Hill measured section displaying the variations in fracture density of the different mechanical units and their correlation to the genetic units.

Cragwald Road Section:

At the Cragwald Road section the stratigraphic interval measured crosses from the Upper Warsaw Shale into the Salem Limestone (Fig. 3.14). Eight genetic cycles have been identified in the Cragwald Road section; six within the Warsaw Formation and two genetic cycles within the Salem Formation (Fig. 3.14). The base of the Warsaw Formation at Cragwald Road consists of a claystone, which represents the transgressive

hemicycle. It is capped by a skeletal packstone with some interbedded mudstones that together are interpreted to be the regressive hemicycle of this genetic cycle. The next genetic unit has a thin-bedded wackestone, which forms the transgressive hemicycle and is then overlain by thick regressive hemicycle composed of crinoidal and bryozoan-rich packstones to grainstones (Fig. 3.14). Overlying the crinoidal bryozoan grainstone is a foram-skeletal packstone bed, which has an unconformity surface at the top. Therefore the third genetic unit identified is compressed to this individual packstone bed. The unconformity is overlain by another regressive hemicycle consisting of crinoidal bryozoan grainstones, the transgressive hemicycle is condensed in the unconformity and has no sedimentary expression (Fig. 3.14). The next cycle has a transgressive hemicycle consisting of a dolomitic peloidal wackestone and a crinoidal-bryozoan grainstone, which represents the regressive hemicycle. The transgressive hemicycle of the last genetic unit measured within the Warsaw Formation at Cragwald Road is represented by a thick dolomitic packstone, which fines upward into a claystone and is capped by a regressive hemicycle of crinoidal dominated grainstone.

The base of the Salem Formation is poorly exposed in outcrop at Cragwald Road. It is represented by a claystone unit, which grades into a slightly dolomitized mudstone. A foram skeletal cross-bedded grainstone overlies the mudstone and hence is interpreted to be the regressive hemicycle, which completes the first genetic unit within the Salem Formation (Fig. 3.14). The next genetic cycle again has a dolomitized mudstone in the transgressive hemicycle and a thick cross-bedded foram grainstone as the regressive hemicycle (Fig. 3.14).

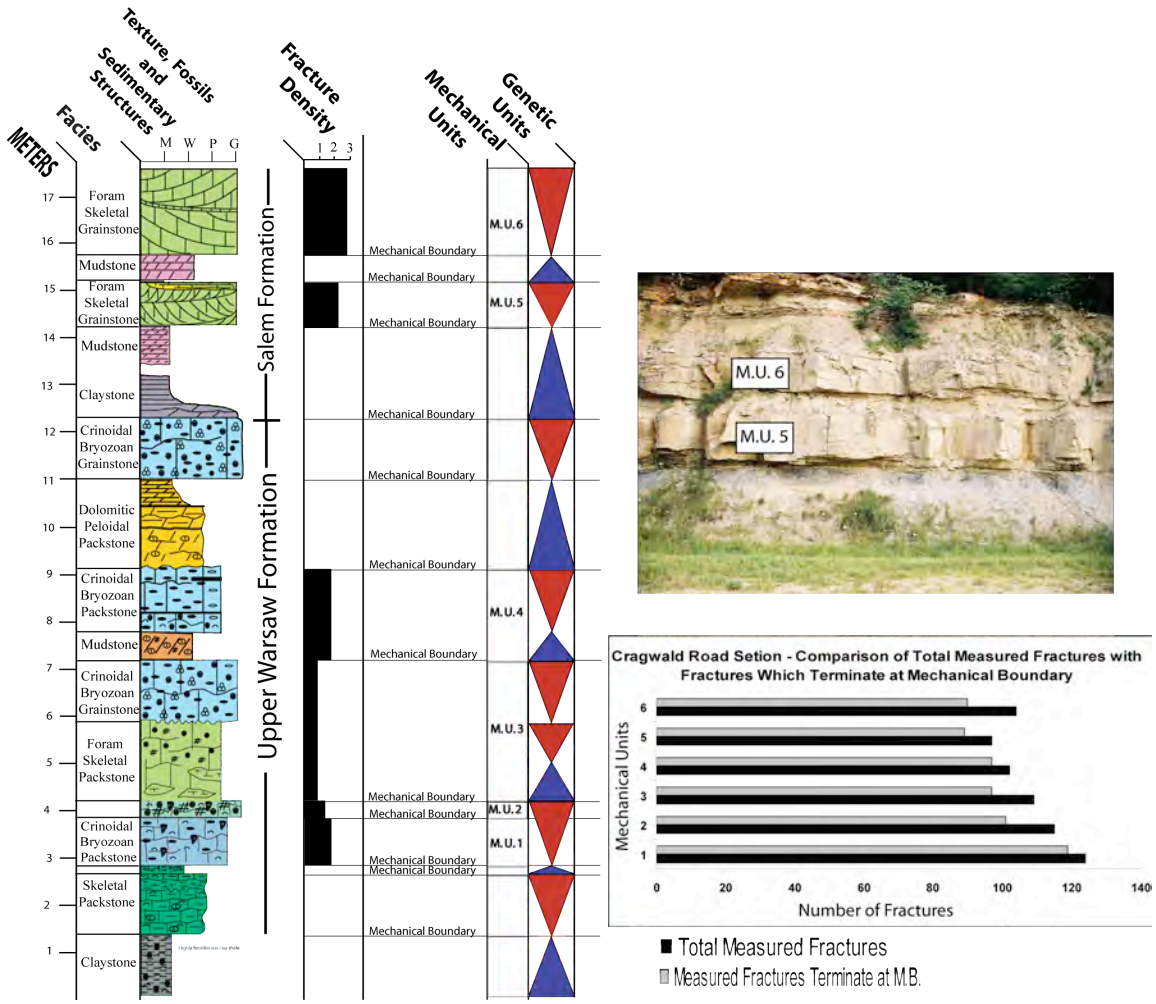

Figure 3.14: Cragwald Road measured section displaying the variations in fracture density of the different mechanical units and their correlation to the genetic units.

A total of six mechanical units were measured at Cragwald Road section. Similarly to the previous section, the majority of the fractures measured within each unit terminated at a specific bedding surface, which is thus defined as the mechanical boundary (Fig. 3.14). Four of the mechanical units identified and measured correspond to the regressive hemicycles of the genetic units. Two mechanical units, however, correspond to more than one hemicycle (mechanical units 3 and 4), (Fig. 3.14). Thus, the conclusion is that the genetic boundaries and their turnaround points mostly correspond to mechanical

boundaries but not always. It is speculated that blasting along the road has caused fractures to cross genetic boundaries because of the superficial fracturing.

Cardinal Quarry Section:

Along the Cardinal Quarry road section the Upper Warsaw and Salem Formations are exposed. The base of the section begins with a regressive hemicycle that consists of a two stacked crinoidal bryozoan packstones (Fig. 3.15). Overlying the packstones is a transgressive hemicycle with a thin hematitic clay-rich layer at the base overlain by foraminifera grainstone. Overlying this transgressive sequence is a spiculitic peloidal wackestone to packstone that grades into a rich peloidal packstone, which forms the regressive hemicycle of the genetic unit (Fig. 3.15). The next genetic cycle consists of a crinoidal bryozoan grainstone in the transgressive hemicycle and a spiculitic dolomitic wackestone that is carved by a foraminifera skeletal grainstone that forms the regressive hemicycle within the Warsaw Formation (Fig. 3.15).

The Upper Warsaw Salem Formation boundary is placed in a claystone on the top of a dolo-wackestone (Rankey, 2003). The base of the Salem Formation consists of the transgressive claystones; above a sharp erosional surface is a thin crinoidal bryozoan grainstone followed of stacked of grainstones to packstones with complex geometries that form the regressive hemicycle of the genetic unit (Fig. 3.15). The transgressive hemicycle within the Salem Formation is composed of a dolomitic peloidal packstone to wackestone which is capped by a thin chert horizon that is topped by an argillaceous mudstone. The regressive hemicycle consists of a peloidal, skeletal grainstone that is topped by a claystone, which represents the next transgressive event (Fig. 3.15).

Seven mechanical units were identified and measured at the Cardinal Quarry section. Of the seven measured sections over 85% of the total number of fractures terminate at bed boundaries that are identified as mechanical unit boundaries (Fig. 3.15). Yet due to the intense heterogeneity of the formations and channel forms, not all the genetic unit boundaries and their turnaround points correspond with mechanical boundaries. Furthermore, the variations in fracture density demonstrate that the regressive hemicycles are more fractured than the transgressive hemicycles (Fig. 3.15).

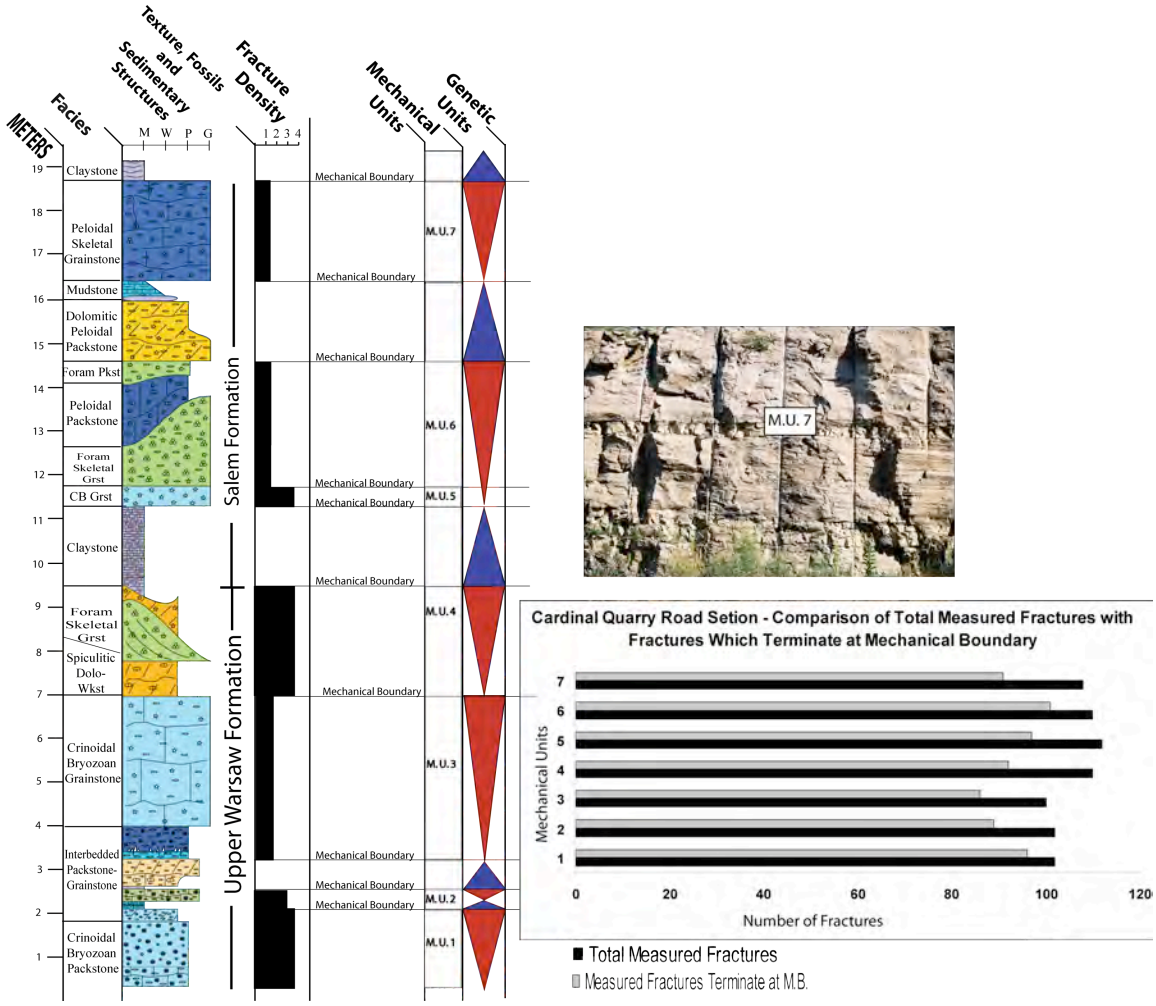

Figure 3.15: Cardinal Quarry measured section displaying the variations in fracture density of the different mechanical units and their correlation to the genetic units.

Flank of Illinois Basin - St. Louis, Missouri - Conclusions

In the Mississippian limestones of Missouri, the genetic unit boundaries correlated well in most to all cases with the mechanical unit boundaries. It can be seen once again that a genetic unit is composed of two mechanical units. The regressive hemicycle controlled mechanical units generally contain a higher fracture density than the transgressive hemicycles, because the grainstones in these Mississippian limestones contained complex internal geometry that created sub-mechanical units. This will be discussed further in the next chapter. Another main observation demonstrated in the Mississippian limestones of Missouri is that lateral facies changes within depositional sequences and complex geometries within facies create also heterogeneities in mechanical stratigraphy. Relations also exist between carbonate beds and chert layers or nodules demonstrating different mechanical strengths of the different units. Where chert is intensely fractured, fracturing is localized in adjacent grainstones, whereas in mudstones to wackestones the fracturing in the chert extends out into the carbonate units. Finally, the observations that these blasted road cuts show consistent and identifiable fracture patterns implies that induced fracturing is controlled by the same mechanical properties as natural fractures.

Paradox Basin, Bluff, Utah

Overview

The Paradox Basin is a northwest-southeast trending, asymmetric basin located in southeastern Utah and southwestern Colorado. It formed in the Middle Pennsylvanian due to reactivation of a complex Precambrian fault system (Baars & Stevenson, 1982). The asymmetric basin topography was produced by major uplift of the northwest-southeast trending Uncompahgre uplift, which forms the prominent eastern and northeastern depositional boundary of the Paradox basin, and relatively minor uplift of tectonic elements to the south, west and north of the basin (Baars & Stevenson, 1982).

A combination of tectonic movement and depositional barriers restricted circulation within the Paradox basin, which resulted in the deposition of evaporites along the northeast-southwest trending basin axis. In the Desmoinesian, high frequency sea level changes produced a cyclic deposition of shallow marine carbonates including the algal mound reservoir facies along the shelf and evaporites and black shales in the basin. In the Paradox Formation of the central part of the basin, there are up to 2000 meters of evaporites (both salt and anhydrite) rhythmically interstratified with black shales (Goldhammer et al., 1991; Choquette, 1983).

The Paradox basin is an asymmetric basin with a thick evaporite sequence in the basin axis and a mixed carbonate/siliciclastic sequence in the southwestern shelf (Peterson and Hite, 1969). On this wide and shallow shelf, cyclic deposition of eolian, fluvial and marine sedimentation occurred, creating a complex sedimentary system. Algal buildups within the carbonate intervals are a major hydrocarbon reservoir (Choquette & Traut,

1963). Algal mound reservoirs occur on the southern margin of the Paradox Basin in an area about 180km by 50km (Choquette, 1983).

Depositional History

The Desert Creek and Ismay members of the Paradox Formation contain the hydrocarbon-producing algal mound fields. High frequency sea-level fluctuations controlled the vertical facies development within small scale (meter scale) genetic units (Goldhammer et al., 1991, 1994; Grammer et al., 1996). Each high-frequency sea level fall and rise produces a depositional cycle of sandstones (at the base) and carbonates (at the top) capped by an exposure horizon and/or a flooding surface (Goldhammer et al., 1991, 1994; Grammer et. al., 1996). Limited sediment supply for the siliciclastic portion and the mismatch between the rate of carbonate production and the rate of sea level change resulted in unfilled accommodation space and lateral thickness variations in these depositional cycles (Grammer et. al., 1996). On the southern margin, cycles consist of a basal sandstone unit that was likely deposited during sea level lowstand and reworked during marine transgression. These are overlain by black shales which mark the maximum flooding interval for the cycles. The overlying carbonates are characterized by a well defined shallowing-upward trend deposited during sea level highstand (Grammer et al., 2000).

Lithofacies Description of Genetic Unit

The eight lithofacies described below are a general composite based on more detailed lithofacies described by Grammer et al. (1996).

An ideal cycle for the Desert Creek, Lower Ismay sections of the Paradox Basin contains a siliciclastic base and shallowing upwards carbonates (Goldhammer et al., 1991 and Grammer et al., 1996).

The ideal cycle taken from Goldhammer et al. (1991) starts with transgressive deposits of eolian dunes that blew across the carbonate platform during sea level fall and were then later reworked and redeposited with calcitic cements. The transgression hemicycle continues with the deposition of the black laminated mudstone which grades into restricted platform mudstone wackestones and then into normal shallow marine wackestones and packstones.

The onset of the intermediate facies represents the maximum flooding surface, with later deposition continuing to shoal upwards into skeletal packstones to grainstones, and is finally capped by oolitic packstones to grainstones.

A modification of this ideal cycle consists of carbonate cycles with no siliciclastic input. For example in the Lower Ismay, the base of the cycle is a spiculitic carbonate mudstone to bioturbated skeletal open marine wackestone, which regresses into a phylloid algal, and a chaetetes zone which is then capped by a fusulinid foram packstone. Also, the phylloid algal mound is not present in all cycles, but a shelfal equivalent is always present. In a mixed carbonate siliciclastic cycle from the Desert Creek the transgressive hemicycle is composed of quartz sandstone and bioturbated skeletal wackestone, with the regression being composed of only oolitic coated grainstones.

Type of Lithofacies	Description
Quartz sandstone facies	The quartz sandstone facies is composed of well sorted fine grained quartz sandstone to siltstone mixed in with skeletal fragments, peloids and lithoclasts, and is cemented with calcite. Sedimentary structures include herringbone cross lamination, tidal current ripples and wave ripples. Minor local burrows and mud drapes occur locally. This facies is interpreted to be transported eolian silts and sand onto the shelf during relative lowstands and subsequently reworked in a tidal environment during transgressions. In other cases there are present hummocky cross stratification and tabular cross bedding, which indicate that the eolian sands were reworked in an open shelf marine environment during the flooding of the platform and hence deposition occurred in the middle to upper shoreface.
Black laminated mudstone facies	This facies occurs as a dark gray to black, dolomitic, silty, organic rich, argillaceous mudstone. Some minor sponge spicules and thin shelled brachiopod fragments are present. Sedimentary structures include lamination and millimeter thick silt stringers. This facies is interpreted to be deposited in an anoxic to anaerobic relatively deep marine conditions during rapid transgressions.
Incipient mound facies	This facies is distinguishable by its sharp basal contact, and is a muddy phylloid algal mudstone to wackestone with a peloidal mud matrix. This facies is interpreted to be a low energy, open marine platform where accumulation of phylloid algal plates and carbonate mud are deposited.
Sponge facies	The sponge facies is a brownish black to dark brownish gray, silty carbonate mudstone with chert nodules. It is dominated by siliceous sponges with low fauna diversity, which includes brachiopods. Sedimentary structures include laminations, bioturbation and nodular to wavy bedding with significant chert presence. The depositional environment of this facies is interpreted to be a highly restricted facies deposited in relatively shallow, low energy subtidal environment during initial flooding of the platform.
Intermediate facies (2)	There are two main types of intermediate facies, as identified by Grammer et al. (2000), 1). Restricted intermediate facies and 2). Diverse intermediate facies. The restricted facies is burrow mottled, has a low faunal diversity and is dominated by brachiopods in a mudstone to wackestone matrix. It represents a low energy, shallow restricted platform facies deposited during the early the stages of platform flooding.

Intermediate facies (2) (continued)	The diverse intermediate facies is a bioturbated skeletal, peloidal wackestone to packstone, with a diverse marine fauna of crinoids, brachiopods, forams and bryozoans. It is highly bioturbated and mottled and interpreted to represent a low to moderate energy, open marine platform, and represents the later stages of platform flooding.
Phylloid algal mound facies	In outcrop this facies morphology varies from flat and elongate (i.e. biostromal) to mound-like with flat bases. The phylloid algal bioherms internal fabric varies from grain-supported algal bafflestones to wackestones and packstones. The most abundant type of phylloid algae is the Ivanovia which is a codiacean green algae, that has a leaf-like form. The phylloid algae is thought to have grown in warm, shallow, moderate energy, open platform marine waters with low tidal ranges.
Non skeletal capping facies (2)	There are two main types of non skeletal capping facies as defined by Grammer et. al. 2000. The oolitic facies contains ooids and coated grain packstones to grainstones. They are generally cross-bedded and represent a shallow water depositional environment of high-energy shoals. The peloidal capping facies is generally composed of peloidal wackestones to packstones, with minor quartz input. They are thin bedded and represent a Peloidal mud flat, which was deposited in intertidal to shallow subtidal environments.
Skeletal capping facies (3)	Three main types of skeletal capping facies are identified by Grammer et al. 2000. These types are based on faunal assemblages, and range from diverse fauna, to crinoidal facies and fusulinid capping facies. The diverse skeletal capping facies are generally packstones, with some wackestones and grainstones, and consists of a diverse assemblage of marine fauna. This facies represents a moderate energy shallow platform facies associated with shoals and channels. The crinoidal facies are generally packstones to grainstones. They are massive with well developed trough-cross bedding. This facies represents a high energy, shallow platform shoal depositional environment. The third skeletal capping facies are the fusulinid dominated wackestones; packstones that are it's interpreted as a low to moderate energy shallow marine subtidal deposit.

Table 3.3: Lithofacies defined from the Lower Ismay and Desert Creek Formations in the Paradox Basin by Goldhammer et al., 1991.

Paradox Basin, Bluff, Utah – Results

Honaker Trail Sections:

Section 1:

The first measured section at Honaker Trail occurs in the top part of the Upper Ismay Formation close to the boundary between the Upper Ismay Formation and the Honaker Trail Formation. The section in total thickness is ~12.5m thick and begins with a regressive hemicycle and consists of three genetic cycles. The regressive hemicycle at the base of the section is composed of grain dominated peloidal packstone. The first genetic cycle above the top of the shoal has a transgressive hemicycle of peloidal wackestones interbedded with finer grained muddier units fining upwards to a more homogeneous mudstone. The flooding surface is sharp and abrupt, and is expressed by the dramatic change from the transgressive mudstones into the regressive hemicycle expressed by the ~4.5m thick grain dominated peloidal packstone. The peloidal packstone/grainstone is capped at the top by a thin cemented horizon which marks the top of the genetic cycle boundary. The next genetic cycle's transgressive hemicycle begins with a meter thick of peloidal/crinoidal mudstone to wackestone, overlain by a ~0.3m thick oolitic grainstone bed which forms the regressive hemicycle of the genetic cycle. Above the oolitic shoal top which forms the genetic cycle boundary another fine grained wackestone represents the transgressive hemicycle of the third genetic cycle, which is capped by another regressive hemicycle of peloidal grainstones ~2.5m thick (Fig. 3.16).

Seven mechanical units were identified based on the mechanical boundaries. The fractures were measured in six different mechanical units. Fractures were measured in the

first regressive hemicycle and 89% of the fractures terminated at the top of the genetic boundary. The next mechanical unit identified which is the transgressive hemicycle of the first genetic cycle, and consists mainly of the black laminated mudstone was not measured for fractures because the turnaround point from transgression to regression is defined as a mechanical boundary because all the fractures present in the thick peloidal packstone does not propagate down into the mudstone unit, thereby defining the base and top of the first transgressive hemicycle as mechanical boundaries and isolating the transgressive hemicycle as a mechanical unit. Again 89% of the fractures present in the regressive portion of the lower genetic cycle do not extend into either the transgressive hemicycle below it or the next genetic cycle above it, where all 99 fractures measured were isolated within the regressive hemicycle, by which our genetic unit sequence boundary is as well a clearly defined mechanical boundary (Fig. 3.16). The third mechanical boundary is identified at the turnaround point of the second genetic cycle where 78% of the measured fractures terminate and do not propagate into the regressive oolitic grainstone. The fracture density in this transgressive hemicycle averages about 6 fractures per meter and is high due to the laminations present in the wackestone (this will be discussed further in chapter 4). 90% of the measured fractures within the regressive hemicycle of the oolitic grainstone terminate at the genetic unit boundary and don't propagate across. The final genetic cycle is again composed of two mechanical units where the first mechanical boundary identified is where 90% of the fractures terminate in the transgressive hemicycle, and this occurs at the turnaround point of the third genetic cycle, and 87% of the fractures terminate in the regressive hemicycle at the top of the genetic cycle boundary. Hence, seven mechanical units are identified in section 1 of

Honaker Trail and the mechanical boundaries identified coincide with the genetic unit boundaries or their turnaround points (Fig. 3.16).

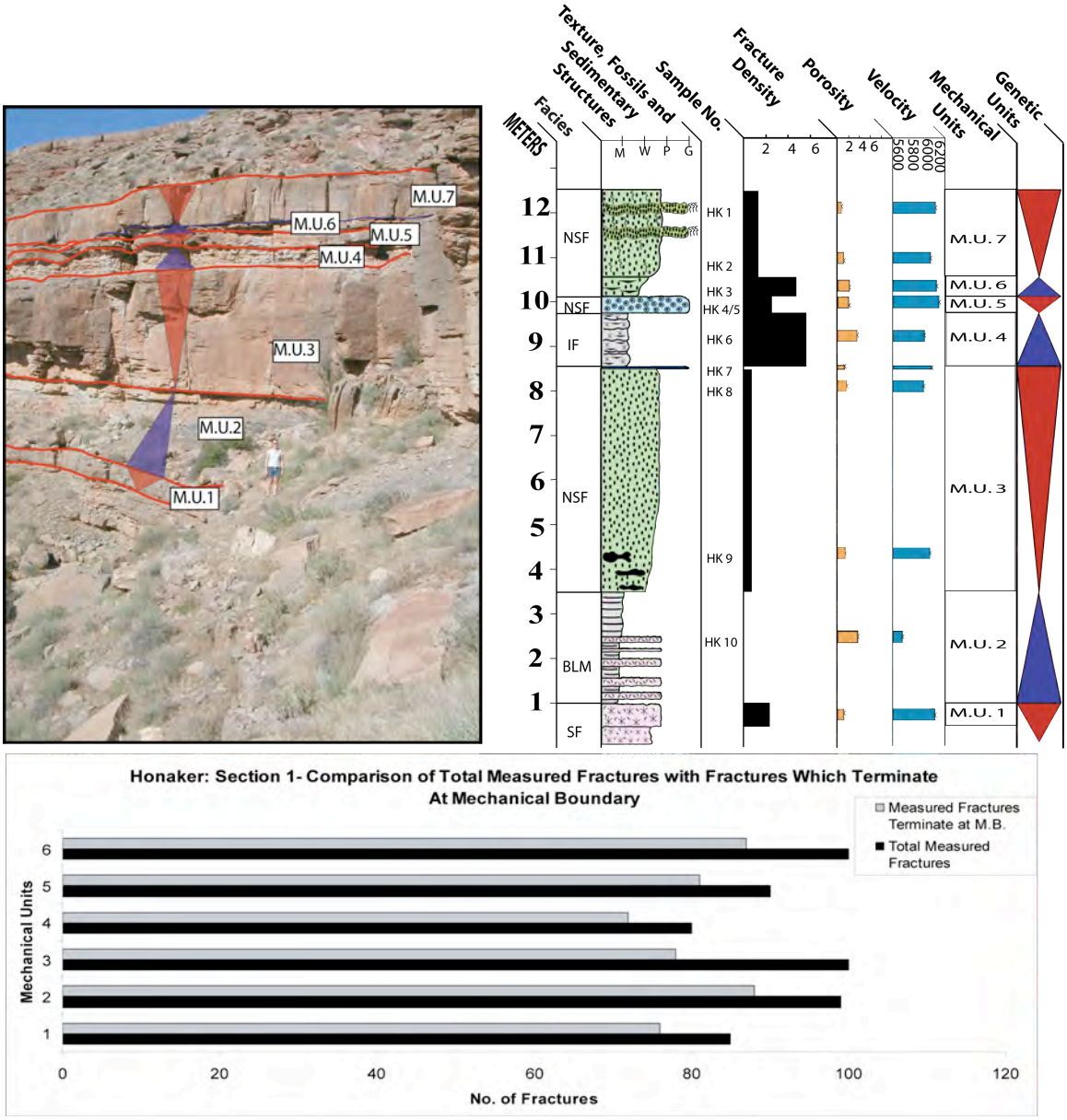

Figure 3.16: Measured Honaker Interval Section 1 at Honaker Trail. Dominant Facies Include; Non-Skeletal Facies and Skeletal Facies (Regressive Hemicycles), Black Laminated Mudstone and Intermediate Facies (Transgressive Hemicycle).

Section 2:

This measured section occurs in the middle part of the Upper Ismay Formation and the total section measured is about 10m thick. The section is composed of three genetic cycles, where the basal genetic cycle begins with a transgressive hemicycle composed of interbedded quartz sandstone and crinoidal mudstones to wackestones and the regressive hemicycle consists of a skeletal, peloidal wackestone to packstone, with an erosional top surface, marking the genetic boundary. Above the genetic boundary, the next genetic cycle begins with 1m thick homogeneous, quartz sandstone which is interpreted to be the transgressive hemicycle and above it ~1.5m quartz sandstone which is typified by bi-directional trough cross bedding and interpreted as the regressive hemicycle of the second genetic cycle, although this can be disputed as the idealized genetic cycle demonstrates that the sandstones is usually always interpreted as the transgressive hemicycle in this area (Grammer et al., 1996). A 0.5m thick mudstone unit forms the next transgressive hemicycle of the uppermost genetic cycle which is overlain by the regressive hemicycle represented as a peloidal skeletal packstone (Fig 3.17).

The fractures were measured in three mechanical units were measured but seven mechanical units were identified based on observations of the mechanical boundaries. The fractures were measured in six different mechanical units. Fractures measured in the first transgressive hemicycle were only measured in the sandstone unit because the other beds were heavily eroded and broken. In the regressive hemicycle of the first genetic cycle 78% of the fractures terminated at the top of the genetic boundary. The next mechanical unit identified which is the transgressive and regressive hemicycle of the quartz sandstones could not be accessed for fracture measurements, but from simple

observations, the mechanical boundaries were clearly observed and recorded (Fig. 3.17). The third mechanical unit measured is at the regressive hemicycle of the peloidal packstone of the top most genetic cycle, where 100% of the measured fractures terminated and did not propagate into the next transgressive portion of the next genetic cycle. Although the measured units were not consistently on-top of each other the mechanical boundaries were clearly observed with the naked eye and hence, seven mechanical units are identified in section 2 of Honaker Trail and the majority of the mechanical boundaries identified coincided with the genetic unit boundaries or their turnaround points except within the first transgressive hemicycle (Fig. 3.17).

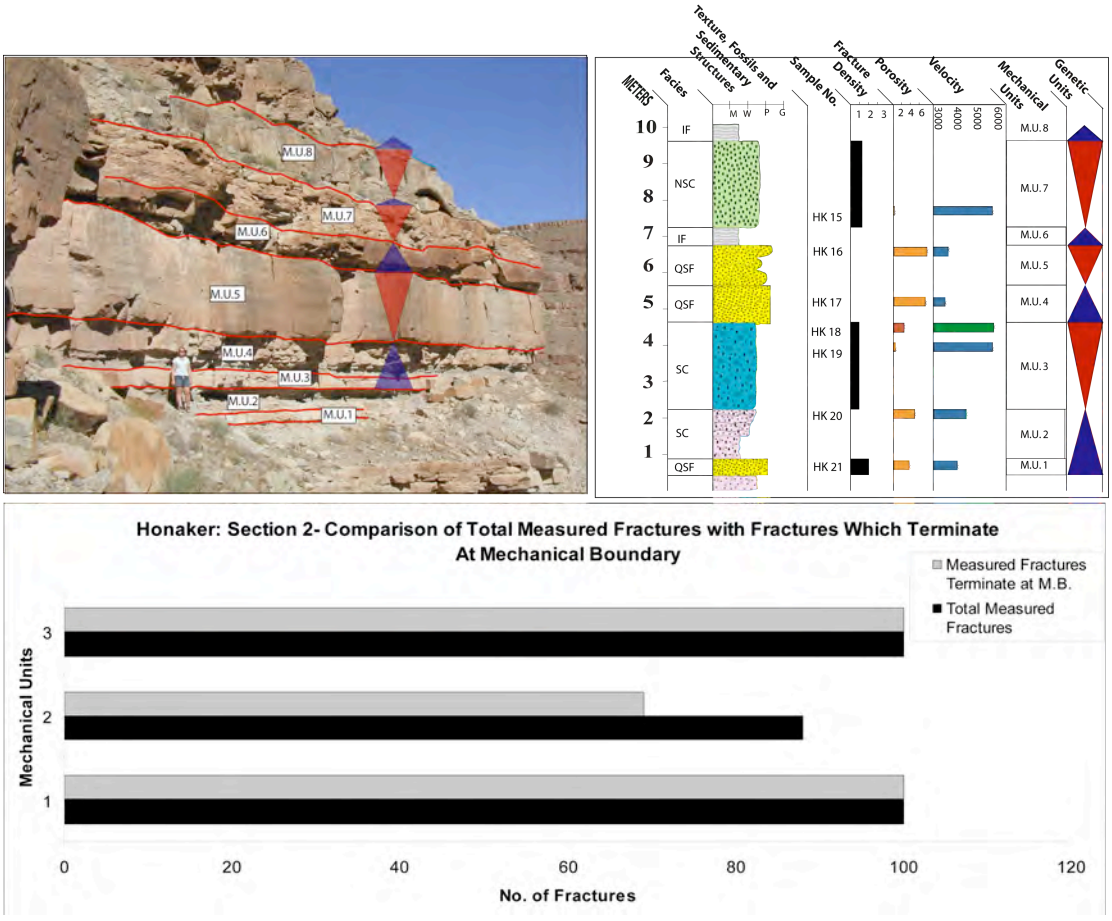

Figure 3.17: Section 2 from the Upper Ismay interval at Honaker Trail. The quartz sandstone is represented in the transgressive and regressive hemicycles. Internal bedforms create a larger fracture density.

Section 3:

Section 3 of Honaker Trail is measured in the lower part of the Upper Ismay formation and covers about 3m in total thickness. Although this section is a short section, it is interesting from the point of view in viewing how caliche surfaces can form mechanical boundaries and are possible barriers to flow. Two genetic cycles are identified in this section. The transgressive hemicycle of the first genetic cycle is a mudstone, which is overlain by a silty, peloidal, skeletal packstone to grainstone which forms the regressive hemicycle and its genetic boundary is clearly present by the ~2.5cm laminated crust. The next genetic cycle above the genetic boundary is represented by the deposit of the quartz sandstone, admixed with peloids and skeletal grains, and the presence of bi-directional trough cross bedding which is interpreted as is consistent with the literature as the transgressive hemicycle (Fig. 3.18).

The fractures were measured in the two mechanical units which were identified based on observations of the mechanical boundaries. All the fractures measured in the first regressive hemicycle terminated at the laminated crust which represents the top of the genetic boundary. The next mechanical unit identified which is the transgressive hemicycle represented by the quartz sandstone also identified a mechanical boundary at the top of the transgression where 100% of the fractures terminated (Fig. 3.18). Therefore the mechanical boundaries identified coincide with the genetic unit boundaries and their turnaround points (Fig. 3.18).

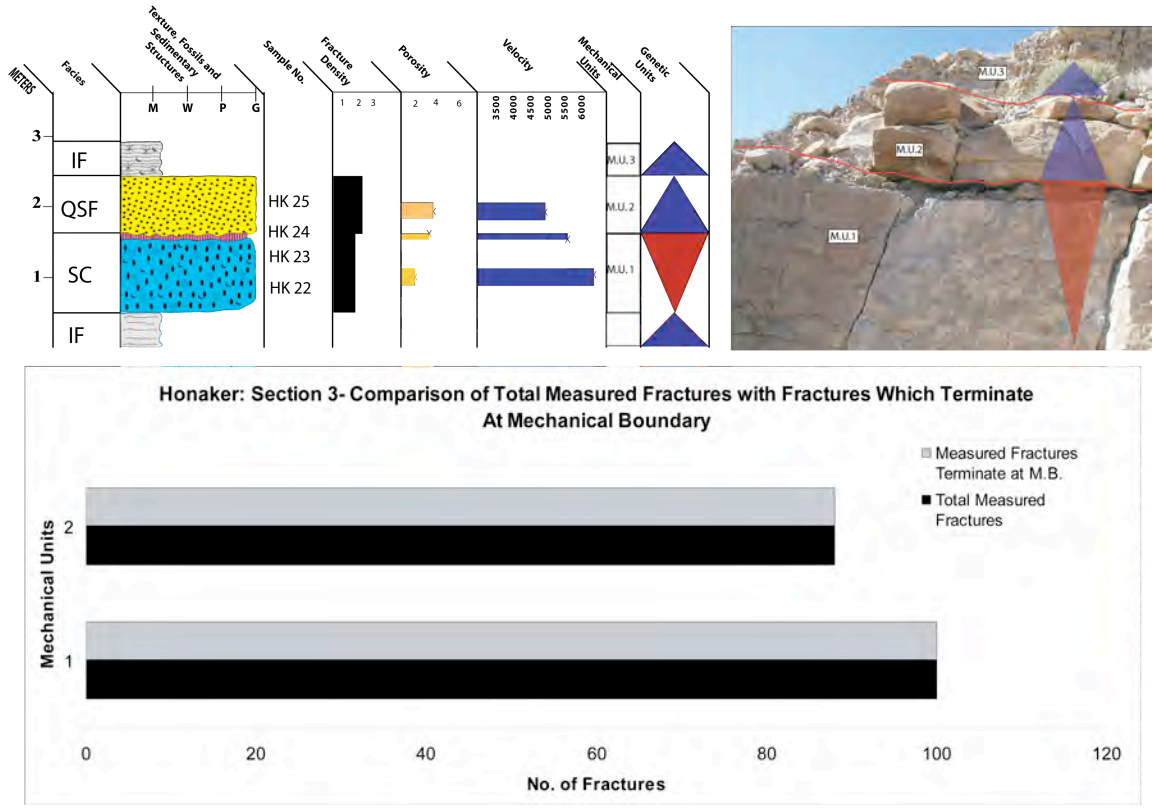

Figure 3.18: Measured Honaker Interval Section 3 at Honaker Trail. Mechanical units correlate well with genetic units.

Section 4:

This section is measured at the boundary between the Upper Ismay formation and the Lower Ismay formation. The section is about 5m thick but the measured section was done on the top surface of the transgressive lag and the laminated crust just above the Hornpoint bed. Two genetic cycles are identified and the section begins with the regressive hemicycle of the phylloid algal where the top of the genetic boundary is a sharp contrast between the algal bed and the transgressive hemicycle of the quartz

sandstone, which represents the onset of the next genetic cycle. The deposition of the infamous Hornpoint bed, forms the regressive hemicycle of the next genetic cycle, where the top of the Hornpoint is marked by a 10cm thick laminated “caliche” crust which marks the top of the genetic boundary. A 10cm thick transgressive lag rich in brachiopods, crinoids and corals mark the onset of the transgressive hemicycle and the next genetic cycle (Fig. 3.19).

The fractures were measured in the two mechanical units which consist of the laminated crust and the transgressive lag was measured using the area method (Fig. 3.19). All the fractures measured in the two units terminated at their corresponding genetic boundaries and turnaround points without displaying a difference in the fracture density, and so the mechanical boundaries identified coincide with the genetic unit boundaries and their turnaround points (Fig. 3.19).

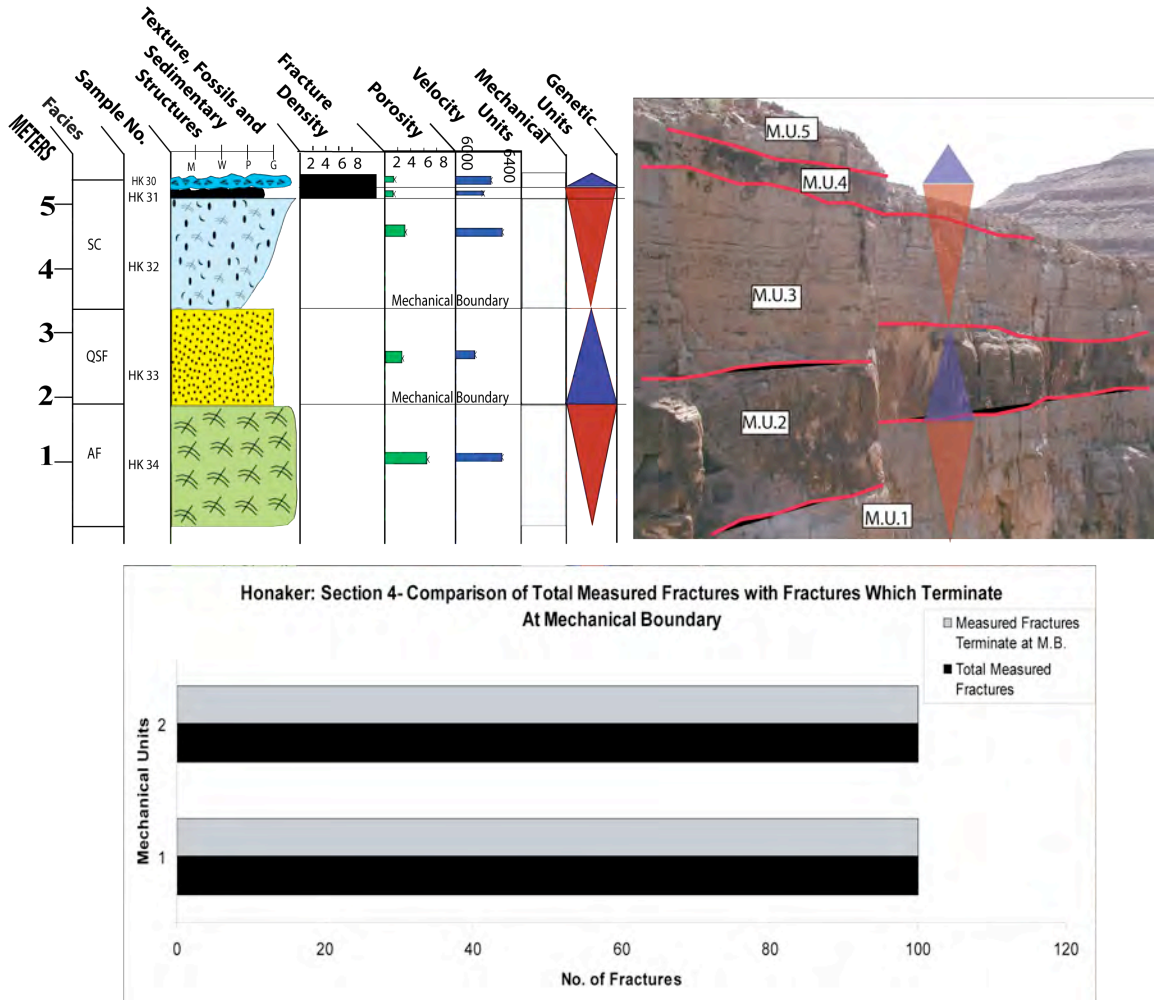

Figure 3.19: Honaker Interval Section at Hornpoint Bed. Dominant Facies Include; Algal/ Skeletal Facies (Regressive Hemicycles), and Sandstone and flooding surfaces (Transgressive Hemicycle).

Section 5:

This section occurs in the Desert Creek Formation and is measured near the boundary to the Lower Ismay Formation. The section is just less than 5m thick, and consists of two genetic cycles. The transgressive hemicycle of the first genetic cycle is a peloidal wackestone/packstone with skeletal grains, gastropods and brachiopods, above the wackestone is a 1m thick oolitic and coated skeletal grained packstone to grainstone which represents the regressive hemicycle of the genetic cycle. An exposure surface occurs at the top of the oolitic grainstone which marks the genetic boundary, and the

crinoidal, peloidal, skeletal wackestone which coarsens upwards into a packstone represents the next transgressive hemicycle of the second genetic cycle, which is heavily bioturbated at the top and indications of a firm ground, is possible, representing a genetic flooding surface. Overlying the packstone above the turnaround point from the transgressive hemicycle into the regressive hemicycle is another oolitic-coated grain packstone to grainstone, which is capped by yet another exposure horizon, as evidenced by brecciation and darkened soil fragments. Above the exposure surface is 0.5m thick muddy laminated wackestones, which demonstrates the onset of another transgression (Fig. 3.20).

All three mechanical units identified were measured for fracture termination and density. Fractures were measured in the first regressive hemicycle and 80% of the fractures terminated at the top of the genetic boundary. The next mechanical unit identified which is the transgressive hemicycle of the second genetic cycle had 81% of the fractures terminating at the turnaround point from transgression to regression is defined as a mechanical boundary. Finally 97% of the fractures present in the regressive portion of the upper genetic cycle do not extend into the transgressive hemicycle above it (Fig. 3.20). The mechanical boundaries identified in this section coincide with the genetic unit boundaries and their turnaround points (Fig. 3.20).

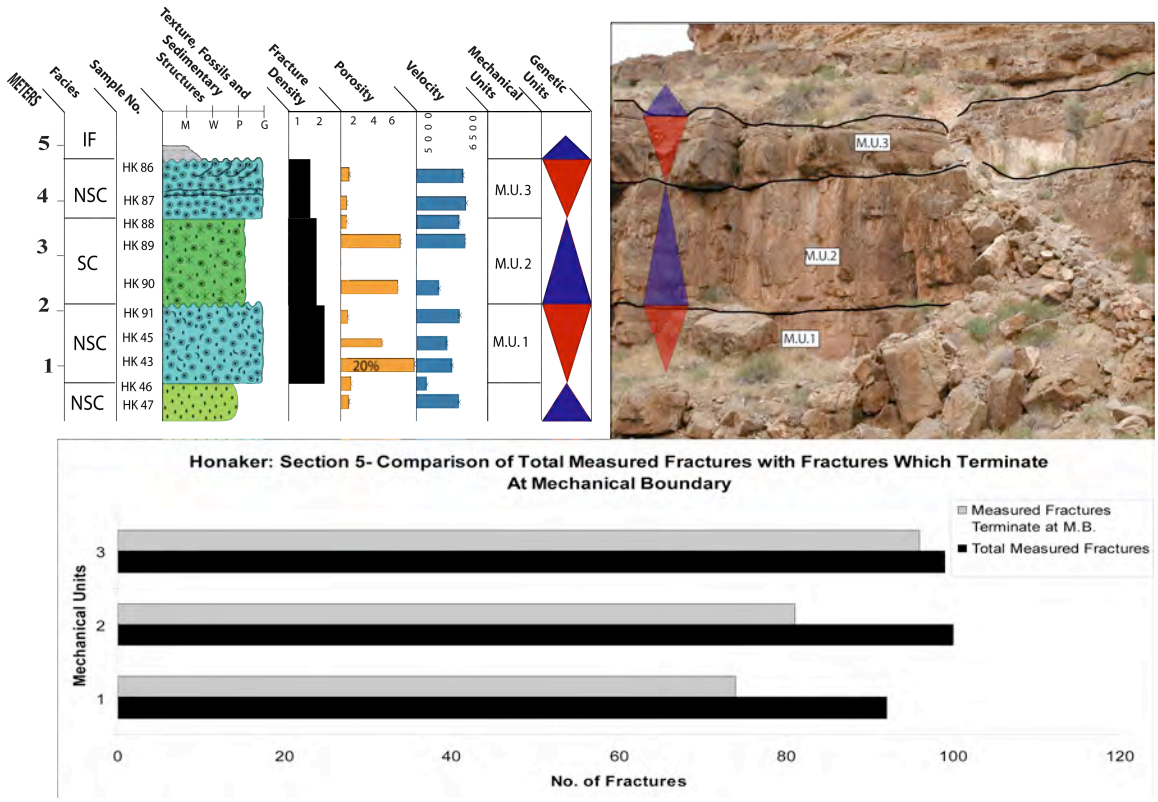

Figure 3.20: Measured Honaker Interval Section 5 at Honaker Trail. Dominant Facies Include; Non-Skeletal Facies (Regressive Hemicycles), and Skeletal/Intermediate Facies (Transgressive Hemicycle).

Section 6:

The final section measured at Honaker Trail, is from the Desert Creek Formation and is 6m thick. Three genetic cycles are present in this section. The basal genetic cycle consists of ~1.5m thick quartz sandstone that contains some wave and current ripples and is interpreted as the transgressive hemicycle. Above the quartz sandstone is the regressive hemicycle which is represented by a 1m thick oolitic packstone to grainstone that is both rippled and cross laminated. At the top of the oolitic grainstone there is some indication of an exposure surface, by minor crust formation which marks the genetic boundary.

The transgressive hemicycle of the next genetic cycle is not expressed and the regressive hemicycle is composed of a fine grained, highly bedded, fossiliferous wackestone to packstone which is also capped by an exposure horizon as indicated by the presence of black pebbles, thus giving us the indication of the presence of a genetic boundary. Above this, another thick oolitic, peloidal packstone to grainstone occurs, that is also capped by an exposure surface evidenced from brecciated clasts, which is also again interpreted to represent the regressive hemicycle of the genetic cycle and hence the transgressive hemicycle is once again not expressed in the rock record. The top of the section ends with the transgressive hemicycle composed of a fine grained, laminated, peloidal, silty, cherty mudstone (Fig. 3.21).

Four mechanical units identified were measured for fracture termination and density. Fractures were measured in the first transgressive hemicycle (quartz sandstone) and 92% of the fractures terminated at the top of the turnaround point. The next mechanical unit identified which is the regressive hemicycle represented by the first oolitic grainstone had 84% of the fractures terminating at its genetic unit cycle boundary and also demonstrates a higher fracture density than the mechanical unit above and below it. Overlying the oolitic grainstone is a second regressive hemicycle and 89% of the fractures terminate at its genetic unit cycle boundary. Finally 90% of the fractures present in the uppermost regressive hemicycle represented by another oolitic grainstone do not extend into the transgressive hemicycle above it; (mudstone bed), (Fig. 3.21). The mechanical boundaries identified in this section coincide with the genetic unit boundaries and their turnaround points (Fig. 3.21).

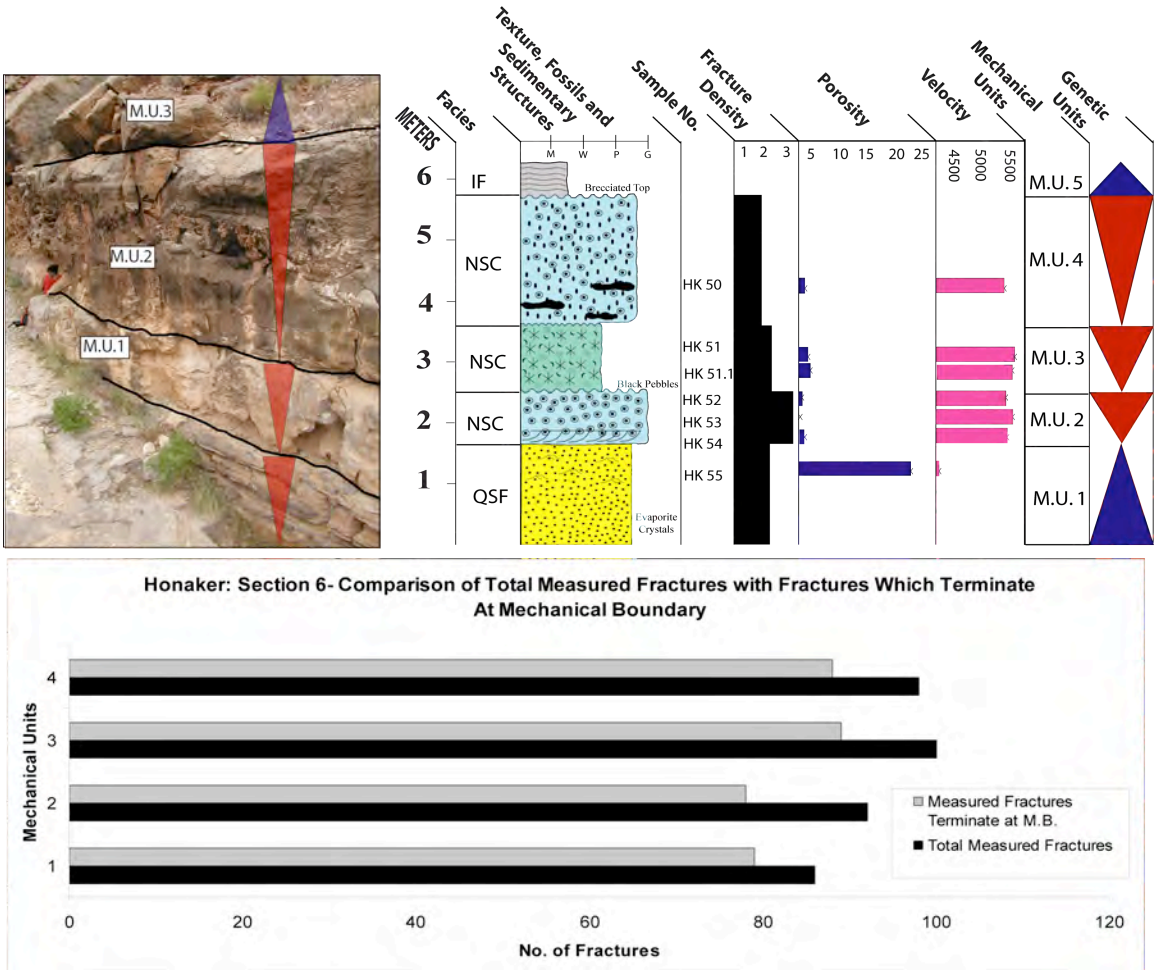

Figure 3.21: Measured Honaker Interval Section 6 at Honaker Trail. Dominant Facies Include; Non-Skeletal/Skeletal Facies (Regressive Hemicycles), and Sandstone/Shales Facies (Transgressive Hemicycle).

Raplee Anticline Sections:

Section 1:

The first measured section from Raplee Anticline begins at the boundary between the Upper Desert Creek Formation and the Lower Ismay Formation (Fig. 3.22). The section is ~16m thick, and is composed of 6 genetic cycles. The base of the section begins with a regressive hemicycle of ~1.8m thick coarse oolitic coated grainstone. At the top of the ooid grainstone is an exposure horizon which represents the base of the Lower Ismay

Formation, and hence is not only a genetic unit cycle boundary but also a sequence boundary. A major transgression follows with the onset of the next depositional genetic unit cycle whereby the transgressive hemicycle is a well sorted carbonate cemented quartz siltstone. Above the quartz siltstone the regressive hemicycle is represented by a combination of different sedimentary beds beginning at the base with a silty rich layer that contains an abundance of rugose corals in living position which has a sharp contact to a condensed wackestone lag, with sole pebbles and conglomerates at the top. A thin bed containing lithoclasts, intraclasts, large crinoidal fragments in a skeletal wackestone bed with diverse fauna and low angle cross bedding forms the top of the genetic unit cycle boundary (Fig 3.23). A 0.5m of non exposure occurs before a thick section of silty, spiculitic argillaceous, skeletal dolomudstone to wackestone with localized bioturbation forms the onset of the next genetic unit cycle which represents the transgressive hemicycle. Overlying it is the regressive hemicycle dominated by phylloid algal bioherms. A stacking of two other regressive hemicycles occur all represented by the phylloid algae. In Grammer et al. (2000), they “lumped” the phylloid algal beds into one major regressive hemicycle, but I modified this interpretation based on indications of minor transgressive hemicycles indicated by the presence of a layer of rugose corals and an upper layer of shaley silty material (Fig 3.23). The top of the phylloid algal layer is interpreted to be the top of the genetic cycle boundary. The next major transgressive hemicycle is represented by the chaetetis wackestone bed of small patch reefs and abundant crinoids. Overlying this is a regressive hemicycle of foraminiferal, skeletal packstone to grainstone with the genetic cycle boundary being capped by the final

transgressive hemicycle measured of well sorted carbonate cemented quartz siltstone (Fig 3.23).

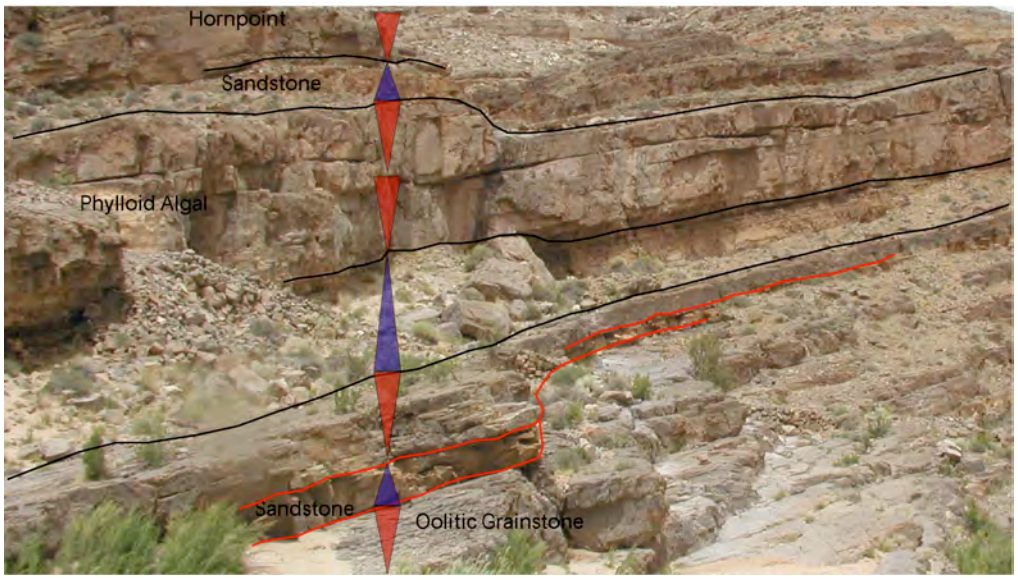

Figure 3.22: Photo outcrop view at Raplee trail displaying the Lower Ismay Formation and the corresponding genetic and mechanical units.

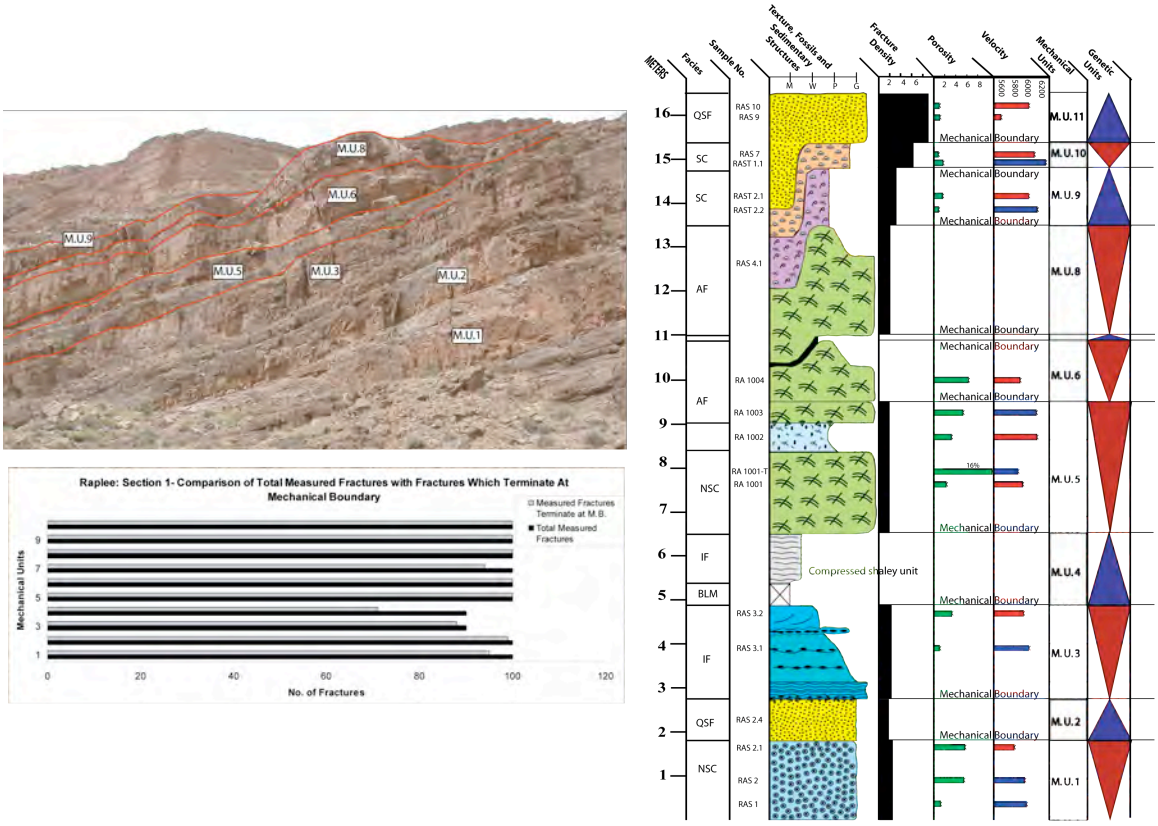

Figure 3.23: Upper Ismay section at Raplee Anticline section 1. Fracture density variations reflect the different mechanical units. The mechanical units correlate with the genetic unit boundaries and internal flooding surfaces.

Ten mechanical units identified in this complex, heterogeneous section beautifully demonstrates the correlation between the genetic hemicycles and the mechanical units (Fig. 3.23). The mechanical units were identified by fracture termination and variations in the fracture density. Fractures measured in the first regressive hemicycle (oolitic grainstone) had a 95% termination percentage at the genetic unit cycle boundary. The top

of transgressive hemicycle represented by the only quartz sandstone in the section averaged a 99% fractures termination at the turnaround point. (Fig. 3.23).The next mechanical unit identified which is the regressive hemicycle represented by various sedimentary beds had 97% of the fractures present in the unit terminating at its genetic unit cycle boundary. The transgressive hemicycle of the next genetic cycle due to poor incomplete exposure, did not obtain any fracture measurements, but the regressive hemicycle of the first phylloid algal bed showed that its base is a mechanical boundary hence making the turnaround point from the poorly exposed mudstone unit a mechanical boundary (Fig. 3.23). The top of the regressive hemicycle is mechanical boundaries where at the genetic unit cycle boundary 79% of the fractures terminated at the top of the second phylloid algae bed. The Overlying the muddy bed which is ~20cm thick forms a minor transgressive hemicycle before the onset of another deposit of phylloid algae which forms the last stacked regressive hemicycle before a major transgression occurs and a prominent mechanical boundary where 100% of the fractures measured terminated. The next major transgression identified 100% of the fractures terminating at the turnaround point between the transgressive hemicycle and regressive hemicycle, where the genetic unit boundary at the top of the regressive hemicycle also demonstrates 100% fracture termination making it a mechanical boundary (Fig. 3.23).

Section 2:

The second measured section at Raplee Anticline is within the Upper Desert Creek formation, is ~8m in total thickness and composed of 4 genetic unit cycles, of alternating oolitic grainstones and quartz siltstones. The base is represented by the regressive hemicycle of an oolitic coated grainstone. The top of the genetic unit boundary shows

evidence of subaerial exposure in the presence of karstified features. The onset of the transgressive hemicycle above the oolitic grainstone is represented by a calcareous quartz siltstone, which then shoals upwards into another 1m thick oolitic coated grainstone which forms the next regressive hemicycle and the top of the cycle with another subaerial exposure. The second genetic unit cycle begins with the transgression of coarse to fine quartz siltstone, which shoals up once again into a ~1.3m thick oolitic grainstone which shows evidence of an exposure surface at the top (Fig. 3.24). Above the top of the genetic unit boundary another ~1m thick oolitic grainstone is deposited, which indicates that the transgressive hemicycle is not expressed in the rock record and we have a stacking of regressive hemicycles. The final genetic unit's transgressive hemicycle begins again with the quartz siltstone, but at the turnaround point a fusulinid foraminifera wackestone bed represents the regressive hemicycle (Fig 3.24).

Eight mechanical units identified were measured for fracture termination and density. Fractures were measured in the first regressive hemicycle (oolitic grainstone) and 92% of the fractures terminated at the top of the genetic cycle boundary. The next mechanical unit identified which is the transgressive hemicycle represented by the quartz sandstone had 89% of the fractures terminating at the turnaround point between transgression and regression. Again 100% of the fractures present in the second regressive hemicycle terminate at the genetic cycle boundary. Overlying the oolitic grainstone is a second transgressive sandstone which the fracture data measured shows that 94% of terminate at the turnaround point and into the next regressive hemicycle. The next regressive hemicycle (oolitic grainstone) has 95% of the fractures terminating at the interpreted exposure horizon below the oolitic bed above it. Also another indication that a

mechanical boundary exists between the two oolitic grainstone is the large variation in fracture density where the upper regressive hemicycle (~1m thick oolitic grainstone) records a fracture density of 20 fractures per meter and the lower regressive hemicycle (~1.3m thick oolitic grainstone) records an average of only 6 fractures per every meter. At the genetic unit boundary between the uppermost oolitic grainstone and sandstone a 95% fracture termination occurs. The last genetic cycle demonstrates that 100% of the fractures present in the uppermost transgressive hemicycle terminate at the turn around point, and overlaying this mechanical boundary is the regressive hemicycle consisting of the fusulinid foram wackestone bed which it genetic unit boundary is also a measured mechanical boundary with 96% of the fractures terminating (Fig. 3.24). Once again it can be shown that the mechanical boundaries identified in this section coincide well with the genetic unit boundaries and their turnaround points (Fig. 3.24).

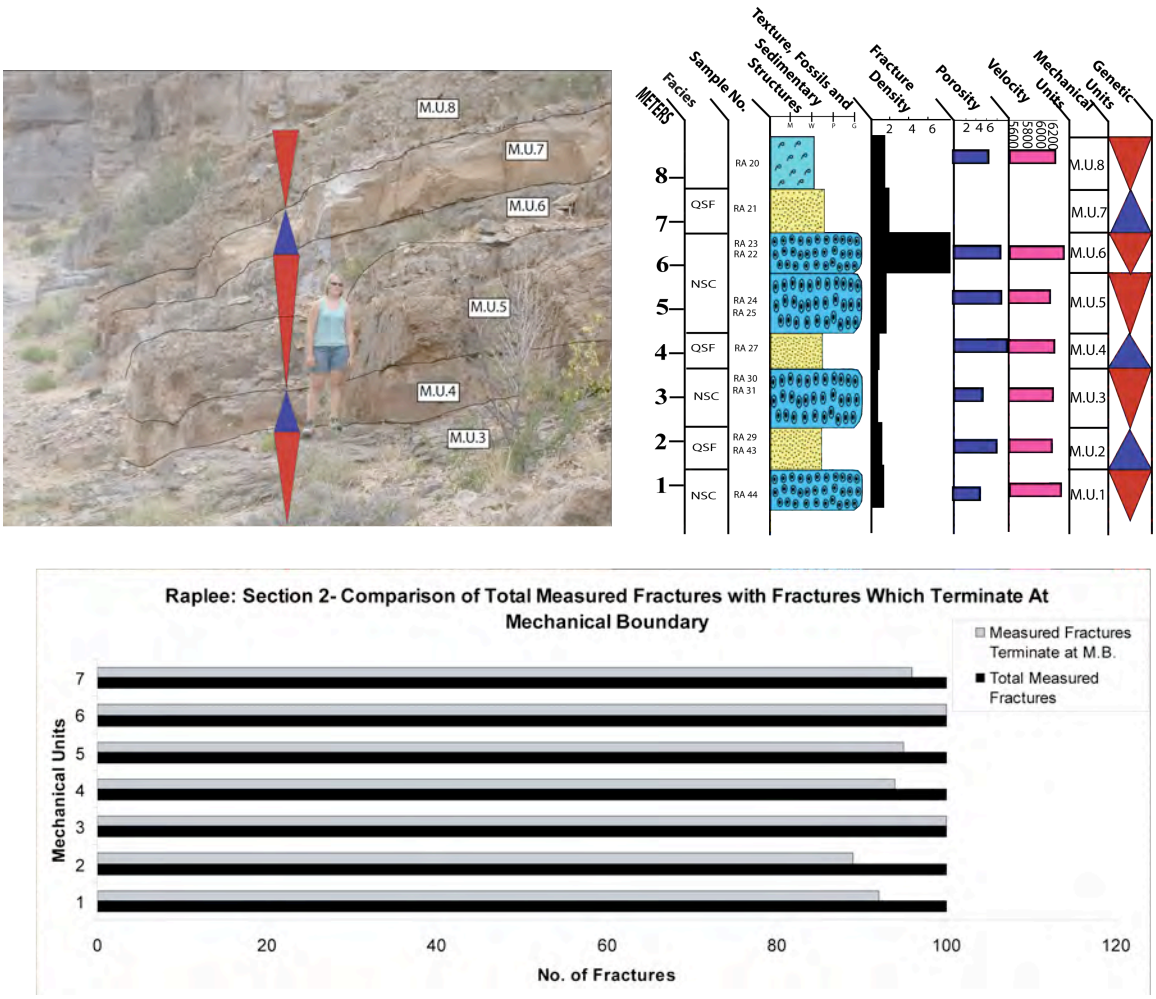

Figure 3.24: Upper Desert Creek section at Raplee Anticline section 2. Fracture density variations reflect the different mechanical units. The mechanical units correlate with the genetic unit boundaries and internal flooding surfaces.

Section 3:

The final measured section at Raplee Anticline is within the Lower Desert Creek Formation, and is composed of three genetic unit cycles and covers a thickness of ~7meters. The base of the section begins with the transgressive hemicycle of fine grained spiculitic carbonate mudstone and the turnaround point is marked by the sharp boundary into the regressive hemicycle which is a ~1.5m thick oolitic coated grainstone with large scale cross stratification. The top of the genetic unit boundary shows evidence of

subaerial exposure in the presence of karstified features. The onset of the next transgressive hemicycle consists of a crinoidal skeletal wackestone overlain by a peloidal, fusulinid packstone to wackestone bed. Overlying this is a crinoidal phylloid algal bed which is identified as being the regressive hemicycle of the second genetic unit cycle (Fig. 3.25). The final genetic cycle begins with a calcareous quartz siltstone, which represents the transgressive hemicycle which then shallows abruptly into a 10cm thick rugose grainstone, which represents the regressive hemicycle of the genetic unit. Above this the next transgressive hemicycle forms with the characteristic spiculitic carbonate mudstone (Fig. 3.25).

Using fracture termination and variations in fracture density four mechanical units were measured and identified. Fractures measured in the first regressive hemicycle (oolitic grainstone) demonstrate that 92% of the fractures terminated at the top of the genetic unit boundary. The next mechanical boundary identified where 94% of fracture termination is present occurs at the top of the fusulinid foraminifera wackestone which is not the top of the transgressive hemicycle, and hence in this case the mechanical boundary coincides above the turnaround point and in the middle of the regressive hemicycle. The next mechanical boundary where 95% of fracture termination is identified occurs at the top of the peloidal, phylloid algae wackestone to packstone which represents a genetic unit cycle boundary. The final mechanical boundary measured is at the top of the transgressive hemicycle where 100% of the fractures present terminate at the turnaround point (Fig. 3.25). The final section measured at Raplee Anticline demonstrates that the majority of the mechanical boundaries identified in this section coincided with the genetic unit boundaries and their turnaround points (Fig. 3.25).

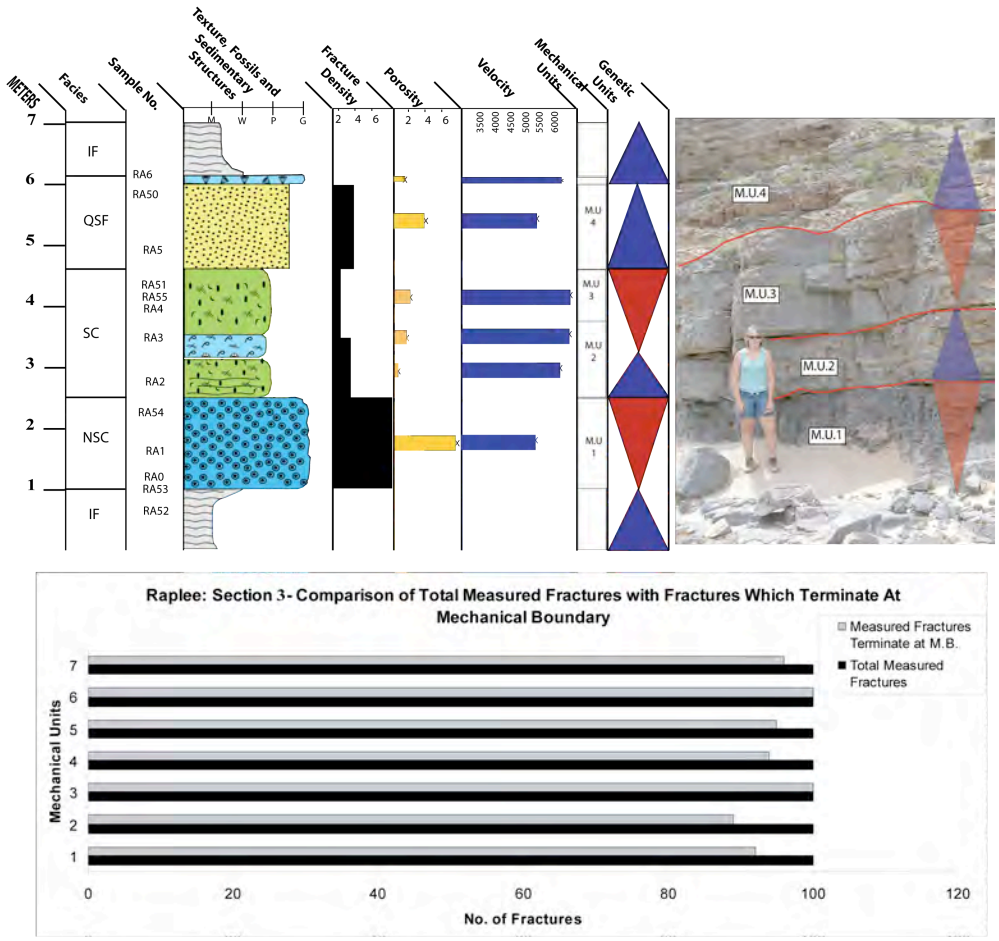

Figure 3.25: Lower Desert Creek section at Raplee Anticline section 3. Fracture density variations reflect the different mechanical units. The mechanical units correlate with the genetic unit boundaries and internal flooding surfaces.

Paradox Basin, Bluff, Utah - Conclusion

The Paradox Basin is one of the best examples found where the genetic unit boundaries and their flooding surfaces are usually found to correlate with the mechanical unit boundaries and hence the high frequency genetic unit boundaries generally are boundaries to fracture propagation (Fig. 3.26).

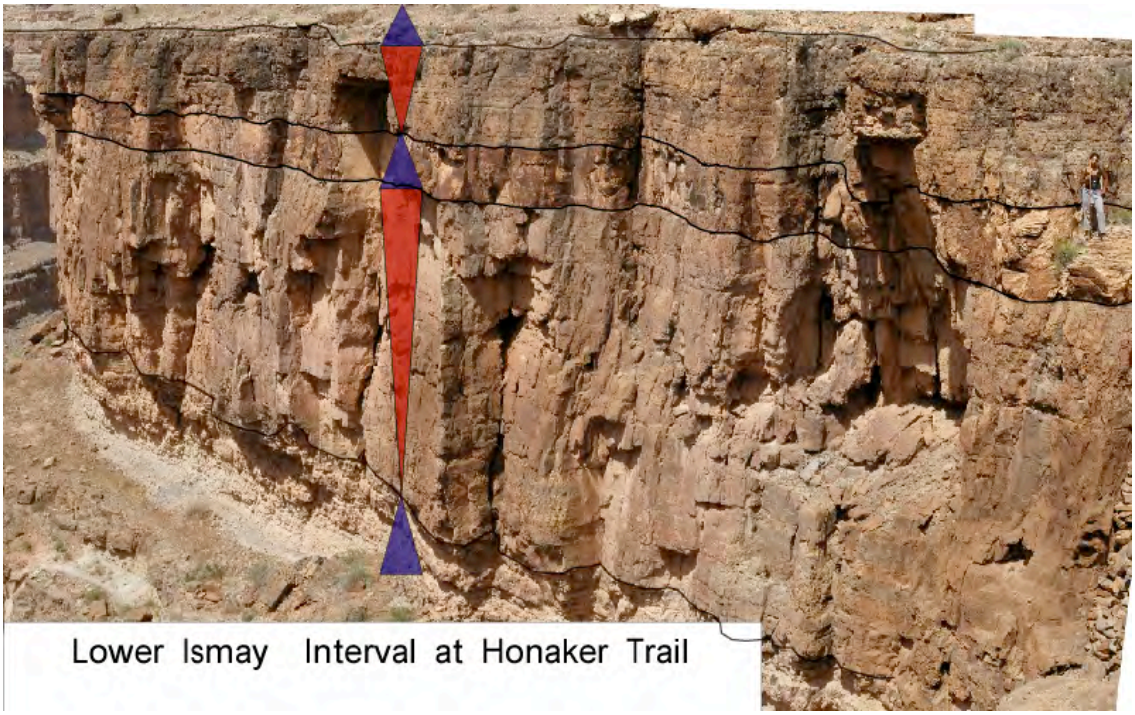

Figure 3.26: Overview of the Lower Ismay interval at Honaker Trail. For scale I am standing on the cross bedded sandstone bed. Large open fractures occur within the phylloid algal unit which majority terminates at the transgressive sandstone bed.

Summary:

Sequence stratigraphy relates changes in vertical and lateral facies distribution to relative changes in sea level. These relative changes also affect early diagenesis, especially in carbonates where, flow of marine and meteoric waters influence the types of pores, cementation and dissolution patterns produced. As a result, in carbonate systems, relative changes in sea level significantly impact the lithology, porosity, diagenesis, bed and bounding surfaces**,** factors that control fracture patterns. In this study, we explicitly explore this concept by integrating stratigraphy with the kinematics and structural regime to evaluate their influence on fracture attributes. Specifically, we focus on the relationship between mechanical boundaries and sequence stratigraphic boundaries in three different settings:

1) Anticlinal Mississippian rocks of Sheep Mountain Anticline, Wyoming

2) 'Undeformed' Mississippian limestones of St. Louis, Missouri area, and

3) Pennsylvanian limestones that are intermixed with clastics in the Paradox Basin, Utah.

Fractures are related to high resolution sequence stratigraphy, where the majority of fractures (80%) terminate at genetic unit boundaries or the internal flooding surface that separates the transgressive from regressive hemicycle. Fractures (20%) that do not terminate at genetic unit boundaries or their internal flooding surface terminate at lower order sequence stratigraphic boundaries or their internal flooding surfaces. For example at Sheep Mountain Anticline, the transgressive units are dominantly dolomitic mudstones and the regressive units are dominantly calcitic grainstones. The generally more brittle dolomites have higher fracture intensity than the calcitic grainstones. Hence, in the Mississippian rocks of Sheep Mountain Anticline, the transgressive hemicycles are more intensely fractured than the regressive hemicycles. In contrast, in the Mississippian limestones of Missouri, the regressive units generally contained a higher fracture density than the transgressive hemicycles, because the grainstones have a complex internal geometry that creates sub-mechanical units.

In our examples, the relationship between fracture spacing and mechanical bed thickness is different than expected, in that it falls below the general linear relationship described in previous studies. Similarly, fracture length distribution is not continuous, but rather clusters at discrete length scales. The reason for the low fracture spacing is the internal bedforms, such as foreset bedding or cross-bedding planes that can act as sub-mechanical

unit boundaries. The clustering of the fracture length is caused by the discrete thickness of the mechanical units that relate to the sequence stratigraphic units.

These results illustrate how integrating sedimentologic and sequence stratigraphic interpretations with data on structural kinematics can lead to refined predictive understanding of fracture attributes.

Chapter 4: Bed thickness, internal bedforms on mechanical stratigraphy and fracture spacing

Chapter three demonstrates that a genetic unit is generally composed of two mechanical units. Not only does the genetic boundary act as a mechanical boundary but the turnaround from a transgression to a regression is a mechanical boundary as well.

Various factors control fracture distribution, spacing and density. Bed thickness, stress regime, lithology, cementation and porosity all play a factor in controlling joint spacing (Cooke and Underwood, 2001; Hanks et al., 1997; Gross, 1995; Helgeson and Aydin, 1991; Narr and Suppe, 1991).

Bed thickness is often considered the most dominant factor in controlling fracture spacing (Gross, 1995). The term "bed thickness" mentioned here is used to define the mechanical bed thickness and may constitute of one or more sedimentary beds. A linear relationship exists between bed thickness and fracture spacing (Hanks et al., 1997; Gross, 1995; Helgeson and Aydin, 1991; Narr and Suppe, 1991).

This 1:1 linear relationship is explained by the stress shadow invoked by each developed fracture, which inhibits the growth and development of another fracture within the stress shadow (Gross, 1995). The diameter of the stress shadow produced by a fracture is equivalent to the length of the fracture (Gross, 1995). At higher levels of strain, fracture infilling occurs, and the 1:1 linear relationship breaks down producing lower fracture spacing to bed thickness ratio (Helgeson and Aydin, 1991; Narr and Suppe, 1991).

Considering the information from the literature and the results present in the Chapter 3, it can be hypothesized that by knowing the genetic units, which gives us a direct correlation to the mechanical units, and their thicknesses, we can thus predict the fracture spacing.

The four sites investigated were measured to test the relationship between bed thickness and fracture spacing (Fig. 4.1).

1. Sheep Mountain Anticline, Wyoming;
2. St. Louis, Missouri;
3. Honaker Trail – Paradox Basin, Utah
4. Raplee Anticline – Paradox Basin, Utah

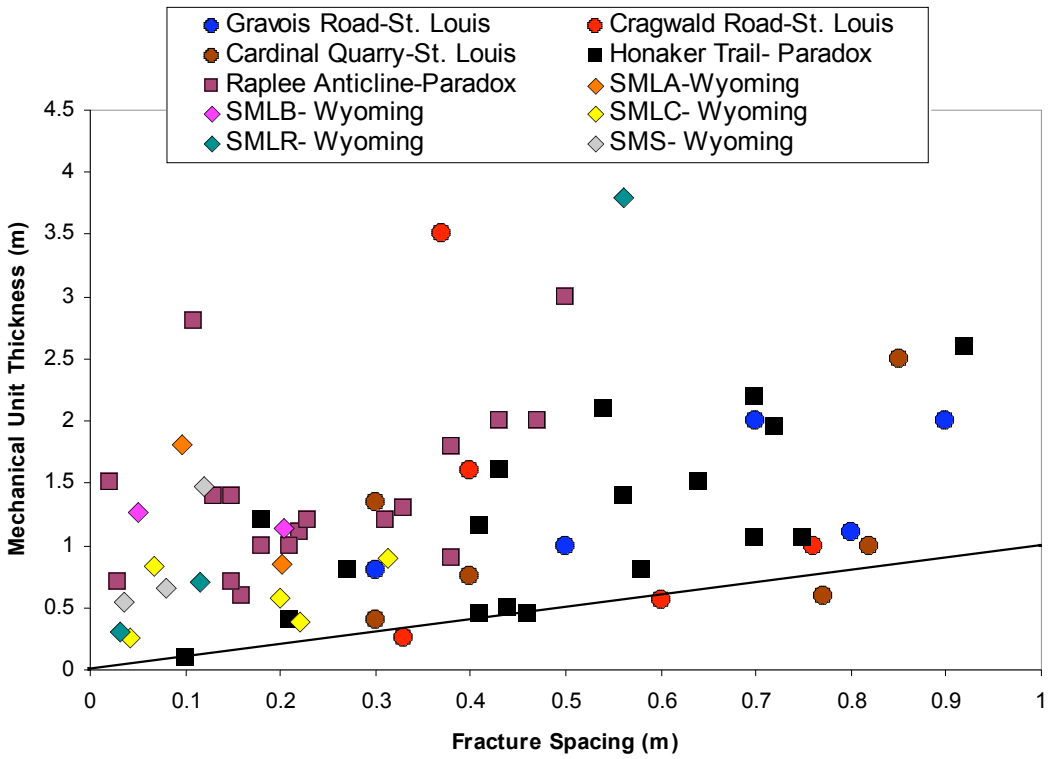

Figure 4.1: Average fracture spacing displayed against mechanical unit thickness for all measured sections and units. The black line represents the 1:1 ratio of expected relationship between bed thickness and fracture spacing.

From the above plot, a large variation exists for fracture spacing per mechanical unit thickness, where the fracture spacing is generally lower than the expected 1:1 ratio. This

chapter will look into the extrinsic effects that cause the fracture spacing to be less than hypothesized.

Methodology and Dataset

The scan density line method (Narr and Lerche (1984), Wu and Pollard (1995) and Engelder et al. (1997) is a traverse line parallel to bedding plane which was used to identify the mechanical units and measure the fracture spacings. All fracture spacings between the fractures which intercept the line are measured. The first fracture is the zero point, and from that fracture the spacing along the strike line is measured to the next fracture. At each fracture, the length of that fracture is measured, and the termination levels are also recorded, to determine the mechanical boundaries. The data is taken from all four study sites.

Wyoming - Sheep Mountain Anticline				
Section	**Mechanical Units**	**Bed Thickness (m)**	**Total No. Fractures**	**Average Fracture Spacing (m)**
SMLA	**1**	**1.81**	**100**	**0.096**
	2	**0.847**	**57**	**0.202**
SMLB	**1**	**1.27**	**102**	**0.05**
	2	**1.14**	**70**	**0.204**
SMLR	**1**	**0.71**	**100**	**0.115**
	2	**0.303**	**85**	**0.032**
	3	**3.79**	**101**	**0.56**
SMLC	**1**	**0.835**	**60**	**0.068**
	2	**0.893**	**50**	**0.314**
	3	**0.57**	**53**	**0.2**
	4	**0.39**	**100**	**0.22**
SMSA	**1**	**1.47**	**54**	**0.12**
	2	**0.543**	**91**	**0.036**
	3	**0.656**	**35**	**0.08**
	4	**0.255**	**50**	**0.043**

Table 4.1: Field Data from selected units within Sheep Mountain Anticline, Wyoming

Missouri, St. Louis -Flank of Illinois Basin				
Section	Mechanical Units	Bed Thickness (m)	Total No. Fractures	Average Fracture Spacing (m)
Gravois	1	2	96	0.7
	2	1	102	0.5
	3	1.1	100	0.8
	4	0.8	110	0.3
	5	2	98	0.9
Cragwald	1	1	124	0.76
	2	0.25	115	0.33
	3	1.4	109	1.4
	4	0.56	102	0.6
	5	1.6	97	0.4
	6	3.5	104	0.37
Cardinal	1	1.35	102	0.3
	2	0.75	102	0.4
	3	5	100	0.8
	4	0.4	110	0.3
	5	0.6	112	0.77
	6	1	110	0.82
	7	2.5	108	0.85

Table 4.2: Field Data from St. Louis, Missouri

Utah - Paradox Basin (Honaker Trail)				
Section	Mechanical Units	Bed Thickness (m)	Total No. Fractures	Average Fracture Spacing (m)
1	1	0.5	85	0.44
	2	5	99	1.48
	3	1.2	100	0.18
	4	0.45	80	0.41
	5	0.4	90	0.21
	6	1.95	100	0.72
2	1	0.45	100	0.46
	2	2.6	88	0.92
	3	2.2	100	0.7
3	1	1.05	100	0.7
	2	0.8	85	0.58
Hornpoint	1	0.1	100	0.1
	2	0.1	100	0.1
4	1	1.6	86	0.43
	2	0.8	92	0.27
	3	1.15	100	0.41
	4	2.1	98	0.54
5	1	1.05	92	0.75
	2	1.5	100	0.64
	3	1.4	99	0.56

Table 4.3: Field Data from Honaker Trail, Paradox Basin, Utah

Utah - Paradox Basin (Raplee Anticline)				
Section	**Mechanical Units**	**Bed Thickness (m)**	**Total No. Fractures**	**Average Fracture Spacing (m)**
1	**1**	**1.8**	**100**	**0.38**
	2	**1.1**	**100**	**0.22**
	3	**2**	**90**	**0.43**
	4	**3**	**90**	**0.5**
	5	**2**	**100**	**0.47**
	6	**1.2**	**100**	**0.31**
	7	**0.6**	**100**	**0.16**
	8	**2.8**	**100**	**0.11**
	9	**1.4**	**100**	**0.13**
	10	**1.3**	**100**	**0.33**
2	**1**	**0.7**	**100**	**0.15**
	2	**1.5**	**100**	**0.02**
	3	**1.0**	**100**	**0.18**
	4	**1.4**	**100**	**0.15**
	5	**0.7**	**100**	**0.03**
	6	**1.2**	**100**	**0.23**
	7	**0.9**	**100**	**0.38**
3	**1**	**1.0**	**100**	**0.21**
	2	**1.2**	**100**	**0.23**
	3	**3**	**100**	**0.5**
	4	**1.8**	**100**	**0.4**

Table 4.4: Field Data from Raplee Anticline, Paradox Basin, Utah

Results

The major result demonstrated in the above dataset is that carbonates do not contain fracture spacing in a simple linear relationship to mechanical unit thickness as found in most sandstones. In many of the sections from all of the three different areas, almost all the fracture spacing falls below the 1:1 expected linear relationship. This indicates that the fracture spacing is more closely spaced than proposed for sandstones by others (Gross, 1995; Cooke and Underwood, 2001; Hanks et al., 1997).

In areas of high strain, infilling of fractures occurs to accommodate increasing strain (Cooke and Underwood, 2001; Hanks et al., 1997; Narr and Suppe, 1991). Hence, the fracture spacing will be more closely spaced than the expected ratio. Nevertheless it

should still maintain a linear relationship to mechanical unit thickness (Cooke and Underwood, 2001; Helgeson and Aydin, 1991; Gross, 1995). Sheep Mountain Anticline and Raplee Anticline are asymmetrical folds, and hence have undergone more strain than the flat bedded sections present in St. Louis, Missouri and Honaker Trail, Utah, (Fig. 4.2).

St. Louis – Missouri

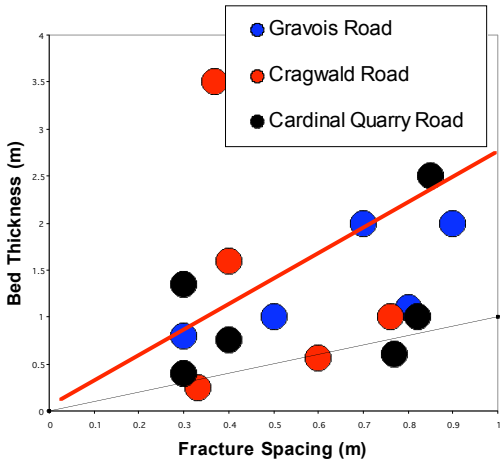

Honaker Trail, Paradox Basin - Utah

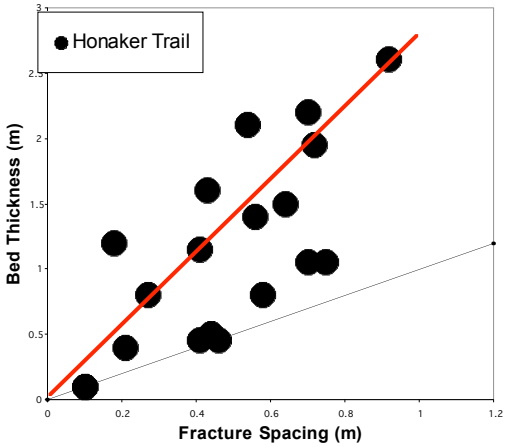

Sheep Mountain Anticline – Wyoming

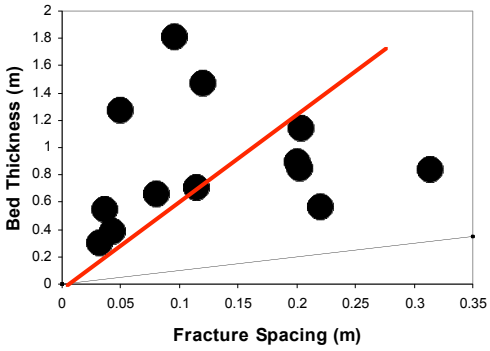

Raplee Anticline, Paradox Basin - Utah

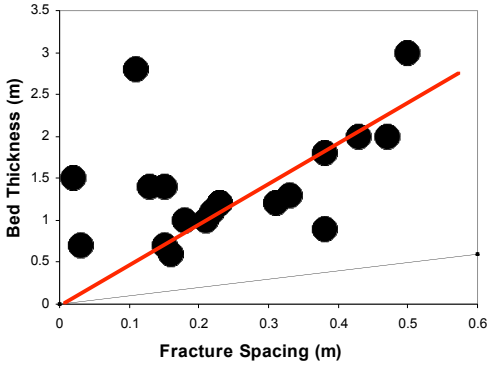

Figure 4.2: Graphs of all four areas mapped out individually for better comparison. The expected 1:1 ration is plotted in black, and the best fit regression line is plotted in red.

Observing each section individually, it can be demonstrated that most of the data points have a good linear relationship with mechanical unit thickness, but not all the fracture spacing data are explained by the 1:1 linear correlation between mechanical unit thickness and fracture spacing.

From figure 4.3, it can be observed that in all the four areas most of the data resides over the 1:1 linear line between mechanical unit thickness and fracture spacing (red line). Secondly, there is a spread in the data above and below this correlation line between fracture spacing and mechanical unit thickness. This means that if we assume the 1:1 correlation line represents the data-points which are related to mechanical unit thickness for that particular strain area, then some of the facture spacing data are much wider than the thickness of the mechanical unit (blue circles), and some of the fracture spacing data are much closer in distance than the mechanical unit thickness (green circles).

Only the Honaker Trail and Missouri dataset contains some data points which lie on the expected 1:1 bed thickness-fracture spacing ratio (black line), and this is due to lesser strain and deformation occurring at both Honaker Trail and St. Louis Missouri in comparison to the anticlines present at Sheep Mountain Anticline in Wyoming, and Raplee Anticline in the Paradox Basin. Hence, the results demonstrate three zonations to a single area, and of the three zonations two can be explained deterministically and the blue circled zone can be hypothesized upon for now.

St. Louis – Missouri

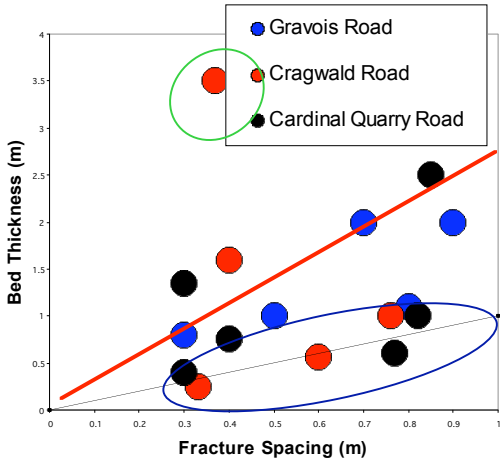

Honaker Trail, Paradox Basin - Utah

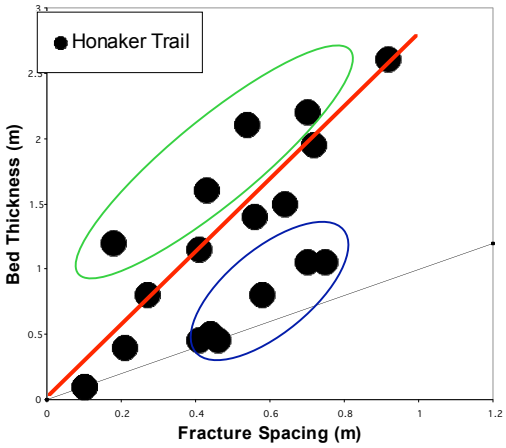

Sheep Mountain Anticline – Wyoming

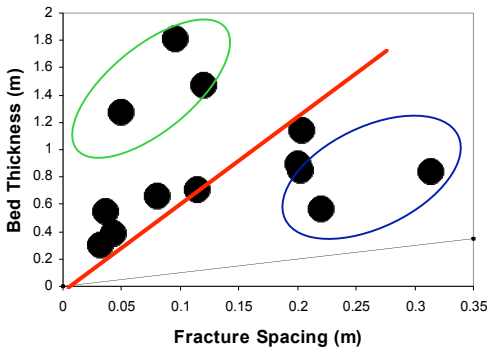

Raplee Anticline, Paradox Basin - Utah

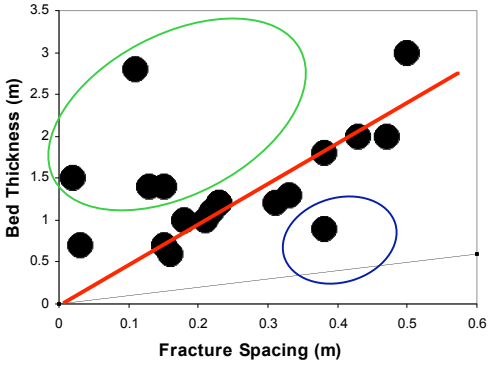

Figure 4.3: Figure breaking down datasets into three zones. First zone is data represented by best fit line (red), second zone is over-expected fracture spacing (data points within blue circles) and third zone is under-expected fracture spacing (data points within green circles).

Discussion

Analysis of data from all beds from the different sections demonstrates that the reason for the low fracture spacing is presence of internal bedforms. Internal bedforms are sedimentary structures associated with the depositional environment. They consist of cross bedding, laminations and introduce complex compartmentalization within the mechanical unit. We observed fracture terminations at surfaces such as laminations, foreset bedding or cross-bedding planes that can act as sub-mechanical unit boundaries.

In Sheep Mountain Anticline about 65% of the fracture spacing data can be explained by the best fit line between bed thickness and fracture spacing accounting for higher fracture saturation due to over strain. However some of the data are anomalously higher than this trend. A data-point in figure 4.4 is selected to further analyze this discrepancy where a 2 meter thick mudstone-wackestone has a fracture spacing of 0.1m (highly oversaturated). The term mechanical unit as stated before is a set of beds that have one continuous fracture set, and because the fractures are continuous through most of the area, it is considered as one mechanical unit. The mechanical unit though is made up of several sedimentary beds which are between 10 and 12cm thick. The laminations act as sub-mechanical layers which create essentially thinner beds that correspond better to the fracture spacing. Hence although the composite of the beds can be termed a mechanical layer it is comprised of smaller mechanical layers which have a greater control on the determination of the fracture spacing.

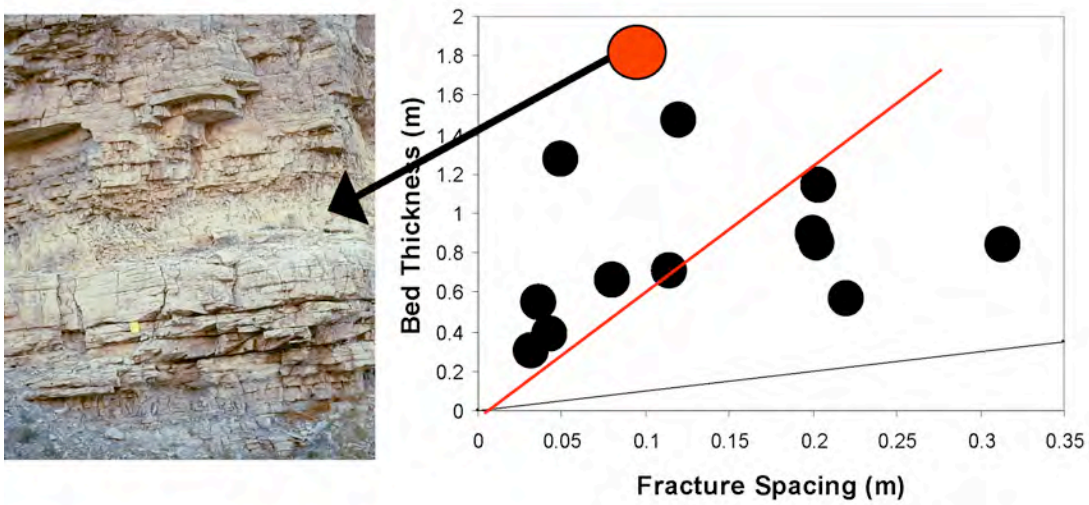

Figure 4.4: Interbedded dolomitic mudstones and calcitic grainstones from Sheep Mountain Anticline demonstrating the variations in fracture spacing. The interbedded dolomitic mudstones are represented by the red dot on the corresponding graph.

In contrast, in the Mississippian limestones of Missouri, not many anomalous oversaturated beds are observed. One exception is in the Cragwald Quarry, where a thick grainstone unit has anomalously high fracture density. The grainstone bed has a complex internal geometry that is caused by cross bedding. The boundaries of the cross beds create mechanical boundaries to small fractures, because of inter-bed slip (Fig. 4.5).

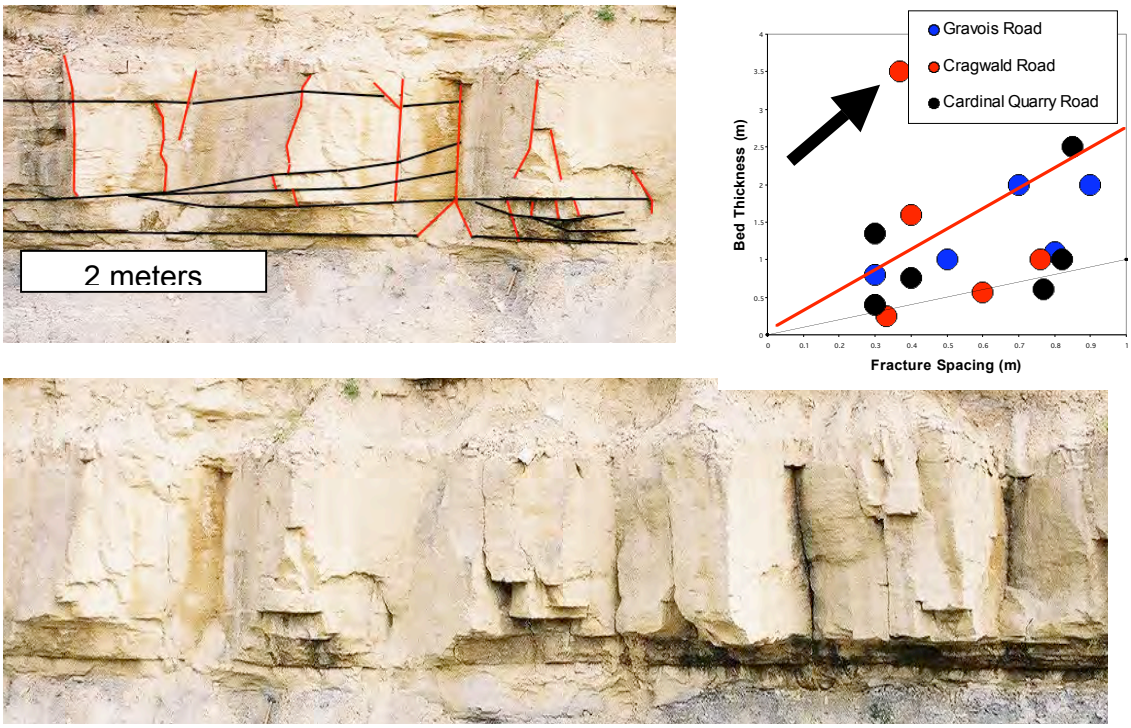

Figure 4.5: Grainstone bed at Cragwald Road section, displaying anomalously different fracture spacing than the other beds in the area. The closely spaced fracture spacing is due to compartmentalization of the mechanical unit by the cross bedding.

In the Paradox Basin, we also observe over-saturated beds in sandstones and carbonate grainstones. At Honaker Trail a sandstone with ~35% carbonate cement fractures more intensely, and the cross bedding surfaces act as sub-mechanical boundaries to the fracturing, hence decreasing the fracture spacing (Fig. 4.6). Fracture spacing is primarily affected by external properties such as bed thickness and internal bedforms and affected to a much lesser degree by lithology, porosity or rock stiffness (Chapter 5). The internal bedforms create complex compartmentalization of the mechanical unit into sub-mechanical units.

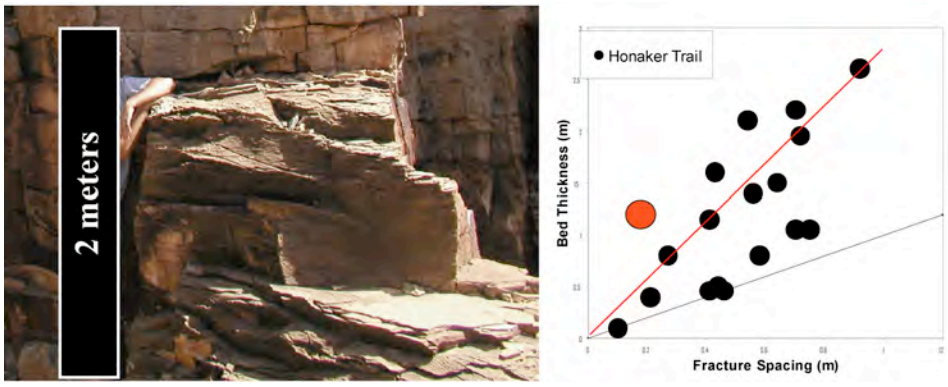

Figure 4.6: Cross bedded sandstone unit at Honaker Trail demonstrating the effect of the internal bedforms in creating complex compartmentalization mechanically.

Similar findings are also present at Raplee Anticline, where a 3 meter thick oolitic grainstone bed is more intensively fractured than other oolitic grainstone beds within the section. The grainstone bed mentioned above is highly cross bedded and some of the fractures are terminating at the cross bedding surfaces. As a whole the mechanical unit behaves in the end as a single unit, because individual fracture terminations connect by crossing over to form a unit that behaves mechanically the same throughout its thickness (Fig. 4.7).

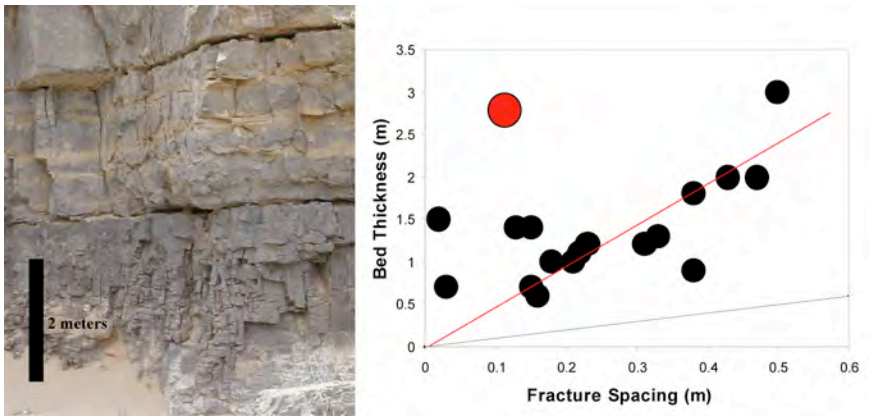

Figure 4.7: Oolitic grainstone unit at Raplee Anticline showing ghost cross bedded laminations where the fractures are depicting as sub mechanical layers.

In conclusion we can observe how the internal bedforms can create sub mechanical units by creating mechanical boundaries with inter-bed slip, within a mechanical unit, thus affecting the 1:1 linear relationship generally found in siliciclastic deposits.

Chapter 5: Fracture termination and fracture spacing in the paradox basin: Effect of intrinsic rock properties

This chapter investigates the controlling factors on fracture spacing and propagation. It has long been established that factors behind joint propagation through different sedimentary layers define the mechanical stratigraphy (Corbett et al., 1987; Narr and Suppe, 1991; Gross et al., 1995; Hanks et al., 1997; Rijken and Cooke, 2001; Lorenz et al., 1997; Underwood et al., 2003). Attributes which define mechanical stratigraphy are the relative thickness of the individual mechanical units, the nature of the mechanical boundary interfaces and the rigidity of each lithologic unit (Cook and Erdogan, 1972; Ladeira and Price, 1981; Helgeson and Aydin, 1991; Gross, 1995; Lorenz et al., 2002; Underwood et al., 2003). Two properties which have been shown to control the propagation of fractures within formations of interbedded brittle and ductile units are: (1) the stiffness contrast between layers, which is controlled mainly by the mineralogy and porosity, and, (2) the yield strength of the more ductile units (Cooke and Underwood, 2001).

In chapter 3 I documented that the majority (80%) of fractures terminate at genetic unit boundaries or a cycle turnaround points, which separate the transgressive hemicycle from the regressive hemicycle. The remaining fractures that do not terminate at genetic unit boundaries or their internal flooding surfaces generally terminate at either the bounding surfaces of internal bedforms such as (laminations, shale partitionings, or cross bed stratification); (Chapter 4). What is still not known is why fractures do not propagate across these stratigraphic boundaries. Currently there are two main hypotheses for fracture termination, these are:

1. The shear rigidity difference between the two rock layers is so large that fracture propagation is stalled (Renshaw and Pollard; 1995).
2. The type of bonding (i.e. how well bonded/molded the beds are to one another without bed slip occurring) at the bedding surfaces (Cooke and Underwood; 2001).

Furthermore, different studies attribute fracture spacing to various controls. Several studies demonstrate that there is generally a linear relationship between joint spacing and bed thickness (Price, 1996, Huang and Angelier, 1989, Wu and Pollard, 1995, Gross et al., 1995, and Narr and Suppe, 1991), whereas other studies such as Yale and Jamieson (1994), Lorenz et al., (1997), Hugman and Friedman (1979) and Hatzor and Palchik (1997) attribute the controls on fracture spacing to be based on the internal properties of the rock. However, as shown in chapter 4 a bed thickness correlation in carbonates is not as straightforward and other factors do come into play. Here I will explore the extent of the intrinsic rock stiffness parameters, bulk moduli, shear moduli, porosity and density on fracture spacing in outcrop from two different strain settings in the Paradox Basin and investigate the effect of the rigidity ratio on fracture propagation or termination.

In Sheep Mountain anticline, Wyoming, we observed that the dolomitic "transgressive" mudstones were generally more fractured than the calcitic "regressive" grainstones (see chapter 3). This initially caused the consensus that rock stiffness controls fracture spacing. Yet, the subsequent study in St. Louis demonstrated no correlation between fracture spacing and internal rock properties (see chapter 4). Key elements of difference between these areas are different strain conditions (anticlinal folded beds versus flat lying regional beds). This study will evaluate which factors dominate fracture spacing.

The study focuses on fracture analysis of upper Desmoinesian strata from the Pennsylvanian mixed carbonate siliciclastic system of the Paradox Basin. We conducted a fracture analysis from the flat-lying strata of the Honaker Trail (6 sections) and the folded, tectonically deformed strata at Raplee Anticline (3 sections). Data at each outcrop section consisted of measurements and descriptions of fracture length, spacing, and fracture orientation where possible. Lithological description and definition of the mechanical stratigraphy based on fracture terminations at significant boundaries is discussed in detail in chapter 3. Continuous exposures allowed for description and collection of a statistically significant data set of attributes of mechanical properties. From each mechanical unit a minimum of 100 fracture lengths and spacing were measured (see chapter 2 for data tables and statistics).

From both sections, a total of 160 samples was collected and used porosity and bulk density determinations as well as velocity measurements to determine dynamic bulk moduli and shear moduli.

Tectonic Setting of Paradox Basin, Utah

The Paradox Basin is an elongate, intracratonic basin that extends from northwestern New Mexico to east-central Utah, covering an area of approximately 27,000 km^2 in the Colorado Plateau province. The tectonic fabric of the plateau was established in Precambrian times and reactivated in Late Paleozoic (Baars & Stevenson, 1982). The Paradox Basin lies at the crossing area of two major lineaments; the Olympia Wichita lineament and the Colorado lineament (Stokes, 1988; Baars and Stevenson, 1982). These Precambrian lineaments were reactivated due to the compression of the Pennsylvanian Ancestral Rocky Mountain Orogeny creating uplift areas with topographic lows (i.e.

Paradox Basin), (Baars & Stevenson, 1982). Most of the structures observed today in the Paradox Basin are due to the west-east compressional forces of the Laramide Orogeny which caused the monoclines across reactivated high angle basement thrust faults, as well as uplift and erosion (White, 1995). The tectonic origin of the Paradox Basin is a controversial subject. Baars and Stevenson (1982) suggested it was an extensional basin with strike slip motion, but a recent study from Barbeau (2003) indicates a foreland origin.

Sequence Stratigraphy

The study area is situated on the southern shelf where during the Pennsylvanian a second-order sequence of cyclic mixed carbonate-siliciclastic system was deposited (Weber et al., 1995; Sarg et al., 1999). The strata are composed of numerous depositional cycles (Goldhammer et al., 1991). An ideal cycle consists of 7 facies deposited during one high-frequency sea level change. During transgression eolian deposits are reworked and overlain by black laminated mudstone. The regressive hemicycle shelf carbonates were deposited and during times of maximum water depth algal mounds developed on several locations that are capped by skeletal/nonskeletal grainstone (Goldhammer et al., 1991; Grammer et al., 1996).

Methodology and Data

Fracture analysis was preformed on two tectonically different areas within the Paradox Basin; these are the flat lying strata of the Honaker Trail Section, and the tectonically deformed strata at Raplee Anticline.

Several representative locations from each site (6 at Honaker Trail and 3 at Raplee Anticline) were analyzed that contained a good variation stratigraphically, and measurable mechanical units. The stratigraphy and identification of the genetic units was analyzed at each location and then the mechanical units were identified and fractures measured using the scan density line method which follows the standard practices (Narr and Lerche, 1984; Wu and Pollard, 1995; Engelder et al., 1997).

The Honaker Trail area underwent significantly less deformation than Raplee Anticline. This is obvious when observing the flat lying beds at Honaker compared to the folded strata at Raplee.

Results

The flat lying beds at Honaker are compared to the folded strata of the asymmetric Raplee Anticline fold. The bed thicknesses in both areas range between 10cm to 300cm with one anomalously large bed at Honaker of 500cm thickness. In figure 5.1 we plot the mechanical bed thicknesses against the coefficient of joint spacing (K), which is the average fracture spacing normalized by the bed thickness. This coefficient ranges between the values 0 and 1. The coefficient of joint spacing for the Raplee data generally ranges from a lower limit of 0.01 to an upper limit of 0.26, with one higher value of 0.42. The Honaker dataset ranges from an upper limit of 1 to a lower limit of 0.26, with a single data point of 0.15.

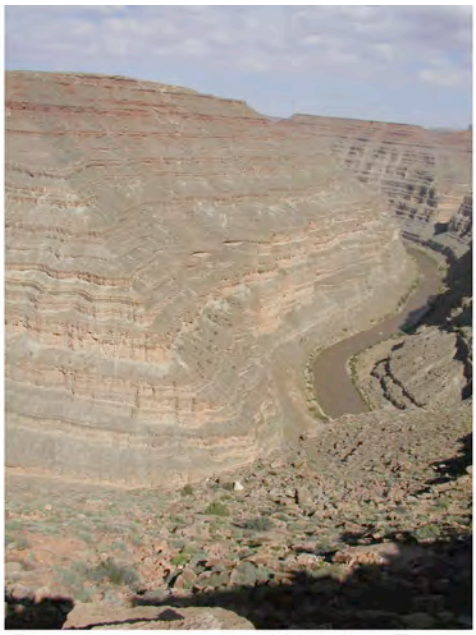

Flatlying strata at Honaker Trail

Fractures are measured in two locations with different strain regimes: Honaker Trail and Raplee Anticline

Raplee Anticline

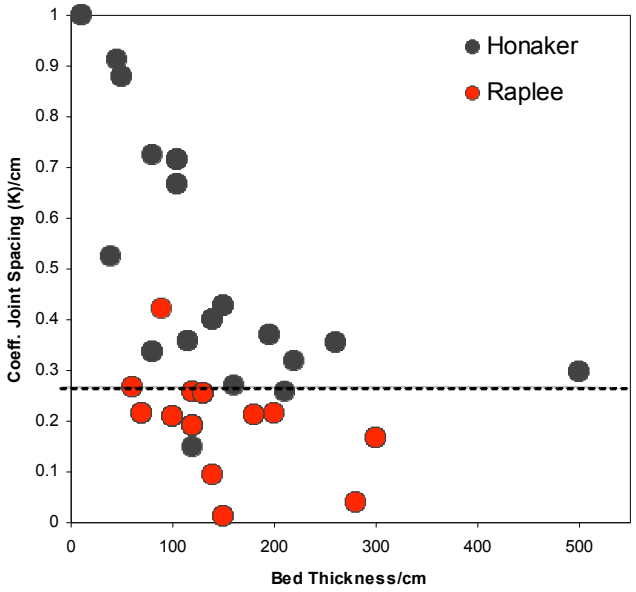

Figure 5.1: A plot of the mechanical bed thickness against the coefficient of joint spacing. The black dots represent Honaker Trail and the red represent Raplee Anticline. The dashed line represents a cutoff in the dataset between the two localities and is at a value of K=0.26.

In siliciclastics a linear relationship is commonly observed between fracture spacing and mechanical bed thickness (Price, 1996, Huang and Angelier, 1989, Wu and Pollard, 1995, Gross et al., 1995, and Narr and Suppe, 1991) except in areas where joint saturation occurs due to continued stress and strain as cited by Becker and Gross (1996). Figure 5.2 explores this relationship in the mixed carbonate-clastic system of the Paradox Basin.

The data from both localities fall below the 1:1 linear relationship expected between the average fracture spacing (which is an average of 100 measured fracture spacing's per mechanical unit). Although a linear type trend may explain some of the data points, there is a considerable scatter of the data points, where a less randomness of the data is observed within the Honaker dataset (R^2=0.53) as compared to Raplee (R^2=0.1).

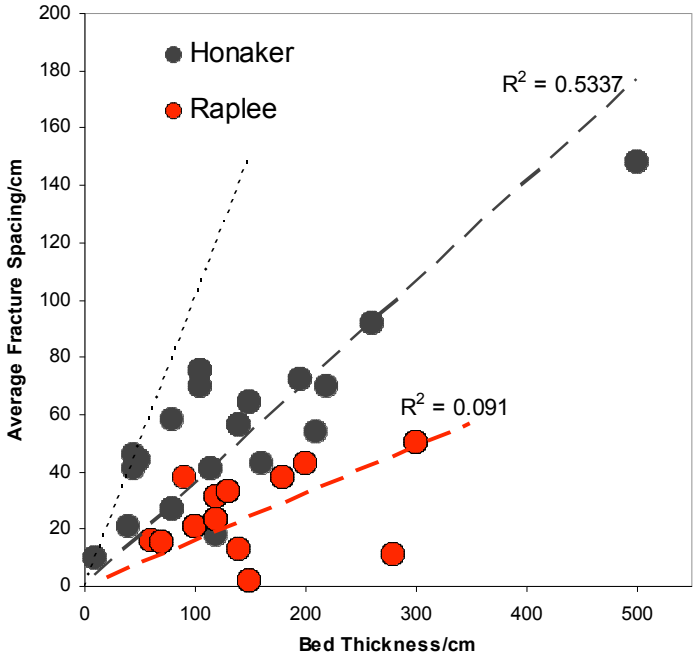

Figure 5.2: Plot of average fracture spacing (cm) against bed thickness (cm) for the Honaker Trail section (black dots) and Raplee Anticline section (red dots). The dotted line is the general linear relationship documented in the literature for bed thickness-fracture spacing. This relationship is commonly found in sandstones.

Since other factors are thought to affect fracture spacing besides bed thickness, such as rock stiffness (Gross et. al., 1995), porosity (Corbett et al., 1987; Engelder et al., 1997),

these factors were hence investigated individually within each location (Figs. 5.3 and 5.4).

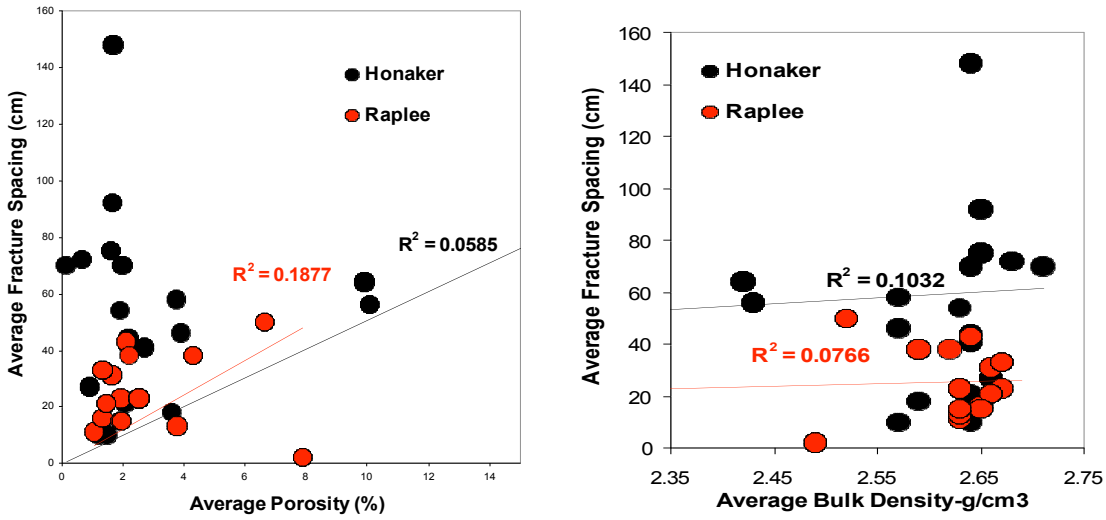

Figure 5.3: Individual plots of porosity (left) and bulk density (right) against average fracture spacing. All demonstrate poor correlation in predicting fracture spacing.

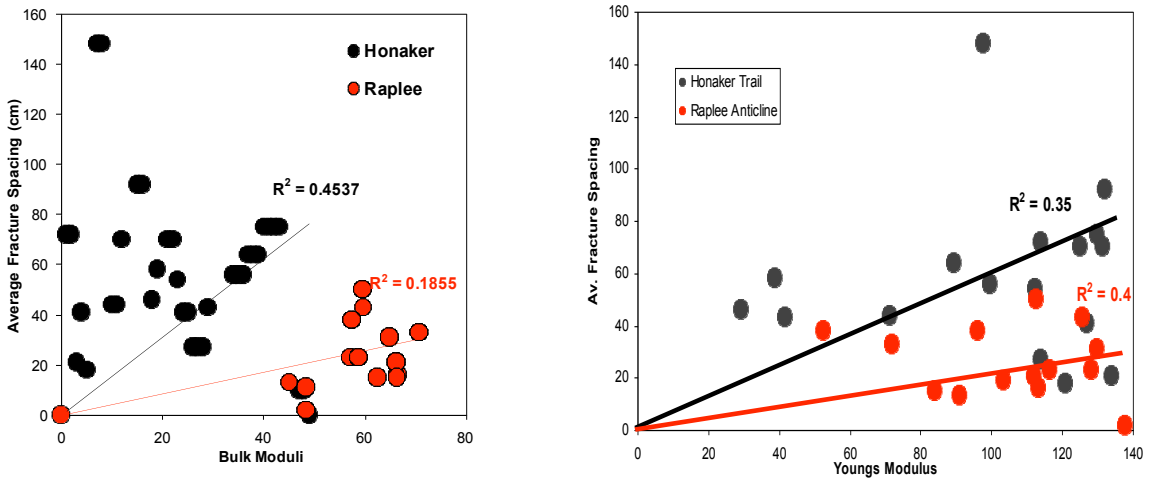

Figure 5.4: Individual plots of bulk modulus (left) and young's modulus (right) against average fracture spacing. All demonstrate poor correlation in predicting fracture spacing.

From the above plots a very poor correlation is found between fracture spacing and the various factors that control the fracture spacing. Hence there is no one singular factor

which can be attributed as the dominant factor in controlling the distribution of the fractures within a bed set. The next step would therefore be to see if a combined effect of the various factors would produce a better coefficient and within each section determine the dominant factor which can be variable from section to section.

Multiple regression plots were then performed to investigate any correlation between fracture spacing and other factors (Fig. 5.5). Plots 5.5A and 5.5B are multiple regression plots of fracture spacing looking at the intrinsic rock properties porosity, bulk density, shear modulus, bulk modulus and velocity. In figures 5.5C and 5.5D, the bed thickness is added into the multiple regression analysis.

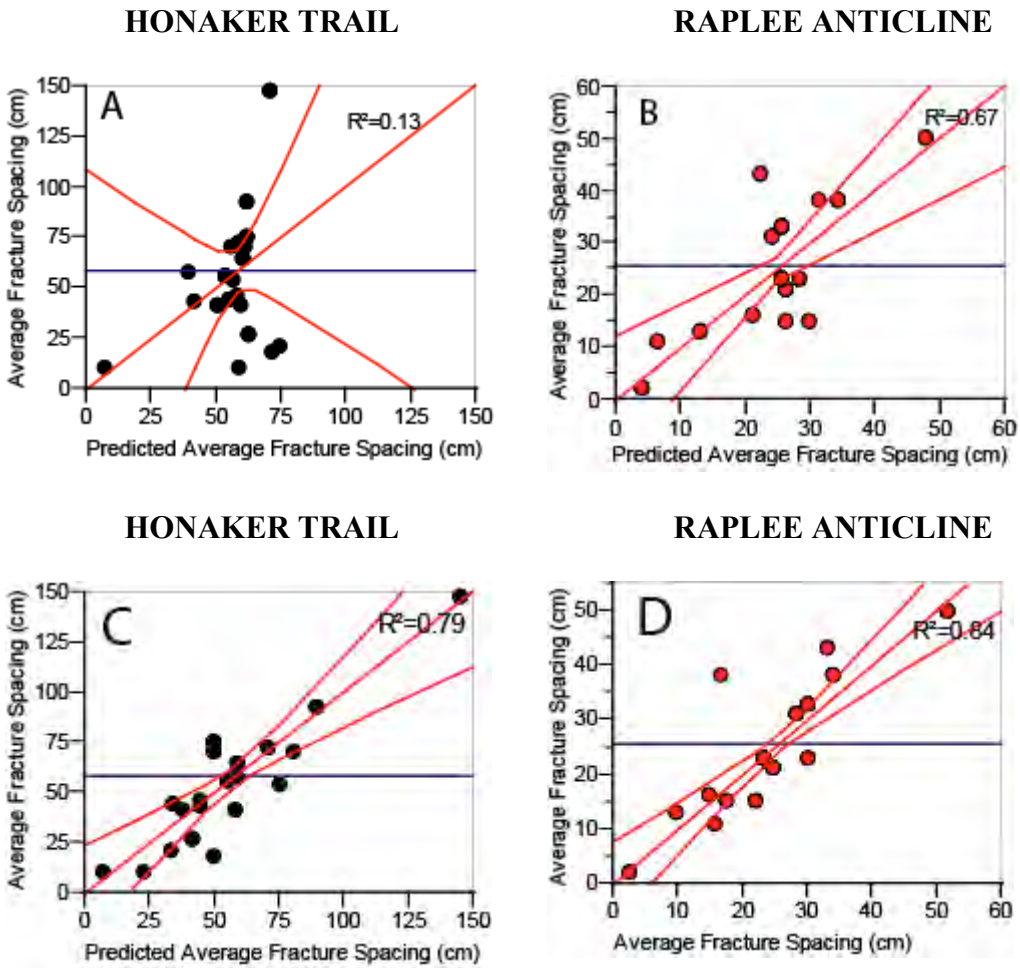

Figure 5.5: Multiple regression plots of the average fracture spacing with internal and external rock properties. 5.5A: Intrinsic rock properties for Honaker Trail. 5.5B: Intrinsic rock properties for Raplee Anticline. 5.5C: Bed thickness and intrinsic rock properties for Honaker. 5.5D: Bed thickness and intrinsic rock properties for Raplee Anticline.

The results show that at Honaker trail the various intrinsic rock properties have little to no influence on the fracture spacing, where R^2=0.13. In contrast at Raplee Anticline a strong correlation of R^2=0.67 is present between the intrinsic rock properties and the fracture spacing. The two intrinsic rock properties which dominate the correlation at Raplee are bulk density and porosity. Yet, when we include the effect of bed thickness then both correlations average out to an R^2=0.8. These results demonstrate that the

average fracture spacing at Honaker is dominantly controlled by bed thickness, and that the internal intrinsic rock properties are the dominating controlling factors on the fracture spacing at Raplee Anticline.

Other fracture determined indices are used in the literature to relate fracture patterns to rock properties. In Table 5.1, many of these indexes were analyzed in multiple regression plots to determine the various influences on the various Indexes. Generally the results are consistent, where at Raplee Anticline higher correlations are achieved on the intrinsic rock properties alone than at Honaker. But with the addition of bed thickness the correlation at Honaker are vastly improved as compared with the smaller correlation improvement observed at Raplee.

Fracture Index	**Honaker Trail Data**		**Raplee Anticline Data**	
	Physical Properties ***(R^2)***	***+ Bed Thickness*** ***(R^2)***	***Physical Properties*** ***(R^2)***	***+ Bed Thickness*** ***(R^2)***
Average Fracture Spacing	0.13	**0.79**	0.67	0.84
Median Fracture Spacing	0.12	0.70	0.52	0.68
Coefficient of Fracture Spacing	0.36	Invalid	0.75	Invalid
Fracture Density	0.44	0.64	0.84	0.93
Fracture Spacing Ratio	0.17	Invalid	**0.97**	Invalid

Table 5.1: Comparison of various fracture indices from the multi-regression analysis.

Engelder et al. (1997) calculated “Fracture Spacing Ratio” which was earlier defined by Gross (1993) by simply dividing the mean bed thickness by the median joint spacing for a particular bed, and observed that samples with low porosity came from units with higher FSR averages than samples with higher porosities.

In the selected dataset the Fracture Spacing Ratio (FSR) has no correlation with the Honaker Trail dataset (R^2=0.17) and a totally opposing relationship with the Raplee Anticline dataset (R^2=0.97). Two Fracture Spacing Ratio residual leverage plots in Table 5.1 are obtained from the Raplee Anticline dataset. Figure 5.6A is the residual leverage plot of the FSR with the average porosity, whereas figure 5.6B is against the bulk density. From these two plots, the scatter in the dataset is more reduced when using bulk density instead of just porosity, which leads us to determine that the bulk density in this situation has the most dominant affect after bed thickness in determining the facture characterization.

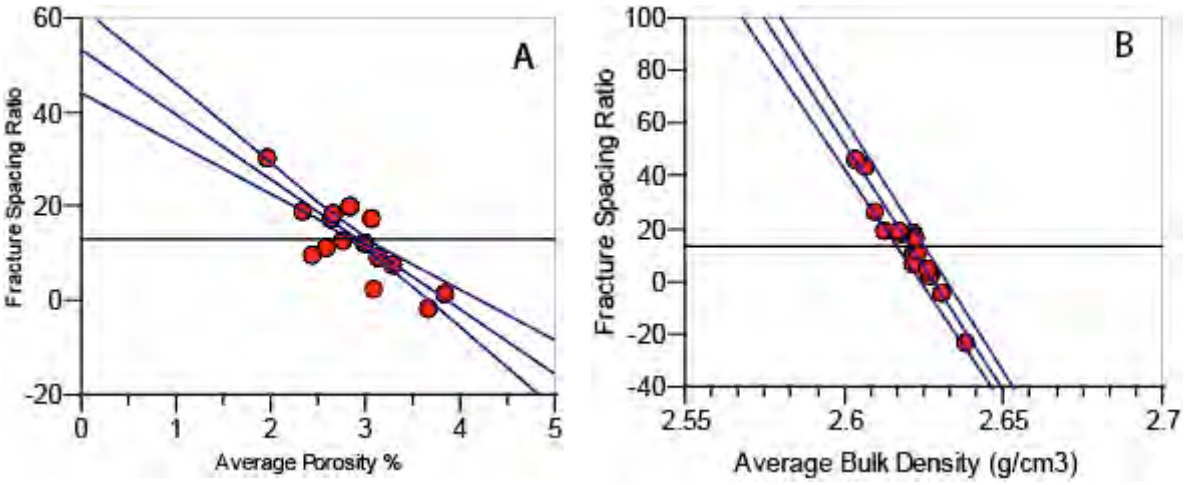

Figure 5.6: Residual plots in predicting fracture spacing. The lower the scatter the better the correlation factor in determining the fracture spacing.

Understanding fracture propagation at mechanical boundaries using rigidity ratios

Renshaw and Pollard (1995) used the shear modulus "rigidity ratio" as an indicator for joint termination at the observed mechanical boundaries and calculated that if the shear

modulus ratio of the softer layer to stiffer layer is < ~0.4, joint termination at that boundary is favored but if μ (Soft)/ μ (Stiff) > ~0.4 then joints will propagate across layer interfaces.

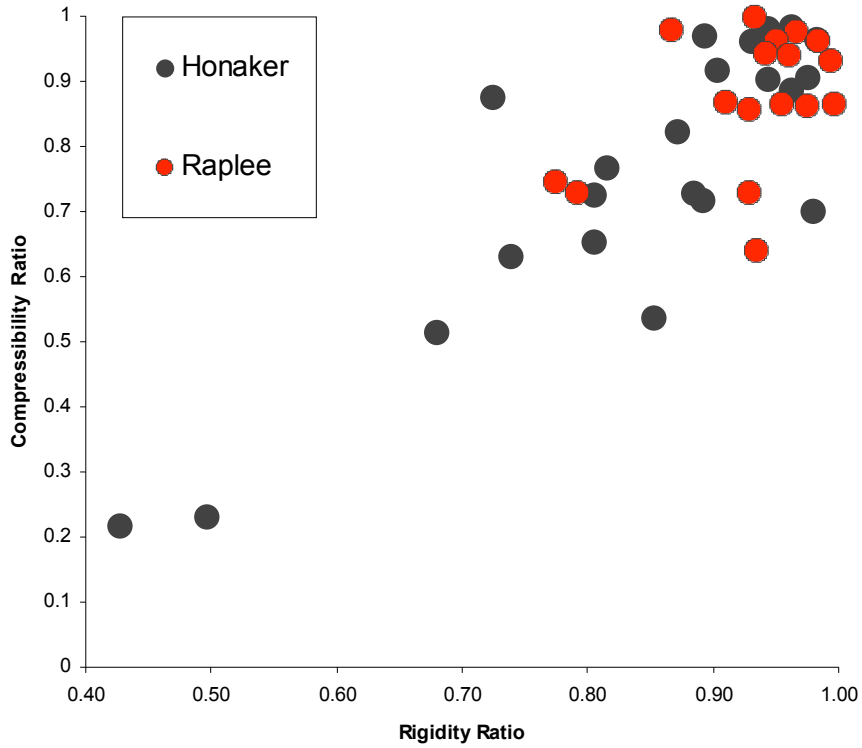

Figure 5.7: Rigidity ratios of the softer mechanical unit over the stiffer unit from the Honaker Trail (black dots) and Raplee Anticline (Red dots). All rigidity ratios are greater than 0.4.

Figure 5.7 shows a plot of the literature derived rigidity ratio (Renshaw and Pollard, 1995) with the compressibility ratio, in order to analyze both stiffness parameters. Two rigidity ratios are low (0.43 and 0.5). Most of the data has a minimum rigidity ratio value of 0.68. Similar calculations were used to determine the compressibility ratio, for consistency purposes. The two anomalous low Honaker points are also the only two lowest points in the compressibility ratio, of values of 0.22 and 0.23 respectively. These

results demonstrate that there is no significant rigidity ratio difference for the existence of mechanical boundaries and fracture termination.

Discussion & Conclusions

The Pennsylvanian strata exhibit similar bed thicknesses and similar stratigraphic characteristics in both areas. The only significant difference between the Honaker Trail section and the Raplee Anticline section is the amount of strain. There are two major discussion points in this section. The first is the controlling factors on fracture spacing, and the second is the causes for fracture termination at mechanical boundaries.

From the multiple regression plots, we can conclude that under low strain conditions, bed thickness tends to have a predominant effect on fracture spacing, whereas the intrinsic properties of the rock have a minor influence. In increasing strain conditions, the internal physical properties come into play and control the fracture spacing, as is observed at Raplee Anticline.

Figure 5.1 shows Honaker Trail and Raplee Anticline have a similar range in bed thickness. However, there is a significant difference in the coefficient of joint spacing between the two with the Raplee Anticline joint spacing averaging 50% less than the Honaker dataset. This difference can be explained by joint infilling due to increased strain conditions at Raplee Anticline.

The infilling of joints which has been described as “joint saturation” or “closely spaced joints” to accommodate increasing strains has long been established in the literature. (Ladeira and Price, 1981; Huang and Angelier, 1989; Narr and Suppe, 1991; Gross et al., 1995; Becker and Gross, 1996; Ji and Saruwatari, 1998; Bai and Pollard, 2000). The difference in the average fracture spacing in figure 5.2 captures the increasing strain

conditions. The average fracture spacing values at Raplee Anticline are half the values present from the Honaker Trail dataset. The data hence confirm fracture infilling due to increasing strain deformation.

Although increasing strain affects joint spacing, a relationship between bed thickness and joint spacing, this is an average result at Honaker trail (R^2=0.5) and non existent at Raplee Anticline (R^2 =0.1); (Fig. 5.5). This leads to the conclusion that there is more than one factor affecting the joint spacing. Figure 5.6, the correlation with average fracture spacing in both Honaker Trail and Raplee Anticline, becomes statistically significant using multiple regression plots. In determining the causes for fracture termination at mechanical boundaries, from the fracture spacing ratio (FSR), Hatzor and Palchik (1997) demonstrated that in carbonate rocks grain size and grain size arrangement can vary dramatically and that the strength of the rock was in a large part due to porosity, where more porous rocks were much weaker than non porous rocks. Corbett et al. (1987) concluded in their work of the Austin chalk that porosity had the highest correlation with rock strength.

Figure 5.7 shows the attempt to asses whether significant differences in rigidity between two mechanical units will inhibit fracture propagation (Renshaw and Pollard; 1995). For fracture termination to occur the rigidity ratio has to be less or equal to 0.4. Our data demonstrate that at both Honaker and Raplee the rigidity difference between layers is above the 0.4 cut off and is not significant enough to inhibit fracture propagation. Yet mechanical boundaries are present and the fractures do terminate, hence another explanation is necessary.

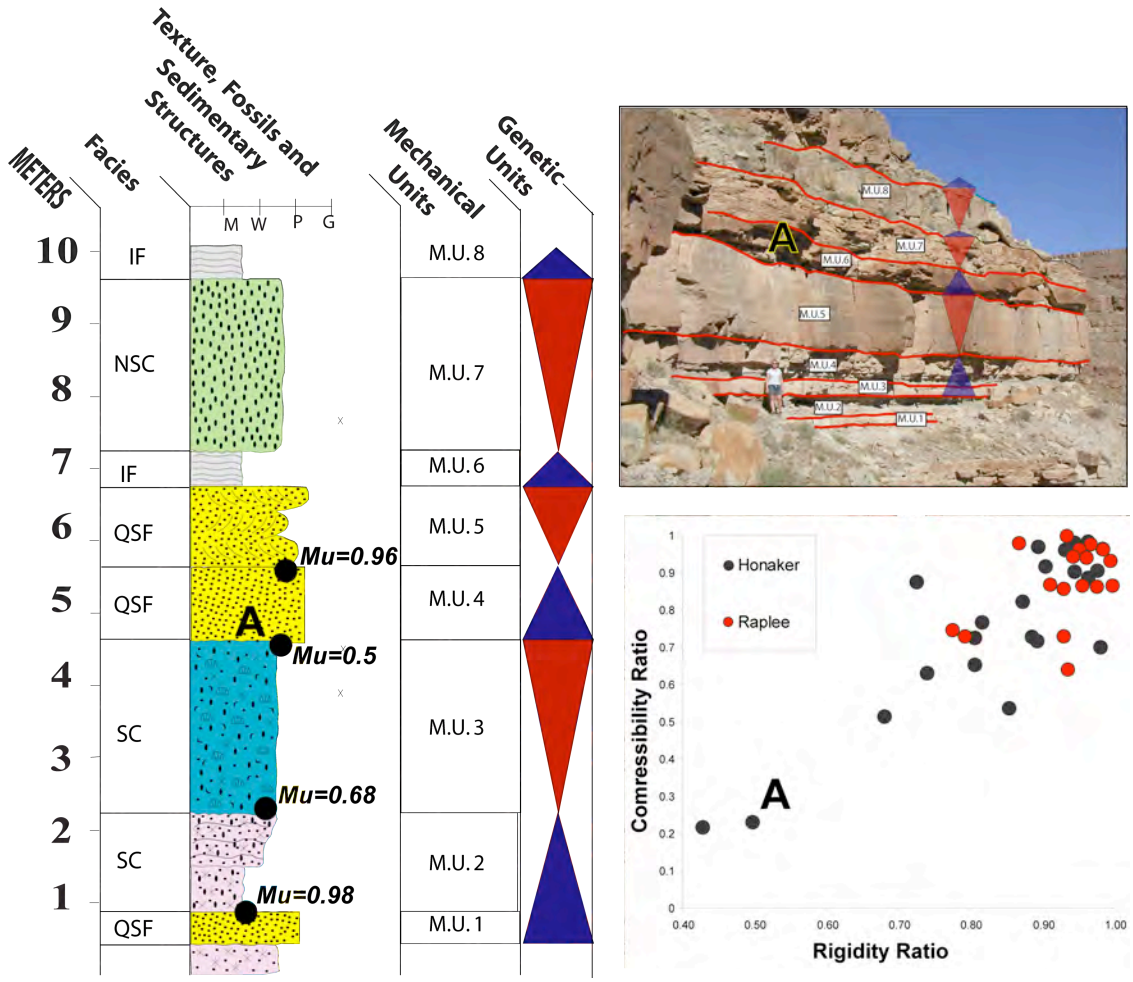

Figure 5.8: Measured section from Honaker Trail, where the genetic boundaries and their turnaround points coincide with mechanical units on the left. Rigidity ratios of the soft to hard layers are plotted on and range from 0.5 to 0.98. On the right is an outcrop photo of the section and on the bottom right is the rigidity ratio plot, showing data point (A), which is anomalously lower than the rest of the data points in the area.

In another study (Shackelton et al., 2005) rigidity ratios below 0.4 causes inhibition of fracture propagation across mechanical boundaries. This study also did not obtain rigidity ratios below 0.4 but also observed mechanical boundaries. They attributed the discrepancy in that rigidity variations existed at time of fracture growth and development, whereas later diagenesis changed the rigidity of the initial rock. Although it is very difficult to know what the initial shear modulus of the rock is during fracturing an alternative explanation is present by Cooke and Underwood (2001).

The Honaker Trail section of figure 5.8 best illustrates the rigidity ratio variations. At the bottom of the section we have a rigidity ratio value of 0.98 between a sandstone bed and a carbonate wackestone to packstone. Even in beds with different lithologies the shear modulus differences are not very large. The quartz sandstone (sample A), labeled in figure 5.8 illustrates that even though it is above a carbonate packstone and hence the lithological and density variation is big it is still insufficient in creating significant shear moduli differences to account for fracture termination at that boundary. Hence an alternative explanation for fracture termination at these boundaries is slip along the bedding contact. Most of the mechanical boundaries coincide with genetic boundaries and their turnaround points, which are markers for significant variations in facies. Hence, this factor may account for bed slip (fig 5.9).

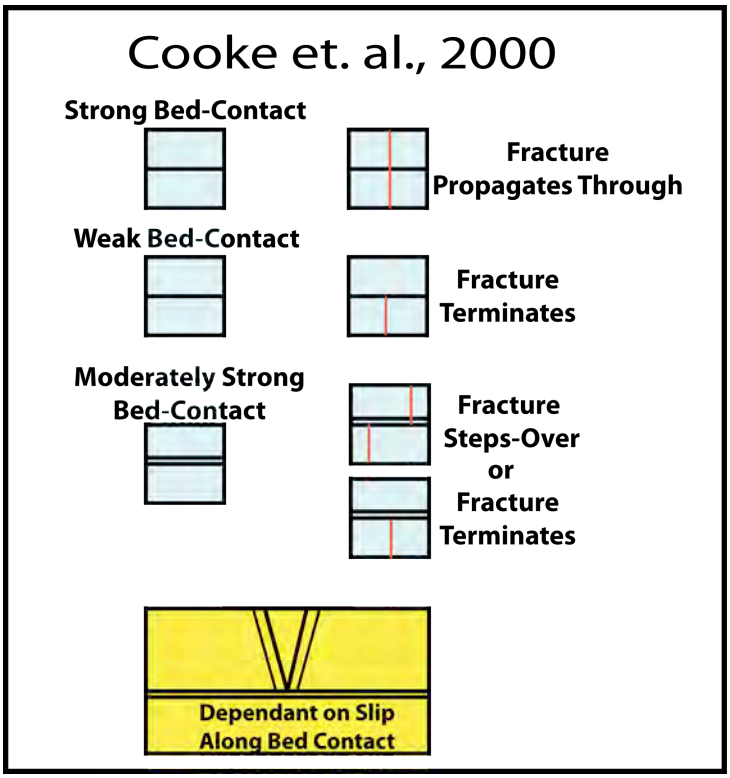

Figure 5.9: Taken from Cooke et al, 2000, this diagram represents fracture propagation, termination or step over through different mechanically bonded boundaries. Sedimentologically, a moderately strong or weak boundary would correlate to genetic boundaries and flooding surfaces.

Genetic boundaries are associated with diagenetic alterations, and periods of no deposition. This factor may also account for poorly bonded layers. Flooding surfaces are usually but not always associated with clay enrichment, which may also account for weak bedding interfaces. These factors may then be the cause for poorly bonded layers, which enhances layer slip and fracture termination by dissipation of the concentrated stress energy (fig. 5.9) as described in Cooke et al., (2000).

The controlling factors on the fracture spacing are determined by the amount of strain conditions the bedrock has undergone. In low strain conditions, the bed thickness dominates and explains 80% of the variability found in the fracture spacing, as observed

at the Honaker Trail section. In high strain conditions, then the intrinsic rock properties of the rock explain 80% of the variability.

Observing intrinsic rock properties with the Fracture Spacing Ratio, most previous literature have associated a relationship between the FSR and porosity. Yet from our results at Raplee Anticline, the bulk density (which takes into account porosity and mineralogy) results in a more significant attribute than porosity (Fig. 5.7).

Finally, the rigidity ratio is not a good measure for determining fracture termination, because it does not take into account later diagenetic events which affect the original rigidity at time of fracturing. Hence a better approach is determining boundaries of bed slip, which generally coincide with high resolution sequence stratigraphic boundaries and their flooding surfaces.

Chapter 6: Thesis Summary

Sequence stratigraphy relates changes in vertical and lateral facies distribution to relative changes in sea level. These relative changes also effect early diagenesis, especially in carbonates where flow of marine and meteoric waters influence the types of pores, cementation and dissolution patterns. As a result, in carbonate systems, relative changes in sea level significantly impact the lithology, porosity, diagenesis, bed and bounding surfaces**,** factors that control fracture patterns. In this study, this concept of facies and diagenetic partitioning is explicitly explored by integrating stratigraphy with the kinematic and structural regime to evaluate its influence on fracture attributes. Specifically, the relationship between mechanical boundaries and sequence stratigraphic (genetic unit) boundaries is evaluated within the Mississippian strata at Sheep Mountain Anticline, Wyoming and the 'undeformed' Mississippian limestones in St. Louis area, Missouri, as well as the Pennsylvanian mixed carbonate-siliciclastic system in the Paradox Basin, Utah.

Fracture analysis was performed with the scan density line method. A comparison of the scan density line method with the area mapping measurement yielded a variation of about 20%At the Paradox Basin, indicating that the scan density line method is a good procedure for measuring fracture patterns. Consequently it is also applied for the other two locations Sheep Mountain Anticline and St. Louis Missouri.

Fracture analyses within the smallest sequence stratigraphic units, the genetic units, reveal that sequence stratigraphic boundaries often act as mechanical unit boundaries. The majority of meso-scale fractures (80%) terminated at genetic unit boundaries or the turnaround point that separates the transgressive from the regressive

hemicycle in each genetic unit. The remaining fractures that did not terminate at their corresponding genetic unit boundaries or their internal turnaround point generally terminated at either internal bedforms (laminations/shale partitionings/ diagenetic surfaces, cross bed stratification) or at lower order sequence stratigraphic surfaces. These results confirm the first working hypothesis of this research, which says that the mechanical unit boundaries correspond to sequence stratigraphic surfaces.

In Sheep Mountain Anticline, the transgressive units are dominantly dolomitic mudstones which are intensely fractured in comparison to the regressive units that are dominantly calcitic grainstones and less fractured. This observation causes speculation that rock stiffness controls the fracture intensity of the units. In contrast, in the Mississippian limestones of Missouri, the regressive units generally have a higher fracture density than the transgressive hemicycles, because the grainstones contain complex internal stratigraphic geometries that create sub-mechanical units. The two other study sites in the Paradox Basin along the Honaker Trail area underwent significantly less deformation than Raplee Anticline and do not show clear differentiation between transgressive and regressive units in fracture intensity. This lack of differentiation is partly due to the sedimentologic and stratigraphic complexity of the facies present within the differing hemicycles that leads to bed internal mechanical unit boundaries. The amount of strain undergone by the facies is important for the fracture intensity. This factor is illustrated in the comparison between the flat lying beds at Honaker and the folded strata at Raplee. This difference in strain produces the fracture density to be twice as high at Raplee anticlines than the density present at Honaker Trail.

The general assumption that bed thickness controls fracture density needs to be modified based on this study. Fracture spacing relates well to bed thickness in mechanical units no greater than 0.5m thick but with increasing bed thickness the relationship between bed thickness and fracture density is not linear and a scatter from the linear-trend is present. This scatter is attributed to the presence of internal bedforms that act as bed-internal mechanical unit boundaries. In addition, largely increased strain conditions like in the tight anticlines at Sheep Mountain and Raplee produce infill fractures and, thus, an higher than expected fracture density.

Several studies in fractures in carbonates attribute the fracture density to be related to the lithology which affects the stiffness of the beds. Data from this study show no clear correlation between "Dunham's" rock texture and fracture density. Similarly, it is assumed that the rock stiffness is directly related fracture patterns. In this study two important parameters that influence rock stiffness, velocity and porosity were measured in the measured strata of the Paradox Basin. Velocity shows in most cases no relation to the fracture patterns observed in outcrop and no correlation is obvious when plotting porosity directly against fracture density. The reason for this lack of correlation may be due partly to that fact that most of the rocks in the Paradox Basin are low in porosity with values from 0.3 to 6%.

The major key findings of this study are:

- Genetic boundaries and higher order sequence boundaries and turnaround points act as mechanical boundaries.

- Fracture length and spacing are primarily affected by external properties such as bed thickness and internal bedforms and affected to a much lesser degree by lithology, porosity or rock stiffness.
- Fracture spacing relates well to bed thickness in mechanical units no greater than 0.5m thick. Correlation of fracture spacing with larger mechanical beds without any internal bedforms is poor, and not well understood.
- Velocity and rock stiffness moduli do not vary enough in the studied carbonates and consequently fail to be mechanical indicators for fracture patterns and behavior.
- The heterogeneity of a mechanical unit that is composed of more than one sedimentological unit makes internal rock properties a poor indicator for defining mechanical units.
- The strata in the Paradox Basin is generally composed of well-cemented, low-porosity rocks. Consequently, a poor correlation exists between fracture density and porosity.
- Raplee Anticline has higher fracture densities than Honaker Trail. This is attributed to the larger strain conditions at Raplee Anticline.

These results illustrate how integrating sedimentologic and sequence stratigraphic information with data on structural kinematics can lead to a more refined predictive understanding of fracture attributes. In conclusion, the gap to understanding the various controls on fracture patterns has lessened, and our understanding into the fracture paradigm has grown, which will enable better understanding of reservoir behavior in future developments.

WORK CITED

Ahr, W.M., 1973. The carbonate ramp: an alternative to the shelf model: Gulf Coast Association of Geological Societies Transactions, v. 23, p. 221-225.

Andersson, J.E., Ekman, L., Nordqvist, R., and Winberg, A., 1991. Hydraulic testing and modeling of a low –angle fracture zone at Finnsjon, Sweden; Journal of Hydrology, v. 126, p. 45-77.

Aydin, A. & Nur, A., 1982. Evolution of pull-apart basins and their scale independence. Tectonics, v.1, p. 91 105.

Baars, D. L. and Stevenson, G.M., 1982. Subtle stratigraphic traps in Paleozoic rocks of Paradox Basin. In Halbouty (1982, Ed.), AAPG Memoir, No. 32, pp.131-158.

Baer, G. and Reches, Z., 1991. Mechanics of emplacement and tectonic implications of the Ramon Dike Systems, Israel. Journal of Geophysical Research, v. 96, p.11895-11910.

Baer, G., 1991. Mechanisms of dike propagation in layered rocks and in massive porous sedimentary rocks. Journal of Geophysical Research, v. 96, p.11911-11929.

Bai, T. and Pollard, D.D., 2000. Closely spaced fractures in layered rocks: initiation mechanism and propagation kinematics, Journal of Structural Geology, v. 22, p. 1409-1425.

Barbeau, D. L., 2003. A flexural model for the Paradox Basin: implications for the tectonics of the Ancestral Rocky Mountains. Basin Research, v. 15, p. 97-115.

Becker, A. and Gross, M.R., 1996. Mechanism for joint saturation in mechanically layered rocks: an example from southern Israel, Tectonophysics, v.257, p. 223-237.

Bellahsen, N., Fiore, P., Pollard, D.D., 2006. Growth of basement fault-cored anticlines: the example of Sheep Mountain Anticline, Wyoming, Geophysical Research Letters 33, L02301, doi: 10.1029/2005GL024189.

Bhattachryya, D.P., and Seely, M.R., 1994, Multiple dolomitization of the Warsaw and Salem formations (Middle Mississippian), western flank of the Illinois Basin: Textural, trace elemental, and isotopic signatures of four types of dolomite-a case study; Diagenesis, *IV*. Developments in sedimentology, v. 51, p. 283-308.

Book: Committee on fracture characterization and fluid flow and U.S. National Committee for rock mechanics, 1996. Rock fractures and fluid flow; Contemporary understanding and applications, National Academy Press.

Boyd, D. W., 1997. Paleozoic history of Wyoming: Proceedings of the 32nd Annual Forum on the Geology of Industrial Minerals.

Caine, J.S., Evans, J.P. and Forster, C.B., 1996. Fault zone architecture and permeability structure, Geology, V. 24, no. 11; p.1025-1028.

Cello, G., Invernizzi, C., Mazzoli, S., and Tondi, E., 2001. Fault properties and fluid flow patterns from Quaternary faults in the Apennines, Italy, Tectonophysics, v. 336, p.63-78.

Chester, F.M., Evans, J.P., and Beigel, R.L., 1993. Internal structure and weakening mechanisms of the San Andreas fault: Journal of Geophysical Research, v. 98, p. 771-786.

Choquette, P.W., 1983. Platey-algal reef mounds, Parodox Basin. In Scholle, P.A., Bebout, D.E., and Moore, C.H., eds., Carbonate depositional environments. American Association of Petroleum Geologists, Memoir 33, p.454-462.

Choquette, P. W., and J. D. Traut, 1963. Pennsylvanian carbonate reservoirs, Ismay field, Utah and Colorado, in R. O. Bass, ed., Shelf carbonates of the Paradox basin: Four Corners Geol. Soc., p. 157-186.

Cluff, R.M., Reinhold, M.L., and Lineback, J.A., 1981. The New Albany Shale Group of Illinois: Illinois Geological Survey Circular 518, 83 p.

Cook T.S. and Erdogan F., 1972. Stresses in bonded materials with a crack perpendicular to the interface, International Journal of Engineering Science, v. 10, p. 677–697.

Cooke, M. L., 2000. Carbonate cyclicity and fracturing – the mechanical stratigraphy connection: AAPG Annual Meeting Abstract.

Cooke, M.L. and Underwood, C.A., 2001. Fracture termination and step over at bedding interfaces due to frictional slip and interface opening, Journal of structural geology, v. 23, p.223-238.

Cooke, M.L., Mollema, P., Pollard, D.D., Aydin, A., 2000. Interlayer slip and joint localization in East Kaibab Monocline, Utah: field evidence and results from numerical modeling, in: Cosgrove, J.W., Ameen, M.S. (Eds.), Geological Society of London Special Publication on Forced Fold and Associated Fractures 169, London, p. 23–49.

Corbett, K., Friedman, M. and Spang, J., 1987. Fracture development and Mechanical Stratigraphy of Austin Chalk, Texas; The American Association of Petroleum Geologists Bulletin, v. 71, No. 1, p. 17-28.

Dyer, R., 1988. Using joint interactions to estimate paleostress ratios. Journal of Structural Geology, v. 10, p. 685-699.

Eberli, G. P., Melim, L. A., Grammer, G. M., Walgenwitz, F., 1996. Stratigraphic control on diagenesis – the key for understanding porosity/permeability distribution in carbonate reservoirs: AAPG Hedberg Conference.

Engelder, T., Gross, M. and Pinkerton, P., 1997. An Analysis of joint development in thick sandstone beds of the Elk Basin Anticline, Montana-Wyoming; Rocky Mountain Association of Geologists, Fractured Reservoirs: Characterization and Modeling Guidebook.

Fabbri, O., Gaviglio, P., Gamond, J.F., 2001. Diachronous development of master joints of different orientations in different lithological units within the same forearc-basin deposits, Kyushu, Japan; Journal of Structural Geology, v. 23, p. 239-246

Goldhammer, R.K., Oswald, E.J. and Dunn, P.A., R.K., 1994. High-frequency, glacio-eustatic cyclicity in the Middle Pennsylvanian of the Paradox Basin; an evaluation of Milankovitch forcing. In: Orbital Forcing and Cyclic Sequences (Ed. by B.P.L. De & D.G. Smith), Spec. Publ. Int. Ass. Sed., v. 19, p. 243−283.

Goldhammer, R.K., Oswald, E.J. and Dunn, P.A., 1991. Hirearchy of stratigraphic forcing: Example from Middle Pennsylvanian shelf carbonates of the Paradox Basin. Kansas Geological Survey 233, p. 361-413.

Grammer, G.M., Eberli, G.P., Van Buchem, F.S.P., Stevenson, G.M., and Homewood, P., 1996. Application of high resolution sequence stratigraphy to evaluate lateral variability in outcrop and subsurface-Desert creek and Ismay intervals, Paradox Basin. SEPM Spec. Publ., p. 235-266.

Grammer, G.M., Eberli, G.P., Van Buchem, F.S.P., Stevenson, G.M., and Homewood, P., 2000. Application of high resolution sequence stratigraphy in developing an exploration and production strategy for a mixed carbonate/siliciclastic system (Carboniferous) Paradox Basin, Utah, USA; Bull. Centre Rech. Elf Explor. Prod., Mem.24, 290 p.

Gross, M. R., 1995. Fracture partitioning: Failure mode as a function of lithology of the Monterey Formation of coastal California: Geological Society of America Bulletin, v. 107, no. 7, p. 779-792.

Gross, M.R., 1993. The origin and spacing of cross joints: example from the Monterey Formation, Santa Barbara coastline, California: Journal of Structural Geology, v. 5, no. 6, p.737-751.

Gross, M.R., Fischer, M.P., Engelder, T. and Greenfield, R.J., 1995. Factors controlling joint spacing in interbedded sedimentary rocks: integrating numerical models with field observations from the Monterey Formation, USA, Geological society special publication, No. 92, p. 215-233.

Hanks, C.L., Lorenz, J., Teufel, L. and Krumhardt, A.P.,1997. Lithologic and structural controls on natural fracture distribution and behavior within the Lisburne Group, Northeastern Brooks Range and North Slope subsurface, Alaska; AAPG Bulletin, v.81, No. 10, p. 1700-1720.

Hatzor, Y. H. and Palchik, V., 1997. The influence of grain size and porosity on crack initiation stress and critical flaw length in dolomites; International Journal of Rock Mechanics, v. 34, No. 5, p. 805-816.

Haq, B.U., Hardenbol, J. and Vail, P.R., 1988. Mesozoic and Cenozoic chronostratigraphy and eustatic cycles. In: C.K. Wilgus, B.S. Hastings, C.G.St.C. Kendall, H.W. Posamentier, C.A. Ross and J.C. Van Wagoner, Editors, Sea-Level Changes: An Integrated ApproachSoc. Econ. Paleontol. Mineral., Spec. Publ. 42, p. 71–108.

Haq, B.U. Hardenbol J. and Vail, R.R., 1987, Chronology of fluctuating sea levels since the Triassic, Science 235, p. 1156–1166.

Heidlauf, D.T., Hsui, A.T. and Klein, G.D., 1986. Tectonic subsidence analysis of the Illinois basin; The Journal of Geology, v. 94, no.6. pp. 779-794.

Helgeson, D.E., and A. Aydin, 1991. Characteristics of joint propagation across layer interfaces in sedimentary rocks: Journal of Structural Geology, v.13, no.8, p. 897-911.

Hennier, J. and Spang, J. H., 1983. Mechanisms for deformation of sedimentary strata at Sheep Mountain Anticline, Bighorn Basin, Wyoming: Thirty Fourth Annual Field Conference; Wyoming Geological Association Guidebook.

Homewood, P., Guillocheau, F., Eschard, R., Cross, T.A., 1992. Correlations haute resolution et stratigraphie gntique: une dmarche intgre, Bull. Centres Rech. Explor.-Prod. Elf- Aquitaine, v.16, p. 357-381.

Homewood, P.W., Mauriaud, P. and Lafont, F., 2000. Best practices in sequence stratigraphy for explorationists and reservoir engineers: Elf EP.

Howe, W.B. and Koenig, J.W., 1961. The stratigraphic succession in Missouri v. 40, State of Missouri Division of Geological Survey and Water Resources, 2nd Series, 185 p.

Huang, Q., and J. Angelier, 1989. Fracture spacing and its relation to bed thickness: Geological Magazine, v.126, no.4, p. 355-362.

Hugman, R. H. H., III, and Melvin Friedman, 1979. Effects of texture and composition on mechanical behavior of experimentally deformed carbonate rocks: AAPG Bulletin v. 63, p. 1478-1489.

Ji, S. and Saruwatari, K., 1998. A revised model for the relationship between joint spacing and layer thickness, Journal of Structural Geology, v.20, No. 11, pp. 1495-1508.

Johnson, G. D., Garside, L. J., Warner, A. J., 1968. A study of the structure and associated features of Sheep Mountain Anticline Big Horn County, Wyoming: Earth Science Bulletin, v. 1, no. 2, p. 25-29.

Kaufman, J., Cander, H.S., Daniels, L.D., and Meyers, W.J., 1988. Calcite cement stratigraphy and cementation history of the Burlington-Keokuk Formation (Mississippian), Illinois and Missouri; Journal of Sedimentary Research, v. 58, p. 312-326.

Kissling, D.L., 1961, Lower Osagean Stratigraphy of East-Central Missouri; Kansas Geological Society, 26th field conference guidebook, pp.142-148.

Kluth, C.F. & Coney, P.J., 1981. Plate tectonics of the ancestral Rocky Mountains. Geology, v. 9, p.10−15.

Knott, S.D., Beach, A., Brockbank, P.J., Brown, L., McCallum, J.E., and Welbon, A.I., 1996. Spatial and mechanical controls on normal fault populations, Journal of Structural Geology, v. 18, Nos. 2/3, p. 359-372.

Kolata, D.R. and Nelson, W.J., 1991. Tectonic history of the Illinois Basin. In: Leighton, M.W., Kolata, D.R., Oltz, D.F., Eidel, J.J. (Eds.), Interior Cratonic Basins. Am. Assoc. Pet. Geol. Memoir 51, p. 263–285

Lacazette, 2000. Natural Fracture Nomenclature, Disk 1, 13 pages, *in* L.B. Thompson (editor) Atlas of Borehole Images, AAPG Datapages Discovery Series 4, American Association of Petroleum Geologists, Tulsa (2 compact disks).

Ladeira, F.L. and Price, N.J. 1981. Relationship between spacing and bed thickness. Journal of Structural Geology v. 3, p. 179–183.

Lane, H.R., 1978. The Burlington shelf (Mississippian, north central United States); Geologica et Palaeontologica, v.12, p. 165-176.

Lasemi, Z., Norby, R.D. and Treworgy, J.D., 1998. Depositional facies and sequence stratigraphy of a Lower Carboniferous bryozoan-crinoidal carbonate ramp in the Illinois Basin, mid-continent USA. In: Wright, V.P. and Burchette, T.P.(eds) Carbonate Ramps. Geological Society, London, Special Publications, v. 149, p.369-395.

Lineback, J.A., 1966. Deep-water sediments adjacent to the Borden siltstone (Mississippia) delta in southern Illinois; Illinois State Geological Survey Guidebook, v. 401, p. 1-21.

Lineback, J.A., 1972. Lateral gradation of the Salem and St. Louis limestones (Middle Mississippian) in Illinois; Illinois State Geological Survey Guidebook, v. 474, p. 1-48.

Lorenz, J.C., Farrell, H.E., Hanks, C.L., Rizer, W.D. and Sonnenfeld, M.D., 1997. Characteristics of Natural Fractures in Carbonate Strata: Carbonate Seismology, Geophysical Developments No.6, p.179-203.

Loucks, R.G. and Sarg, J.F. 1993. Editors, Carbonate Sequence Stratigraphy, AAPG Memoir 57, p. 545.

Meyers, J. W., 1978. Carbonate cements: Their regional distribution and interpretation in Mississippian limestones of southwestern New Mexico: v. 25, p. 371-399

Mitchum, R.M., 1977. Seismic stratigraphy and global change of sea level, Part 1: Glossary of terms used in seismic stratigraphy, in Payton, C.E. (ed.), Seismic stratigraphy – applications to hydrocarbon exploration. AAPG Memoir 26, p.117-133.

Narr, W. and Lerche, I., 1984. A Method for Estimating Subsurface Fracture density in Core, AAPG Bulletin p. 637-648.

Narr, W., Suppe, J., 1991. Joint spacing in sedimentary rocks. Journal of Structural Geology, v. 13, p. 1037 –1048.

Nelson, R.A., 1985. Geologic analysis of naturally fractures reservoirs: Gulf Publishing Co., Houston, 320p.

Peterson, J.A., and Hite, R.J., 1969. Pennsylvanian evaporite-carbonate cycles and their relation to petroleum occurrence, southern Rocky Mountains: American Association of Petroleum Geologists Bulletin, v. 53, p. 884-908.

Price, N.J., 1996. Fault and joint development in brittle and semi-brittle rock: Oxford, England, Pergamon Press, 176p.

Posamentier, H.W., Vail, P.R., 1988. Eustatic controls on clastic deposition II-sequence and systems track models. In: Wilgus, C.K., Hastings, B.S., Ross, C.A.,

Posamentier, H.W., Van Wagoner, J.C., Kendall, C.G., 1988. (Eds.), Sea-level Changes: An Integrated Approach. SEPM (Society for Sedimentay Geology) Special Publication 42, p. 125-154.

Rankey, E.C., 2003. Carbonate-filled channel complexes on carbonate ramps: an example from the Peerless Park Member [Keokuk Limestone, Visean, Lower Carboniferous (Mississippian)], St. Louis, MO, USA: Sedimentary Geology, v.155, p.45-61

Renshaw, C. E., Pollard, D.D., 1995. An experimentally verified criterion for propagation across unbounded frictional interfaces in brittle, linear elastic materials. International Journal of Rock Mechanics and Mining Science and Geomechanics Abstracts, v. 32, p. 237-249.

Rijken, P. and Cooke, M.L., 2001. Role of shale thickness on vertical connectivity of fractures: application of crack-bridging theory to the Austin Chalk, Texas, Tectonophysics 337, p. 117–133.

Rock Fractures and Fluid Flow: Contemporary Understanding and Applications, 1996. Commission on Geosciences, Environment and Resources- Online Book.

Sarg, J.F., Markello, J.R., and Weber, L.J., 1999. The second-order cycle, carbonate-platform growth , and reservoir, source, and trap prediction. SEPM Spec. Publ. No. 63, p. 11-34.

Shackleton, R., Cooke, M. and Sussman, A., 2005. Evidence for temporally changing mechanical stratigraphy and effects on joint network architecture, Geology, v. 33, p. 101-104

Smith, L. B., and Eberli, G. P., 2000. Sequence Stratigraphic Distribution of Reservoir-Quality Dolomite, Madison Formation (Mississippian), Wyoming and Montana, American Association of Petroleum Geologists Annual Meeting, Program with Abstracts, p. A139.

Smith, L.B., Eberli, G.P. and Sonnenfeld, M.D., In Press, Sequence stratigraphic and paleogeographic distribution of reservoir quality dolomite, Madison Formation, Wyoming and Montana: AAPG.

Smith, L. B., Eberli, G. P**.** and Sonnenfeld, M.D., 2004. Sequence stratigraphic and paleogeographic distribution of reservoir-quality dolomite, Madison Formation, Wyoming and Montana submitted to Grammer, G. M., Harris, P. M., and Eberli, G. P. (eds.), Integration of Outcrop and Modern Analogs in Reservoir Modeling. AAPG Memoir 80, p. 67-92.

Sonnenfeld, M.D., 1996. Sequence evolution and hierarchy within the lower Mississippian Madison limestone of Wyoming: SEPM, p.165-192.

Stevenson, G.M. & Baars, D.L., 1986. The Paradox; a pull-apart basin of Pennsylvanian age. In: Paleotectonics and Sedimentation in the Rocky Mountain Region, United States (Ed. by J.A. Peterson), v. 41, p. 513–539. Am. Ass. Petrol. Geol.

Stokes, W.L., 1988. Geology of Utah (2nd printing). The Utah Museum of Natural Histroy; Occasional paper no.6, 280 p.

Swart, P.K. and Melim, L.A., 2000. The origin of dolomites in Tertiary sediments from the margin of Great Bahama Bank; Journal of sedimentary research, v. 70, No. 3, p.738-748.

Teufel, L. W., Clark, J. C., 1984. Hydraulic fracture propagation in layered rocks: experimental studies of fracture containment. Society of Petroleum Engineers Journal, v. 24, p. 19-34.

Underwood, C.A., 1999. Stratigraphic controls on vertical fracture patterns within the Silurian dolomite of Door County, Wisconsin and implications for groundwater flow: Master's thesis, University of Wisconsin-Madison, Wisconsin, 193p.

Underwood, C.A., Cooke, M.L., Simo, J.A. and Muldoon,M.A., 2003. Stratigraphic controls on vertical fracture patterns in Silurian dolomite, northeastern Wisconsin, AAPG Bulletin, v.87, No.1, p. 121-142.

Vail, P.R., Mitchum, R.M., Jr., Todd, R.G., Widmier, J.M., Thompson, S., III., Sangree, J.B., Bubb, J.N. and Hatleilid, W.G., 1977. Seismic stratigraphy and global changes of sea level. In: C.E. Payton (Editor), Seismic Stratigraphy-Applications to Hydrocarbon Exploration. Am. Assoc. Pet. Geol. Mem., 26, p.49-212.

Van Wagoner, J.C., Mitchum, R.M., Campion, K.M., Rahmanian, D., 1990. Siliciclastic sequence stratigraphy in well logs, cores, and outcrops: concepts for high-resolution correlation of time and facies. American Association of Petroleum Geologists Methods in Exploration Series 7, 55 p.

Weber, L.J., Wright, F.M., Sarg, J.F., Shaw, E., Harman, L.P., Vanderhill, J.B. and Best, D.A.1995. Reservoir delineation and performance. SEPM short course, No. 34, p.1-30.

White, J.V., 1995. Diagenesis and porosity distribution of Pennsylvanian Paradox Formation carbonates (Upper Ismay), Southeast Utah. M.A. Thesis, The University of Texas at Austin, 100 p.

Wiltschko, D. V., Medwedeff, D. A. and Millson, H. E., 1985. Distribution and mechanisms of strain within rocks on the northwest ramp of Pine Mountain block, southern Appalachian foreland: a field test of theory: Geological Society of America Bulletin, v. 96, p. 426-435.

Wu, H. and Pollard, D.D., 1995. An experimental study of the relationship between joint spacing and layer thickness: Journal of structural geology, v. 17, No.6, p.887-905.

Yale, D.P. and Jamieson Jr, W.H., 1994. Static and Dynamic mechanical properties of carbonates; Rock Mechanics (reprinted) p. 463-471.

Zhang, X. & Sanderson, D. J., 1998. Numerical study of critical behavior of deformation and permeability of fractured rock masses: Marine and Petroleum Geology, v. 15, p. 535-548.